Space Sci Rev (2020) 216:25
https://doi.org/10.1007/s11214-020-0645-3

Oxygen Isotopes and Sampling of the Solar System

Trevor R. Ireland[1] · Janaina Avila[1] · Richard C. Greenwood[2] · Leon J. Hicks[3] · John C. Bridges[3]

Received: 3 December 2019 / Accepted: 12 February 2020 / Published online: 3 March 2020

Abstract Oxygen is the dominant element in our planetary system. It is therefore remarkable that it shows substantial isotopic diversity both in mass-dependent fractionation, because it is a light element, and in mass-independent fractionation, primarily associated with variation in abundance of ^{16}O. On Earth, the primary variation in isotopic composition is related to temperature-dependent kinetic mass fractionation between hydrosphere and atmosphere. Meteorites provide samples of primitive bodies, that have not experienced melting, and planetesimals that have melted early in their history. Samples of Mars, Vesta, and the Moon are present in the meteorite collections. In meteorites, the cosmochemical fractionation related to the abundance of ^{16}O provides a useful classification scheme. Inclusions in chondrites show a large range in ^{16}O abundances from highly enriched (solar) through to compositions closer to terrestrial (planetary). The variability in ^{16}O appears originally to be related to predissociation and self-shielding of carbon monoxide likely in the primordial molecular cloud. Within the chondrite parent bodies, exchange between ^{16}O-poor fluids and relatively ^{16}O-rich solids created isotopic mixing lines. This model makes specific predictions for isotopic compositions of silicates and water ice throughout the solar system. One prediction, that the Earth should be isotopically heavier than the Sun, appears to be verified. But other tests based on oxygen isotopes within the solar system require either remote analysis or sample return missions. Remote analysis will require new instrumentation and analytical techniques to achieve the precision and accuracy required for three oxygen isotope analysis. Methodologies associated with cavity ring-down spectroscopy appear promising. Sample return appears viable only for the inner solar system including Mars and asteroids.

Role of Sample Return in Addressing Major Questions in Planetary Sciences
Edited by Mahesh Anand, Sara Russell, Yangting Lin, Meenakshi Wadhwa, Kuljeet Kaur Marhas and Shogo Tachibana

✉ T.R. Ireland

[1] Research School of Earth Sciences, The Australian National University, Canberra, ACT 2601, Australia

[2] Planetary and Space Sciences, School of Physical Sciences, The Open University, Milton Keynes MK7 6AA, United Kingdom

[3] Space Research Centre, School of Physics and Astronomy, University of Leicester, Leicester LE1 7RH, United Kingdom

While sample return missions to either Venus or Mercury appear highly challenging, the scientific benefits are immense both in oxygen isotope characterisation, and in a variety of other geochemical analyses. Measurement of three oxygen isotopes throughout the solar system would further our concepts for formation of other solar systems, and give us insight into the general mechanisms of planetary system formation and the role of water in the formation and evolution of the chondrite parent bodies and planets.

Keywords Oxygen isotopes · Sample return · Remote analysis · Cosmochemistry

1 Introduction

Oxygen is a most remarkable element. It is the most abundant element on Earth. Combining with silicon it forms silicates, which are the most abundant minerals in the mantle and crust. The interrelationship with the oxidation state of iron potentially controls the core size of the terrestrial planets. Combining with hydrogen it forms water, a molecule which can single handedly define the habitability of a planet. Liquid water defines Earth. Water ice is common in the outer solar system. Condensation of water at the snow line of the early solar system potentially allowed the rapid formation of Jupiter. Understanding the processes that control oxygen in the materials of the solar system is therefore fundamental.

Another remarkable characteristic of oxygen, and the main focus of this paper, is the isotopic variability of oxygen in the solar system. Oxygen shows large mass dependent fractionation on Earth, especially between hydrosphere, atmosphere, and water precipitation. Calibration of these fractionations has allowed temperature proxies to be developed that allow insights into Earth's climate in the past.

In extraterrestial samples, including primitive and differentiated meteorites and their solar condensate components, variations associated with the abundance of ^{16}O are predominant. These can range from an 8% enrichment in ^{16}O to 20% deficits relative to terrestrial oxygen isotope ratio (e.g., Ireland 2012; Yurimoto 2018). The source of this isotopic diversity appears to be related to the chemistry of carbon monoxide rather than any particular nucleosynthetic carrier. Carbon monoxide can experience photodissociation under UV radiation, and self-shielding of the different isotopologues can create isotopic diversity (Bally and Langer 1982; Lada et al. 1994). One of the main products of this dissociation is water that is isotopically enriched in ^{17}O and ^{18}O. This mechanism yields testable predictions for the composition of the Sun, and for the compositions of silicates and water ice on outer solar system moons. A fundamental achievement of the NASA Genesis mission (Burnett et al. 2003) was to show that indeed the Earth is different from the Sun in a way that is consistent with the predissociation and self-shielding model (McKeegan et al. 2011).

The exploration of our solar system with respect to the nature and distribution of oxygen isotopes is therefore a priority in attempting to understand the formation processes of our solar system. Potentially this will guide our understanding of the formation of other exoplanetary systems.

The key to further our understanding of oxygen isotope compositions lies in the ability to either accomplish remote analysis of the three stable oxygen isotopes, or to bring samples back from solar system bodies. The analysis of three oxygen isotopes on Earth is enabled by the use of rather extreme chemical processing (use of highly reactive fluorine compounds) and analysis with rather heavy magnetic sector mass spectrometers. Neither of these aspects is particularly well suited to space flight. The alternative of a sample return mission is expensive, risky, and difficult. Still, if we are to realise an ambition to measure oxygen isotopes

throughout the solar system, a combination of remote analysis and sample return missions will almost certainly be required.

This paper reviews the systematics of oxygen isotopes in our solar system including nomenclature, analysis protocols, isotopic processing on Earth as a guide to processes in the solar system, and the extent of isotopic diversity revealed in the solar system. The terrestrial oxygen isotope geochemistry section has been guided by the classic texts of Faure (1986) and Hoefs (2009). The extraterrestrial work is initiated from reviews of oxygen isotopes in the solar system by Ireland (2012), Greenwood et al. (2017), and Yurimoto et al. (2008). From these starting points we look at various possibilities to further our understanding of the solar system through remote analysis and sample return missions.

2 Oxygen Isotope Measurements

2.1 Nomenclature

Oxygen has three stable isotopes: ^{16}O (99.76%), ^{17}O (0.04%) and ^{18}O (0.20%), where the percentages in brackets refer to approximate overall terrestrial abundances. Oxygen isotope ratios show significant variation at the percent level in terrestrial materials as well as solar system materials. While a determination of absolute isotope abundances requires stringent measurement calibrations, in general usage an oxygen isotope composition is expressed as isotope ratios relative to the major isotope ^{16}O, i.e. ^{17}O/^{16}O and ^{18}O/^{16}O.

Measured oxygen isotope ratios are then generally calibrated to a reference material and expressed as a deviation from that reference material in units of parts per thousand, i.e.,

$$\delta^{17}\mathrm{O} = \left[\left(^{17}\mathrm{O}/^{16}\mathrm{O}\right)_{\mathrm{meas}}/\left(^{17}\mathrm{O}/^{16}\mathrm{O}\right)_{\mathrm{std}} - 1\right] * 1000\ (‰)$$

$$\delta^{18}\mathrm{O} = \left[\left(^{18}\mathrm{O}/^{16}\mathrm{O}\right)_{\mathrm{meas}}/\left(^{18}\mathrm{O}/^{16}\mathrm{O}\right)_{\mathrm{std}} - 1\right] * 1000\ (‰)$$

where the subscript "meas" refers to the measured isotope ratio and "std" refers to the reference standard ratio.

2.2 Standards

The most common currently used reference material is V-SMOW, which is the Vienna Standard Mean Ocean Water standard. The original SMOW represented a mix of a number of ocean water samples from around the world that have been distilled to form pure water (Craig 1961). The limited supply of SMOW had been addressed by the International Atomic Energy Agency (based in Vienna) producing the replicate V-SMOW. The oxygen isotope ratios of this material are:

$$^{17}\mathrm{O}/^{16}\mathrm{O} = 0.0003799 \pm 8 \text{ (a ratio of approximately 1 in 2632 parts)}$$

$$^{18}\mathrm{O}/^{16}\mathrm{O} = 0.00200520 \pm 43 \text{ (a ratio of approximately 1 in 499 parts).}$$

The original determination for the absolute ^{18}O/^{16}O ratio of SMOW was carried out by Baertschi (1976) and this value is still taken as the reference for this ratio to fix the delta scale. The direct determination of ^{17}O/^{16}O of SMOW, or V-SMOW, is not a common practice. With the advent of dual-inlet multiple-collector mass spectrometers, relative differences between samples and standards are determined, rather than absolute values. Thus, the

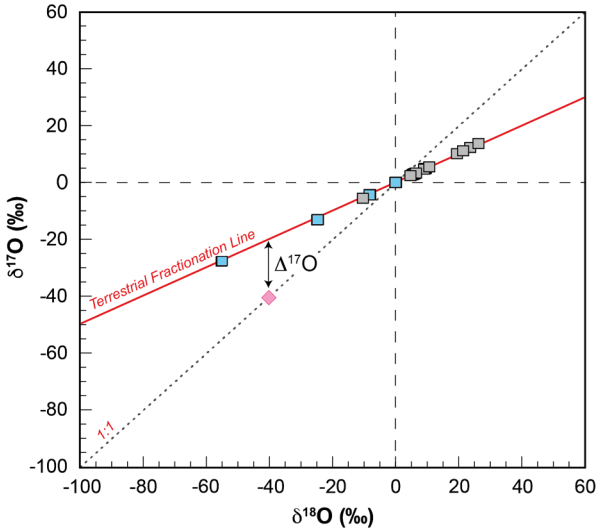

Fig. 1 The Oxygen three-isotope diagram. Oxygen isotope ratios are referenced to deviations from SMOW to generate the delta scale. Mass dependent fractionation related to kinetic isotope mass fractionation lies on the Terrestrial Fractionation Line of slope of approximate 1/2 (i.e. $\delta^{17}O = 0.5 * \delta^{18}O$). $\Delta^{17}O$ refers to the deviation of a composition from the mass dependent fractionation line, and is expressed as the distance to the TFL at the given $\delta^{18}O$ (i.e. $\Delta^{17}O = \delta^{17}O - 0.52 * \delta^{18}O$). For the red diamond at $\delta^{18}O = -40‰$ on the slope 1 reference line, the $\Delta^{17}O$ is $-19.2‰$. Oxygen isotope compositions of meteoritic water (blue squares) and terrestrial silicate and oxide minerals (grey squares) from Tanaka and Nakamura (2012) are consistent with mass dependent fractionation

$^{17}O/^{16}O$ ratio determined by Li et al. (1988) has an uncertainty of approximately 2‰, but this uncertainty is not propagated to measurements because the measurements are made in direct reference to the standard gas (e.g. Jabeen and Kusakabe 1997). A more complete discussion of the issues of calibration to SMOW are provided in Pack and Herwartz (2014) and Miller et al. (2015).

2.3 Mass Dependent Fractionation

Isotope compositions are known to change on Earth through mass dependent fractionation (MDF). For small degrees of MDF, a linear approximation may be used to describe the relationship between $\delta^{17}O$ and $\delta^{18}O$, with the slope being a function of the mass difference in the ratios, i.e. $(17-16)/(18-16) = 1/2$ (Fig. 1). If exact nuclidic masses are used, then the constant is 0.501. However, the interrelationship between $\delta^{17}O$ and $\delta^{18}O$ is not strictly constant and depends on the processes involved; Matsuhisa et al. (1978) noted a range in the fractionation factor between 0.50 and 0.53.

Typically in isotope geochemistry, the $^{17}O/^{16}O$ ratio is not measured. This is because of the functional relationship between $\delta^{17}O$ and $\delta^{18}O$, and also because of the increased difficulty of measuring $^{17}O/^{16}O$. The lower abundance of $^{17}O/^{16}O$ requires longer measurement times to achieve appropriate precision. Moreover, a common analytical mass spectrometric protocol involves the production and measurement of CO_2 where $^{18}O/^{16}O$ is represented by $^{12}C^{18}O^{16}O/\ ^{12}C^{16}O_2$. (i.e. mass 46/mass 44). However, in this case, mass 45 cannot be used for the $^{17}O/^{16}O$ ratio because of the isobaric $^{13}C^{16}O_2$ molecule interfering with $^{12}C^{17}O^{16}O$. Measurement of three oxygen isotopes requires the measurement of O (or O_2) directly, often

released from silicate minerals with fluorine or fluorine compounds (i.e. F_2, BrF_5; Clayton and Mayeda 1963).

2.4 Mass Independent Fractionation

The purpose of measuring three oxygen isotopes is to ascertain if the mass dependence relationship holds, and if not, to identify the process responsible. Deviation from an assumed mass fractionation law is often referred to as Mass Independent Fractionation (MIF), although this particular expression has connotations of there being no relationship with mass dependent fractionation, which may, or may not be the case. A more generic expression is non-mass dependent fractionation and essentially expresses a departure from the accepted mass fractionation law.

This departure is quantified by calculating the residual $\Delta^{17}O$ (Fig. 1), where

$$\Delta^{17}O \approx \delta^{17}O - 0.52 * \delta^{18}O$$

In this case the value of 0.52 was adopted by the Chicago laboratory as an average value of the range found by Matsuhisa et al. (1978). Other laboratories have adopted different values, such as 0.5247 at the Open University based on a linearization method of a number of silicate standards (Miller 2002). However, Pack and Herwartz (2014) advocated a much steeper slope of 0.5305, which is the theoretical high temperature limit for equilibrium fractionation. It should be noted that at extremely high precision levels, such differences in fractionation factors will result in small shifts in $\Delta^{17}O$, and these will be systematically related to $\delta^{18}O$.

In the expression for $\Delta^{17}O$, the deviation of the composition from MDF is explicitly ascribed to the $^{17}O/^{16}O$ ratio. It should be remembered that departures from the MDF line are related to specific processes and reactions and that they may have a large MDF component as well as a MIF. Furthermore, while $\Delta^{17}O$ is a useful algebraic construct, it does not inform particularly well as to the cause of the shift away from the MDF line.

2.5 Analytical Techniques

2.5.1 Gas Source Mass Spectrometry

Gas source mass spectrometry (GSMS) is generally referred to as a bulk analytical technique because the sample is removed from its original context and chemically treated to release oxygen. The material can be solid, liquid, or gas, but the analytical methodology is based on the introduction of a gas (e.g. CO_2, O_2) to the mass spectrometer. However, for analysis of $\delta^{18}O$ and $\delta^{17}O$, oxygen must be used as the source gas because of the presence of unresolvable isobars with CO_2, and specifically with the major species $^{12}C^{16}O^{17}O$ and $^{13}C^{16}O_2$ at mass 45.

The controlled and complete release of oxygen from rocks is not straightforward (see review by Greenwood et al. 2017). Early chemical release of oxygen was based on "bombs", robust sealable containers made of a metal (e.g. Ni) that could be taken to elevated temperature (and thence internal pressure) to promote chemical reaction. Still, the temperature can only be taken to several hundred °C (e.g., ClF_3-HF at 430 °C or F_2-HF at 420 °C for periods of 6 to 20 hours, Baertschi and Silverman 1951) potentially resulting in incomplete reaction. Introduction of potential contaminants to the sample is an issue as hygroscopic NiF_2 is produced during heating of Ni bombs; NiF_2 can react with released sample oxygen compounds potentially compromising O isotopic ratios. The large surface area of the bombs can also contribute significantly to blank levels.

The development of laser fluorination techniques revolutionised oxygen isotope mass spectrometry (Sharp 1990). In this procedure, the sample is locally heated to extremely high temperatures (c. 1200 °C) by a focussed infrared laser, facilitating rapid reaction with the reaction agent e.g. F_2, BrF_5. The direct heating of the sample lowers blanks because the whole containment device is not heated.

The released oxygen is then cleaned up in a gas handling system before introduction to the mass spectrometer. A standard configuration is a dual inlet source that allows for rapid switching between a reference gas (the working standard) and the "unknown" gas, facilitating calibration to the V-SMOW reference scale. Mass spectrometry is generally carried out with a magnetic sector mass spectrometer typically at low resolution (c. 250 M/ΔM) in multiple collector configuration (^{16}O, ^{17}O, ^{18}O simultaneously collected in independent Faraday cup detectors). It is routinely possible to analyze 0.5 to 2 mg mineral and whole-rock samples with a precision in $\Delta^{17}O$ of better than ±0.03‰ (2σ) (Greenwood et al. 2017).

2.5.2 *Secondary Ion Mass Spectrometry*

Secondary ion mass spectrometry (SIMS) is based on a primary ion beam sputtering (ablating) a target mineral and analysis of the emitted secondary ions (Ireland 2014; Sangély et al. 2015). Sputtering with an energetic primary beam (of order 10–20 keV) results in ejection and ionisation of atoms and molecules from the target. The target is exclusively solid, and in particular, highly polished solid mineral species allow for the best reproducibility of isotope measurements. The sample must be coated with an electrically conductive material (C, Al, Au, etc.) so as to maintain the potential of the secondary ions being accelerated in the extraction field and passing into a double-focussing magnetic sector mass spectrometer.

For oxygen isotope analysis, a Cs^+ primary beam is typically used and bombardment with a positive ion beam, and extraction of negative ions (and electrons) causes sample charging. The charging effects can be neutralised with electrons delivered to the target either as a flood or as a targeted beam (e.g., Ávila et al. 2020; Kita et al. 2009).

For measurement of ^{18}O and ^{16}O, relatively low mass resolution is required to separate ^{17}OH from ^{18}O (M/ΔM ≈ 2000, where ΔM refers to the width of the peak at 10% peak height). This allows the slits used to define the ion beam, and in particular the source slit to be kept relatively wide allowing most of the O^- ion signal to be analysed. However, for three isotope measurement the measurement conditions are more complicated. In particular the presence of $^{16}OH^-$ adjacent to $^{17}O^-$ requires higher mass resolution (Fig. 2) because the $^{16}OH^-$ peak can be higher than the $^{17}O^-$, and particularly if hydrated species are being analysed. This requires higher mass resolution than predicted based on the nuclidic masses because of tailing of $^{16}OH^-$ under the $^{17}O^-$. To achieve this the source slit is narrowed restricting the transmission of O^- into the mass spectrometer. The first three oxygen isotope measurements were made on the small-magnet-radius Cameca ims-3f ion microscopes (McKeegan 1987), but now this type of analysis is largely carried out on large-radius ion microprobes where high precision is required (Ickert et al. 2008; Kita et al. 2010; Loiselle et al. 2019).

The detection system for oxygen isotope analysis is typically based around a multiple collector. For two isotope measurements (such as $^{18}O/^{16}O$), Faraday cups in current mode are used, where the current is measured through high ohmic resistors (10^{11}–10^{12} Ω). The small amount of material consumed in an analysis (typically ∼ 0.2 to 1 ng) limits the ion signal and so for ^{17}O an electron multiplier can be used to improve signal to noise. However, the electron multiplier is subject to gain drift (and associated dead time drift), which

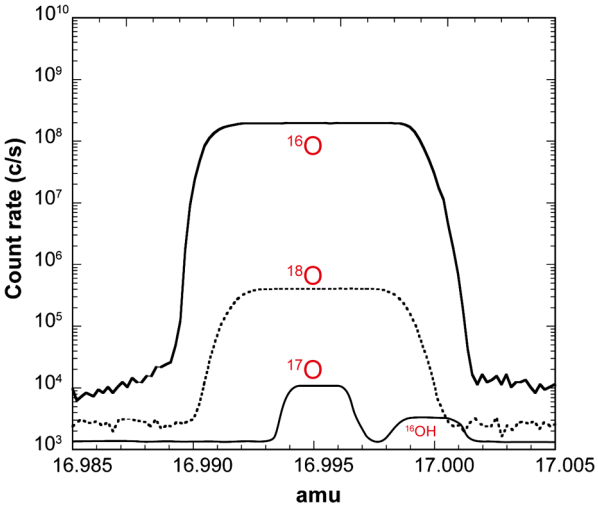

Fig. 2 Mass spectra of the oxygen isotope mass region. X-axis is determined by the $^{17}O^-$ mass position. For measurement of $^{18}O^-$ a mass resolution of ca. 2000 (M/ΔM) is required to resolve $^{18}O^-$ from the interferences of $^{17}OH^-$ and $^{16}OH_2^-$. However, to resolve $^{17}O^-$ from $^{16}OH^-$ a higher mass resolution of ca. 5000 (M/ΔM) is needed to completely resolve the hydrate contribution from $^{17}O^-$ with insignificant tailing contribution

can limit the accuracy of the measurement. Modification of a Faraday cup detection system where the feedback resistor is replaced by a capacitor has proven to be successfully to resolve subpermil variations in $\Delta^{17}O$ (Ireland et al. 2014; Loiselle et al. 2019).

2.5.3 Time-of-Flight Mass Spectrometry

An alternative to magnetic sector mass spectrometry is provided by time-of-flight mass spectrometry (TOF-MS). In this case the mass separation is enabled through the conversion of the extraction potential energy into kinetic energy. Lighter ions have higher velocity than heavier ions allowing time resolution of the individual species from a pulsed source (Wiley and McLaren 1955). The pulsed source can be an ion source (e.g. TOF-SIMS), or a laser, or any configuration that allows for rapid switching (ON/OFF) of the ion beam. The TOF spectrometer is based on having a drift length where the individual species can separate according to velocity. Detection of the signal is through an electron multiplier or a channel plate. Electron multipliers typically have very low background allowing for highly sensitive detection. Channel plates are composed of a resistive slab of material that has holes ("channels") that act as individual multipliers allowing multiple arrivals to be detected. Both detection systems are subject to dead time resulting in multiple coincident arrivals not being detected. The chief benefit of TOF-MS for space flight considerations is that the mass spectrometer is quite simple and a heavy magnetic sector mass spectrometer is not needed. On the other hand, the pulsing of the ion beam with a limited number of ions per pulse severely limits the number of ions collected and hence precision. Recently, new developments on the TOF-MS data acquisition method have been proposed to overcome the lack of high dynamic range. Kawai et al. (2018) presents a technique that combines simultaneously waveform-averaging and ion-counting data acquisition to measure target ions with a high concentration difference. The averaging mode and ion-counting mode are used simultaneously for high and low abundant ions, respectively.

For mass spectrometry on space missions, TOF-MS is a preferred method because it is relatively light and has a low energy consumption. The drift length can be straight and include electrostatic reflection, or can be configured in to a continuous flight path such as in a cyclotron.

2.5.4 Cavity Ring-Down Spectrometry

A novel technique for oxygen isotope analysis is based on the absorption of infrared radiation by water, or other O-bearing, molecules. Laser light is reflected in a cavity with a characteristic decay. If a gas is introduced, a faster decay proportional to abundance of the species occurs at relevant absorption lines. Absorption coefficients for the relevant lines have been determined to allow three isotope measurements in water and minerals (O'Keefe and Deacon 1988; Barker et al. 2011). It offers the possibility of a simple apparatus that is used in the field on Earth for triple oxygen isotope analysis. Even for saline waters, $\delta^{18}O$ measurements to the level of 0.1‰ levels have been achieved (Skrzypek and Ford 2014).

2.5.5 Accuracy and Precision

Precision relates to the level of uncertainty obtained in a given analysis. The fundamental limitation in mass spectrometry is typically taken as the number of ions available. According to Poisson counting statistics, the precision is limited to $1/\sqrt{N}$, where N is the number of counts. For an isotope ratio, it is largely determined by the numerator counts because the denominator is the major isotope. Precision can also be affected by noise in the system, for instance Johnson noise in the electrometer systems associated with Faraday cups.

Precision of oxygen isotope measurements is primarily determined by the amount of material available for analysis. This is typically a characteristic of the analytical technique where the procedure is optimised for a specific amount of material, which has been traded off with the ability to detect heterogeneity within a number of samples. For GSMS, this could be a specified amount of material such as a few mg, while for SIMS, the sample size is the amount of material sputtered during the course of a single spot, which might be as small as 1 ng for oxygen isotope analysis.

For GSMS, sample sizes are selected that optimise the precision that can be obtained through Faraday cup measurements. The signal strength can be adjusted to minimise electrometer noise and the analysis controlled to yield optimum precision and accuracy. Analytical time is not an issue. Ultimate precision at a level of 0.03‰ is attainable.

For SIMS, the spot size (and spot depth) control the amount of material in a single analysis. Precision for a given spot is typically of the order of 0.1‰ for $^{18}O/^{16}O$. For a $\Delta^{17}O$ measurement, the precision is poorer simply because of the low abundance of ^{17}O. For single spot analysis of spots of ca. 15 μm and a $^{16}O^-$ ion beam at 10^8 c/s, the ^{17}O count rate is 40000 c/s and so to get the minimum counts for 0.1‰ in ^{17}O (i.e. 10^8 counts) would take 2500 seconds. However, an analysis of this time would probably cause other changes in the ion emission, which would affect accuracy. A typical maximum analytical time for this type of SIMS analysis might be of order 1000 s, yielding a precision of order 0.3‰. Even then, this requires a stable primary ion beam as well as good stability in all other aspects of the instrument (electrical control, magnetic fields, etc.).

For TOF, the precision depends to a certain extent on the type of ionisation system, usually laser or focussed ion beam. The source controls the amount of material available as well as the ionisation. However, the main limitation for TOF spectrometers is the amount of material that can be included in a single pulse, and the time between pulses. Effectively, a TOF-MS spends most of its time waiting for the ions to arrive at the detector so that there is no interference between pulses of different species.

The *accuracy* of an analysis pertains as to how close the measurement comes to the true composition. A determination of accuracy is typically carried out by analysing reference materials, samples of known composition, and assessing reproducibility of those analyses.

It is extremely difficult to calibrate a measurement to determine absolute isotope abundances and this is generally regarded as unnecessary.

Accuracy is a particular issue for in situ techniques, where matrix composition may affect the ionisation yields and cause changes in the instrumental mass fractionation. As such, SIMS works best on well-defined matrices which have been characterised for chemistry and mineralogy (crystal structure) and for which well-matched standards and reference materials are available (Ireland 2014). SIMS cannot analyse mixtures particularly well. In some cases, atomic or molecular ion species can be used to assess the mix of two minerals and a calibration can be obtained, but in general SIMS measurements of complex matrices yield complex results.

GSMS has the ability through complete acid digestion (etc.) and release of oxygen to avoid any matrix effects. That is, for triple oxygen isotope measurements, only oxygen is ever introduced into the mass spectrometer and this can be run in reproducible conditions.

3 Terrestrial Oxygen Isotopes (Planet Earth)

Oxygen is present as a major component at Earth's surface: in silicate minerals in rocks, as free molecular oxygen in the atmosphere, and as water in the hydrosphere. These reservoirs, and their interactions, are part of the Earth system and can be characterised with oxygen isotopes. From a planetary science perspective, the detail available from the oxygen isotopic analysis of terrestrial materials is pretty much overwhelming. Furthermore, the Earth system as a whole is unique in the solar system in having surface water liquid, solid, and gas as coexisting phases. Effectively this is what makes Earth a habitable planet, and the resulting interactions in biogeochemistry are also evident.

3.1 Hydrosphere

The key processes of the water cycle are evaporation and condensation with fractionation between liquid and vapour (see Cappa et al. 2003). Water vapour that has evaporated from the surface of the ocean is enriched in ^{16}O, with $\delta^{18}O = -9.2‰$ (at 25 °C). However, this fractionation is strongly temperature dependent and ranges from +14‰ at −20 °C to +5‰ at 60 °C (Dansgaard 1964; Cappa et al. 2003). Condensation of water vapour to form precipitation enriches $^{18}O/^{16}O$ such that the composition is similar to the original seawater. The air mass carrying the water vapour becomes further enriched in the light isotope as condensation and precipitation proceed. If this is viewed as an open system, then the isotope compositions of vapour and liquid follow a trend defined by Rayleigh distillation (Dansgaard 1964). However, mixing of air masses probably result in compositions that are not strictly relatable via Rayleigh processing although the general trend of freshwater having lower $\delta^{18}O$ than seawater typically holds.

The strong temperature dependence of oxygen isotope composition of evaporating and condensing water is best viewed in terms of the change in oxygen isotope composition of water precipitation with latitude (Dansgaard 1964). At high latitudes, where the mean annual temperature can fall to below −30 °C, $\delta^{18}O$ is below −30‰ (Fig. 3). The precipitation record in ice cores allows model temperatures of sea surface temperatures to be estimated. These records can be traced back for hundreds of thousands of years into the past (Epstein et al. 1965; Johnsen et al. 1972; Siddall et al. 2003; Mayewski et al. 2004). While the ice records are restricted in time, other fossil proxies can then be used such as precipitation of silica, carbonate, and phosphate from seawater as occurs in various life forms (diatoms,

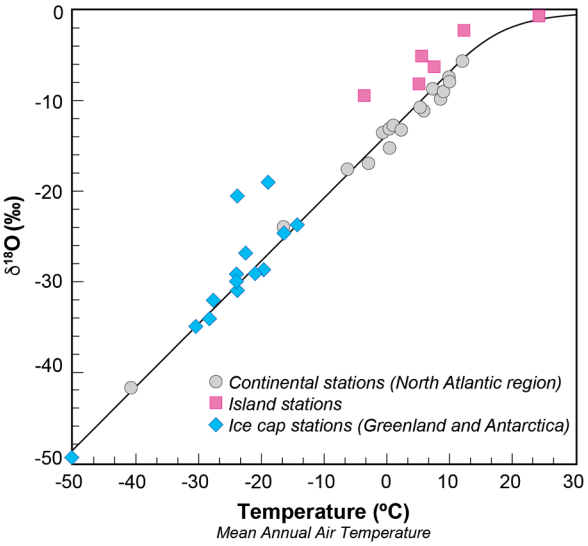

Fig. 3 Oxygen isotope compositions of meteoric waters are closely related to the annual mean temperature of the site of precipitation indicating a temperature related kinetic fractionation. This same effect can be used to model global sea water temperatures from ice cores. After Dansgaard (1964)

foraminifera, and conodonts respectively). Oxygen isotope analysis of fossil materials can then be used to estimate surface temperatures back through the Phanerozoic, provided the system remains closed to later re-equilibration with for example ground waters.

3.2 Atmosphere

Earth's oxygen-rich atmosphere is believed to have formed from progressive addition of oxygen through the Archean as a waste product of photosynthesising cyanobacteria (Holland 2006). Originally Earth appears to have had a reducing atmosphere, potentially similar to the N_2-CH_4 atmosphere found on Titan. Oxygen was initially taken up in oxidation of Fe^{2+} in the oceans with precipitation of magnetite forming Banded Iron Formations (Cloud 1973). In the Great Oxidation Event near the beginning of the Proterozoic, free oxygen became ultimately stable in the atmosphere, and led to stratospheric production of ozone (O_3) and concomitant shielding of Earth's surface from harmful UV radiation. This is reflected in the end of non-mass-dependent S isotope fractionations from SO_2 photodissociation that can only occur and be preserved in a low oxygen atmosphere (Farquhar et al. 2000; Pavlov and Kasting 2002). Detrital uraninite and pyrite, which are susceptible to weathering breakdown in oxidising conditions, disappeared from sedimentary sequences (see Johnson et al. 2014), and, deposition of large-scale Banded Iron Formations ceased (Cloud 1973).

Molecular oxygen (O_2) and stratospheric ozone (O_3) have distinct oxygen isotope compositions (Fig. 4) and the isotopic shift does not obey a mass dependent fractionation law (Heidenreich and Thiemens 1986; Thiemens 1999). Ozone oxygen isotope compositions can be enriched in $\delta^{17}O$ and $\delta^{18}O$ by over 10% (Schueler et al. 1990). It appears that this enrichment is related to stabilisation of asymmetric molecules, which favours those molecules with ^{17}O and ^{18}O. The fractionation lies on a line of slope 1 on the oxygen three isotope diagram.

3.3 Igneous Rocks

Oxygen is a major constituent in all of the principal mantle mineral phases: olivine $[(Mg, Fe)_2SiO_4]$, clinopyroxene $[Ca(Mg, Fe)Si_2O_6]$, orthopyroxene $[(Mg, Fe)SiO_3]$, and

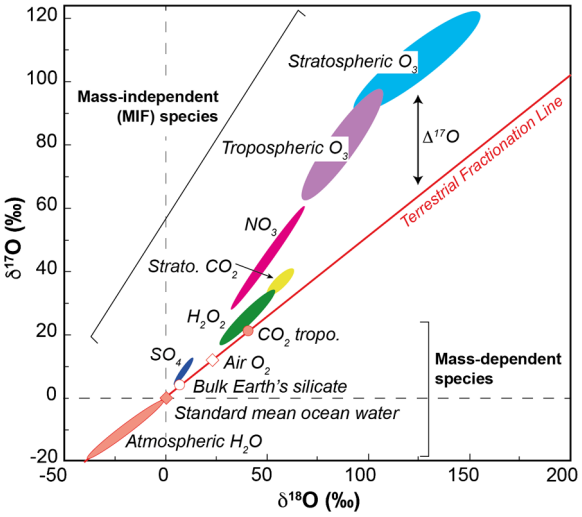

Fig. 4 Oxygen isotopic compositions in Earth's hydrosphere and atmosphere. Kinetic fractionation of oxygen isotopes follows mass dependent fractionation signified as the Terrestrial Fractionation Line. This includes Earth's oceans, surface level Air O_2 and bulk silicate compositions, and the large temperature related fractionation of atmospheric H_2O, which becomes isotopically light towards the poles. Mass independent fractionation occurs in the Earth's stratosphere and troposphere and is related to UV photolysis breaking oxygen molecules to form ozone. More energy states exist for asymmetric molecules leading to a build up of ^{17}O, ^{18}O-rich ozone. Equilibration of ozone with other species (CO_2, NO_2, SO_2) leads to MIF enrichments in these species as well. (Adapted from Thiemens 1999)

spinel $[(Mg, Fe)(Al, Cr)_2O_4]$. As such it constitutes around 50% of Earth's mantle. Earth's crust is a consequence of partial melting in the mantle and the preferential partitioning of incompatible elements into the melt. The Earth's crust has minerals with higher SiO_2 and alkali metals (Na, K) (quartz, feldspars) and lower Mg and Fe (both retained as compatible elements in the mantle). Oxygen isotopes also reflect this trend with quartz and feldspars having heavier oxygen (higher $\delta^{18}O$) leading to a trend of increasing $\delta^{18}O$ from ultramafic mantle rocks through basalts and gabbros and then granites and pegmatites (Fig. 5). In terms of oxygen isotopes, mantle rocks have $\delta^{18}O$ values in a narrow range from +5 to +6.5‰ relative to the SMOW reference, with granites and pegmatites ranging up to +13‰. The total range of $\delta^{18}O$ in igneous rocks at ca. 8‰ is not especially large but sufficient analytical resolution is available to distinguish the rocks according to igneous fractionation of specific minerals and the resultant bulk rocks. In igneous rocks not affected by atmospheric components, the isotopic mass fractionation appears to be entirely mass dependent and no $\Delta^{17}O$ effects are evident.

Oxygen isotopes are observed to partition into different phases in different proportions. The fractionations between coexisting minerals are consistent and can be shown to be temperature dependent. As such, a measurement of suitable phases can be used as a geothermometer (Taylor and Epstein 1962a,b).

3.4 Sedimentary Rocks

Clastic sedimentary rocks reflect the compositions of the particles that comprise the bulk rock. As such, sedimentary rocks can show heterogeneity reflecting differing proportions

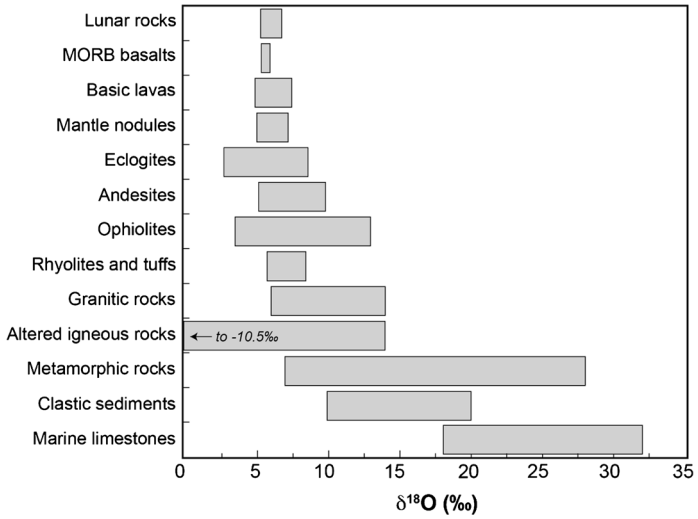

Fig. 5 Range of mass dependent fractionations (expressed as $\delta^{18}O$) in terrestrial reservoirs. Igneous rocks typically show a narrow range of compositions. Alteration of igneous rocks by meteoric water leads to isotopically light compositions. Biogeochemical reactions can lead to isotopically heavy fossils which are deposited as limestones. (Adapted from Hoefs 2009)

of differing source materials. Those source materials can be derived directly from igneous rocks, or can have more complex histories such as from metamorphic rocks. A characteristic of sedimentary rocks is their grain size, porosity, and permeability. The spacing between grains often allows the introduction of meteoric and/or marine water and so sedimentary rocks can be affected by low temperature reactions involving water and replacement of fine grained minerals.

A particular issue for sedimentary rocks is the formation of clay minerals. Notwithstanding the composition of the water reacting with silicate minerals to form clays, oxygen isotope fractionation factors at Earth surface temperatures for minerals such as montmorillonite and kaolinite are quite large at around $+27‰$ in terms of $\delta^{18}O$ (Savin and Epstein 1970).

Biological activity in the oceans can also fix oxygen in to a variety of phases such as silica, carbonates, and phosphates. Some of the species can reflect a near equilibrium with ocean water while others show variable compositions and systematic biases (i.e., kinetically induced MDF). As such, sediments composed of diatoms [SiO_2], coccoliths and foraminifera [$CaCO_3$], and conodont elements [$Ca_5(PO_4)_3(OH)$] can all reflect the changing oxygen isotopic composition of ocean water, which is typically responding to ice volume on Earth (Shackleton and Opdyke 1973).

3.5 Metamorphic Rocks

Metamorphic rocks can be mixtures of components from igneous, sedimentary, or metamorphic sources and inherit a variety of oxygen isotope signatures. This can include the extreme compositions of clay minerals and meteoric water. In a fully equilibrated metamorphic rock, the crystallisation of a new assemblage leads to a new fractionation of oxygen isotopes between the stable minerals. Equilibration temperatures in metamorphic rocks are lower and thence larger oxygen isotope fractionations are evident between minerals (Taylor and Epstein 1962b). These can also be used as geothermometers (Garlick and Epstein 1967).

However, the tendency of metamorphic systems to not be fully equilibrated, as well as late stage changes in fluid compositions, can cause perturbations.

3.6 The Earth System

Earth is a dynamic planet with 4.5 billion years of history. A lot of the events that led to the growth of Earth are probably the same as formed the other terrestrial planets. Earth's overall oxygen isotope composition was inherited from the planetesimals that contributed to it followed by efficient mixing and equilibration.

Earth is unique in the solar system in having solid, liquid, and gaseous water present. As such, water-rock interactions are important in geological processes. The formation of oceanic crust is followed by hydration reactions (serpentinisation) and subduction at convergent boundaries. Subduction is associated with dehydration, and then contribution to arc volcanoes, which release volatiles into the atmosphere, with some water likely recycled back into the mantle. The presence of water leads to a change in the physical nature of the mantle making it more plastic and amenable to convective overturn. This recycling has carried on over aeons and appears to be another unique aspect of Earth.

4 Extraterrestrial Oxygen

Oxygen is the most common element in the stony meteorites that come to Earth. Robert N. Clayton pioneered the characterisation of oxygen isotopes in extraterrestrial materials and his analytical prowess, thoroughness, and eye for detail offered insights into cosmochemical processes that still colour the field to this day (Clayton 1993, 2003). The discovery of three-oxygen isotope anomalies in meteorite inclusions was profound (Clayton et al. 1973). This completely changed our previous view of the hot homogeneous solar nebula (e.g. Grossman 1972). Isotopic anomalies were found in bulk meteorites, allowing oxygen isotopic compositions to become an essential tool in identifying clans of meteorites of common provenance, and effectively leading to the characterisation of meteorite parent bodies (Clayton et al. 1976).

While geochemical isotopic variations are dominated by mass dependent effects, cosmochemical oxygen isotope systematics in extraterrestrial materials are dominated by variability in ^{16}O. This was originally described as a mixing line in Allende inclusions between a ^{16}O-rich component ($\delta^{17}O \approx \delta^{18}O \approx -40‰$; $\Delta^{17}O \approx -20$) and a fractionated component close to the terrestrial fractionation line, yielding a slope of approximately 0.94. This line is commonly referred to as CCAM (for Carbonaceous Chondrite Anhydrous Mixing; Clayton et al. 1977). Young and Russell (1998) subsequently defined a pure ^{16}O mixing line (slope 1) that includes the ^{16}O-enriched composition of the CAIs, as well as the compositions of the ordinary chondrites. Another representation of ^{16}O mixing in the early solar system is the PCM line (Primitive Chondrules Mineral line; Ushikubo et al. 2012), which is based on the dispersion observed in chondrules from the Acfer 094 carbonaceous chondrite.

4.1 Chondrite Meteorites and Their Components

4.1.1 Bulk Chondrites

Chondrites are regarded as the building blocks of the terrestrial planets. They are essentially cosmic breccias and are regarded as primitive in that they have never been melted and preserve materials of different provenance from the early solar system. A range of materials

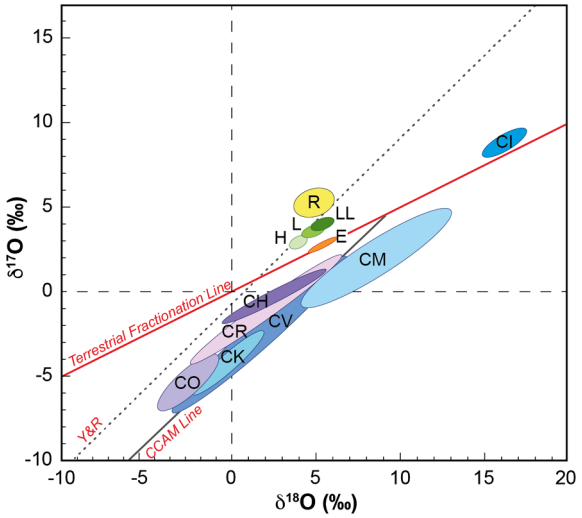

Fig. 6 Oxygen isotope compositions of chondrites are characteristic of different groups and are used for classification. Ordinary chondrites (H, L, LL) are enriched in $\delta^{17}O$, $\delta^{18}O$ with a progressive increase in $\Delta^{17}O$ from H to L to LL. R chondrites have the highest $\Delta^{17}O$ of any of the chondrite groups, while Enstatite chondrites are not resolved from terrestrial. Carbonaceous chondrite compositions appear to be derived from a mixture of mass dependently fractionated oxygen (e.g. CI chondrites), and a ^{16}O-rich reservoir located on the CCAM mixing line. Reference lines shown are the terrestrial mass fractionation line, CCAM (Carbonaceous Chondrite Anhydrous Mineral) mixing line with slope of 0.95 (Clayton et al. 1977), and the ^{16}O fractionation line with slope = 1 (Young and Russell 1998)

exists in these breccias from high temperature inclusions through to the low temperature matrix, which has commonly experienced interaction with water. Chondrites are the most common type of meteorite falls, with Ordinary (O) chondrites by far the most common of these.

Ordinary chondrites have been split in to H, L, and LL groups based on the Fe metal abundance and compositions of the ferromagnesian silicates (see Van Schmus and Wood 1967). H chondrites have the highest overall Fe abundance, coupled with high Fe metal abundance and thence the lowest Fe substitution (i.e., as Fe^{2+}) in to ferromagnesian silicates. The L chondrites have lower total Fe abundances, lower Fe metal contents and higher Fe substitution into ferromagnesian silicates. The LL group are characterised by having the lowest total iron, low metal content, but the highest iron substitution in ferromagnesian silicates. Van Schmus and Wood (1967) used the fayalite content of olivine to distinguish the three groups with H (16–20% Fa), L (21–26%Fa) and LL (27–31% Fa).

The other chondrite types are the enstatite (E) chondrites, carbonaceous (C) chondrites, Rumuruti (R) chondrites, and Kakangari (K) chondrites. The enstatite chondrites are noteworthy in that they are extremely reduced (Van Schmus and Wood 1967); all Fe is present as metal and oxygen is in sufficient deficit that some metallic silicon is present in the Fe metal, and Ca is typically present in oldhamite (CaS). Carbonaceous chondrites have a large fraction of matrix material with a high volatile component (organics, water) and typically mostly oxidised Fe. Rumuruti (Bischoff et al. 2011) and Kakangari (Weisberg et al. 1996) chondrites are quite rare and have similarities to carbonaceous chondrites in terms of matrix abundance, but also have similarities to other chondrite types.

Oxygen isotope compositions of the chondrite families are presented in Fig. 6. The O chondrites show a progressive shift in terms of increasing $\delta^{17}O$ and $\delta^{18}O$ from H to L to LL,

and hence increasing $\Delta^{17}O$ (Clayton et al. 1983, 1991). The changes are relatively small, but distinct. In terms of $\Delta^{17}O$, H chondrites are $+0.7‰$ with L chondrites at around $+1.0‰$, and LL chondrites $+1.2‰$. The R chondrites continue this trend with even higher $\Delta^{17}O$ of $+2.0‰$. E chondrites have compositions that appear to be coincident with the TFL (i.e. $\Delta^{17}O$ of $0‰$; Clayton et al. 1984). The Kakangari chondrites have $\Delta^{17}O$ of -1.2 to $-1.8‰$, similar to the CR chondrites (Weisberg et al. 1996).

The carbonaceous chondrites show a wide range in oxygen isotopic compositions for the various subtypes. CI chondrites, have compositions of non-volatile elements close to solar abundances (Wang et al. 2019), but have strongly mass fractionated oxygen ($\delta^{18}O \approx +16‰$) and lie close to the TFL (Clayton and Mayeda 1999). CM chondrites also contain mass fractionated oxygen (up to $+12‰$), but lie significantly below the TFL indicating ^{16}O enrichment. CV chondrites lie close to the ^{16}O-mixing line with ranging down to $\delta^{17}O \approx \delta^{18}O$ of $-4‰$, with similar characteristics for the other carbonaceous chondrite groups. The bulk CI and CM carbonaceous chondrites appear to have been affected by alteration by water on their parent bodies.

4.1.2 Chondrules and CAIs

Chondrites contain high temperature inclusions. The most notable of these are chondrules, whose name provides the name of the rock type, chondrites. Chondrules are dominantly composed of ferromagnesian minerals (olivine, pyroxene), plus mesostasis (glass), some opaque Fe oxides (ilmenite, magnetite) and less commonly Fe metal and sulphide (Connolly and Jones 2016). The oxygen isotope compositions of chondrules in O chondrites lie on a trend of slope ~0.8 on three isotope plots (Bridges et al. 1999).

Chondrules in carbonaceous chondrites show a wider variety of ^{16}O enrichment compared to OC and EC. Populations of chondrules with ^{16}O-rich compositions are common. Clayton et al. (1983) found that chondrules in Allende ranged from $\delta^{18}O$ of $+4$ to $-3‰$. Ushikubo et al. (2012) reported two populations with $\delta^{17}O \approx \delta^{18}O \approx -4‰$ and $-10‰$ from the primitive Acfer 094 carbonaceous chondrite. However, these enrichments are small compared to highly forsteritic relic cores in chondrules, which can have $\delta^{17}O \approx \delta^{18}O \approx -50‰$ (Yurimoto and Wasson 2002). The most ^{16}O-enriched chondrule, found in the Acfer 214 carbonaceous chondrite, has $\delta^{17}O \approx \delta^{18}O \approx -80‰$ (Kobayashi et al. 2003).

Calcium, aluminium-rich inclusions (CAI) are the oldest materials formed in the solar system, and were the first objects to be found with large isotopic anomalies. Clayton et al. (1973) found Allende CV3 CAIs to have ^{16}O-rich compositions (i.e. $\delta^{17}O \approx \delta^{18}O \approx -40‰$; $\Delta^{17}O \approx -20‰$). The enrichment was observed to be mineral dependent with the most ^{16}O-enriched compositions found in pyroxene and spinel while melilite is closer to the TFL (Fig. 7). This has been related to thermal processing in the solar nebula (Ryerson and McKeegan 1994), or to parent body processes including aqueous alteration (e.g. Krot et al. 2019).

The ^{16}O-rich composition was initially interpreted as a nucleosynthetic component that came in to the solar system during the early stages, and potentially associated with other supernova debris products such as ^{26}Al (Clayton et al. 1977). However, the oxygen isotope anomalies are different from isotopic anomalies in other elements in that the variation is in the most abundant isotope and the range of variability is comparatively extremely large. Refractory minerals and inclusions from Murchison CM2 meteorite have been shown to have even larger anomalies, with up to $60‰$ enhancements in ^{16}O (Fahey et al. 1987; Ireland et al. 1992; Liu et al. 2009; Kööp et al. 2016).

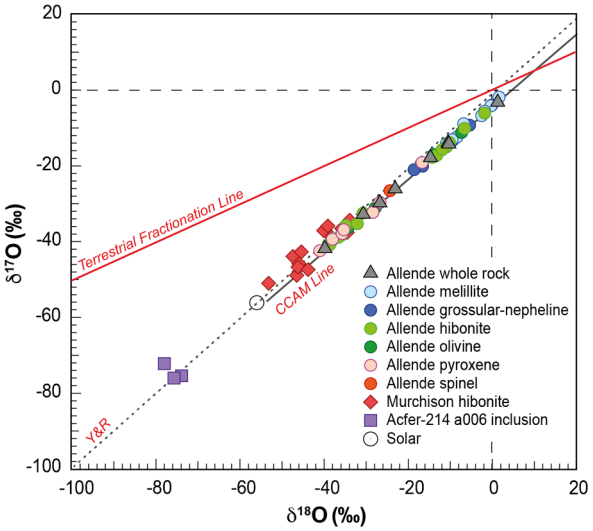

Fig. 7 Oxygen isotope compositions of CAIs are mineralogically controlled in Allende inclusions. Melilite and secondary minerals such as grossular and nepheline are ^{16}O-poor compared to olivine, pyroxene and spinel (Clayton et al. 1977). Whole rock (WR) measurements are also shown; other data are from density separates with dominant mineral indicated. The Allende mineral separates define CCAM, the Carbonaceous Chondrite Anhydrous Mixing line. Murchison hibonite compositions extend to an even more ^{16}O enriched compositions than Allende inclusions (Liu et al. 2009) and approach the solar oxygen isotope composition inferred from solar wind measurement (McKeegan et al. 2011). Also shown is the extreme ^{16}O enrichment measured thus far, that being in glass from the a006 inclusion in the Acfer 214 carbonaceous chondrite (Kobayashi et al. 2003). Terrestrial Fractionation Line shown, as well as a slope 1 reference line passing through the solar composition (broken line)

4.1.3 Mineralogical Controls on Oxygen Isotopic Compositions in Ordinary Chondrites

Bridges et al. (1995, 1999) used three isotope, laser fluorination analyses of mineral separates to show that there is a mineralogical control on the oxygen isotopic compositions of chondrules and clasts in ordinary chondrites. Silica polymorphs (notably cristobalite and tridymite), feldspar and feldspathic-composition glass all have relatively heavy δ^{18}O and δ^{17}O compared to olivines and pyroxenes (Fig. 8). The most ^{16}O-poor composition identified was $\delta^{18}O = +13‰$ and $\delta^{17}O = +9.5‰$, $\Delta^{17}O + 3.0‰$. Furthermore, both laser fluorination on mineral separates and subsequent SHRIMP analyses have shown that the largest isotopic differences between the co-existing ferromagnesian and feldspathic/silica phases have been preserved in the least equilibrated ordinary chondrites e.g. Semarkona, Krymka and Adrar 003 (Bridges et al. 1999; Bridges and Ireland 2015). Other ion probe studies confirm that olivines in ordinary chondrites have relatively ^{16}O-rich compositions, falling closer to the terrestrial fractionation line (e.g. Kita et al. 2010; Saxton et al. 2010). In order to explain this mineralogically controlled isotopic fractionation, Bridges et al. (1999) proposed that the diffusion of ^{16}O-poor water through the OC parent bodies would lead to the isotopic patterns observed. This is due to the propensity for framework silicates and glasses to allow relatively rapid exchange with a fluid. For instance, a high degree of isotopic equilibration can be attained rapidly for feldspar—H_2O exchange e.g. less than 100 years for a 10 mm grain of albite at 400 °C (Giletti et al. 1978). Silica polymorphs and feldspathic glass have

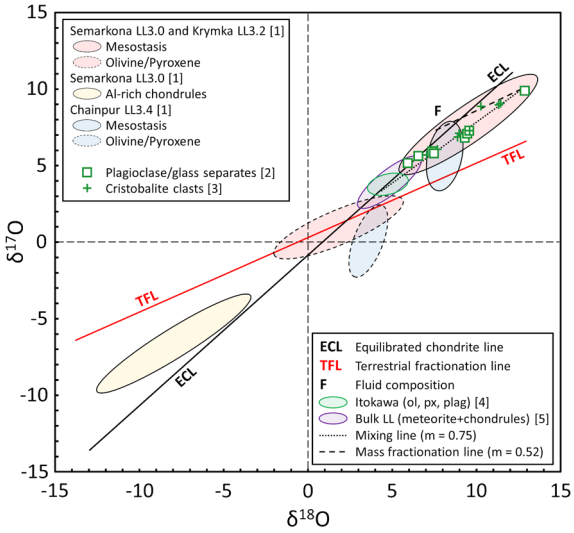

Fig. 8 Oxygen 3-isotope diagram of fluid-solid exchange in ordinary chondrites. Data from [1] Bridges and Ireland (2015); [2] Bridges et al. (1999); [3] Bridges et al. (1995); [4] Nakashima et al. (2013); [5] Clayton et al. (1991). The most highly thermally unequilibrated ordinary chondrites preserve a mineral specific oxygen isotopic fractionation and mass balance. Framework silicates and glass are ^{16}O-poor, whereas olivine, pyroxene are more ^{16}O-rich relative to bulk chondrule and clast isotopic compositions. This is the result of ^{16}O-poor fluid-^{16}O-rich solid exchange processes at low temperatures. We envisage the hydrous fluid reservoir originating on a slope 1.0 line, with mass dependent exchange between that and ^{16}O-rich solids

similar exchange properties. In contrast, gas-solid equilibration times for forsterite and low Ca pyroxene are many orders of magnitude longer.

Magnetite grains in Semarkona LL3.0 analysed by SIMS showed Δ^{17}O of up to +5‰, consistent with the presence of an ^{16}O-poor parent body fluid from which the magnetite formed by oxidation of metal (Choi et al. 1998). These mineralogical-isotopic studies highlight the importance of fluid process on the chondrite parent bodies in setting the oxygen isotopic compositions of chondrules and clasts. There is a large body of independent mineralogical evidence for the significance of fluid-mineral reactions in the OC parent bodes, including corroded chondrule mesostasis (Grossman et al. 2000), smectite clays and magnetite in chondrite matrix e.g. (Alexander et al. 1989; Brearley and Jones 1998; Hutchison et al. 1987). The oxygen isotopic data that show the greatest mineral specific fractionations, preserved in the least equilibrated ordinary chondrites, suggest that the OC isotopic mixing lines and associated aqueous activity predate thermal metamorphism and equilibration on the parent bodies.

The importance of low temperature fluid isotopic exchange processes on oxygen isotopes has been recognized for the carbonaceous chondrites as well, where the large extent of fluid activity—compared to the ordinary chondrites—has led to some minerals being partially equilibrated, leading to a slope 0.94 line on δ^{17}O *v.* δ^{18}O plots (Krot et al. 2019). This is analogous to the slope 0.8 line in OC chondrules and clasts (Bridges et al. 1995, 1999). However, the added complexity of carbonaceous chondrites, with abundant CAIs and highly ^{16}O-rich components, described in the previous section, means that the relatively simple mixing lines preserved in the OCs are not always as easily defined.

We discuss the origin and isotopic composition of the associated water further in Sect. 7.3.2.

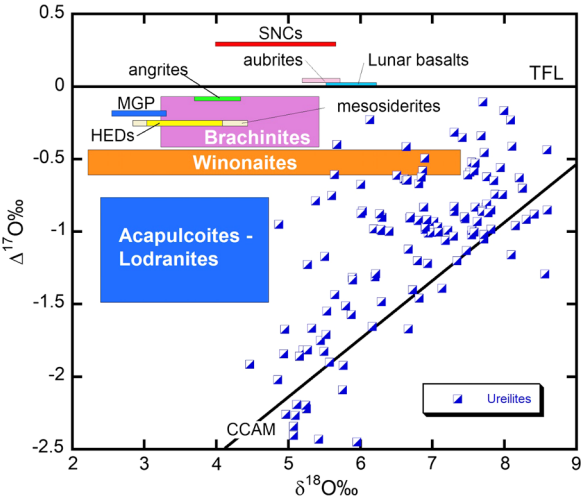

Fig. 9 Oxygen isotopic composition of planetary and asteroidal achondrites (modified after Greenwood et al. 2017). Coloured boxes: $\pm 2\sigma$ variation of group mean values (see Greenwood et al. 2012 for further details). Ureilite data: Clayton and Mayeda (1996), Bischoff et al. (2010), Rumble et al. (2010), Horstmann et al. (2012), Bischoff et al. (2014), Greenwood et al. (2017); SNC data: Franchi et al. (1999); Lunar basalt data: Greenwood et al. (2018); Aubrite data: Barrat et al. (2016); Acapulcoite-Lodranite clan: Greenwood et al. (2012); Brachinite data: Greenwood et al. (2012); Winonaite data: Greenwood et al. (2012); Abbreviations: MGP: main group pallasites, HEDs: Howardite-Eucrite-Diogenite suite, TFL: Terrestrial Fractionation Line, CCAM: Carbonaceous Chondrite Anhydrous Minerals line (Clayton et al. 1977; Clayton and Mayeda 1999)

4.2 Achondrites

Achondrites are meteorites that experienced variable degrees of high temperature processing, such that they lack primary "chondritic" components, including chondrules, CAIs, amoeboid olivine aggregates (AOAs) and matrix (Krot et al. 2014; Scott et al. 2015). Achondrites are derived both from asteroids and larger planetary bodies (specifically Mars and the Moon) and accordingly we refer to the former as asteroidal achondrites and the latter as planetary achondrites. The oxygen isotope composition of planetary and asteroidal achondrites is shown in Fig. 9.

4.2.1 Asteroidal Achondrites

Asteroidal achondrites tend to be divided into two broad subtypes: (i) primitive and (ii) differentiated achondrites (Weisberg et al. 2006; Krot et al. 2014; Scott et al. 2015). Primitive achondrites have near-chondritic bulk compositions, but non-chondritic textures and are thought to represent the products of low degrees of partial melting of a chondritic precursor material (Weisberg et al. 2006; Krot et al. 2014). Differentiated achondrites are compositionally more evolved and have well-developed igneous textures (Mittlefehldt et al. 1998; Krot et al. 2014). Differentiated achondrites are most likely derived from asteroids that experienced moderate to high degrees of partial melting (Krot et al. 2014; Scott et al. 2015).

Since primitive and differentiated achondrites show a complete gradation in terms of the extent to which they underwent melting and mobilization, there is disagreement about which individual groups should be assigned to each of these broad categories (Greenwood

et al. 2017). Based on their heterogeneous oxygen isotopic compositions (Fig. 9), Greenwood et al. (2017) suggested that the acapulcoite-lodranite clan, winonaites and silicate-bearing IAB and IIICD irons, brachinites and ureilites are all best considered to be primitive achondrites. In contrast, due to their relatively homogeneous oxygen isotopic compositions (Fig. 9), Greenwood et al. (2017) included the angrites, aubrites, howardite-eucrite-diogenite suite (HEDs), mesosiderites and pallasites as differentiated achondrites.

In addition to achondrites that fit within the well-defined groups, an increasing number of both primitive and differentiated "ungrouped" achondrites are being identified. In a similar way to the ungrouped irons (Chabot and Haack 2006), ungrouped achondrites are of potential significance in that they increase the number of asteroidal bodies from which we have samples to investigate in the laboratory. Thus, Greenwood et al. (2020) estimated that in addition to the 15 to 17 parent bodies from which the primitive and differentiated "grouped" achondrites are derived, ungrouped achondrites may sample a further 28 to 34 parent bodies, significantly increasing the number of "igneous" asteroids from which we have samples.

Meteorites are linked to possible source asteroids through spectral similarities in the visible and near-infrared (Burbine 2016). However, in most cases it is not possible to make fully diagnostic meteorite-asteroid linkages, as most asteroids do not have sufficiently distinct reflectance spectra that would make any potential fit unambiguous (Burbine 2016). A further complication is that in most cases asteroid surfaces are likely affected by space weathering processes (Hapke 2001; Burbine 2016), which could cause a mismatch between the laboratory-derived and asteroidal spectra. Consequently, asteroids are generally linked to meteorites on the basis of taxonomic classes (DeMeo et al. 2009), rather than at the level of unique asteroidal bodies.

The HED-4 Vesta link appears to be a clear exception to the problem of identifying the asteroidal source of a particular group of meteorites. McCord et al. (1970) were the first to measure the reflectance spectra of 4 Vesta and match it to the eucrites. Since then there has been a general acceptance that the HED suite is derived from the Vesta family, which appears to be collisionally linked to asteroid 4 Vesta (McSween et al. 2011). The mesosiderites have also been linked to 4 Vesta (Greenwood et al. 2006, 2015), most recently by Haba et al. (2019), although no conclusive evidence to support this relationship was obtained by the NASA Dawn spacecraft (Peplowski et al. 2013).

4.2.2 Martian Meteorites and Mars Igneous Rocks

As of November 2019 there are 139 known martian meteorite samples (Meteoritical Bulletin database) of which about half are paired, i.e., there are about 65 distinct martian meteorites. The oxygen isotope composition for 98 individual martian meteorites is shown in Fig. 10a.

McSween (1984) first proposed that the shergottite-nakhlite-chassignite (SNC) clan of meteorites were derived from Mars. Prior to this, the energy of any potential impact on Mars had been deemed to be too small to allow ejection of martian material from the surface of Mars into an orbit that could bring them to Earth. The SNC meteorites are believed to come from Mars for three main reasons: geologically young ages, retention of trapped gases with composition similar to martian atmosphere, and high D/H ratios. Of these, the most decisive evidence was trapped noble gases from the martian atmosphere, as determined by the Viking spacecraft in 1976 (Pepin 1985).

The majority of the martian meteorites can also be further subdivided into groups, which include the shergottites (the most abundant, and in turn having basaltic, olivine-phyric and lherzolitic petrographic types), nakhlites (olivine clinopyroxenites), and the chassignites (dunites) (Fig. 10a). In addition, there is the ALH 84001 orthopyroxenite. A recently discovered meteorite NWA 7034 and its pairs including NWA 8114 form a new type of martian

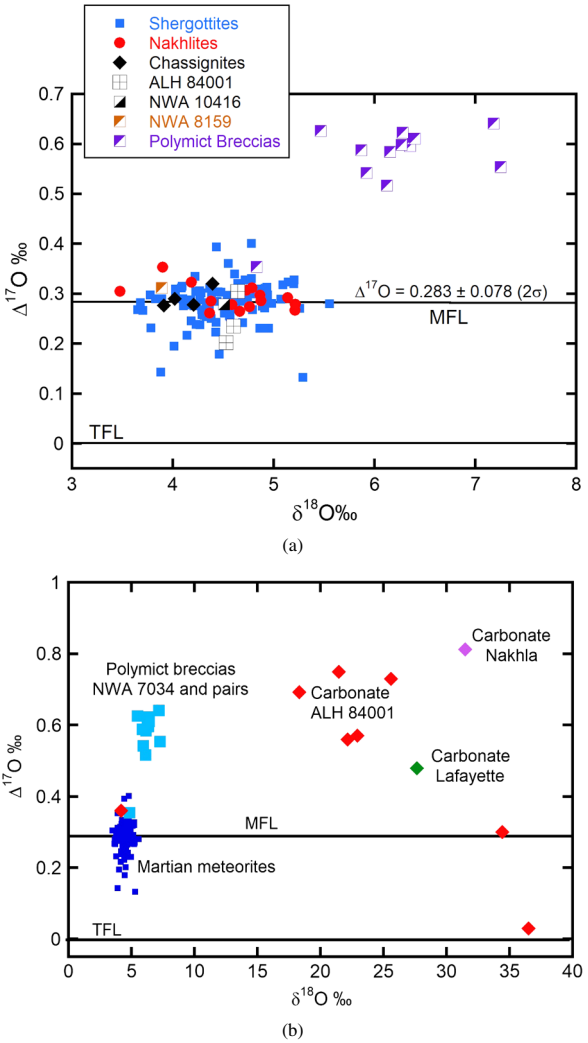

Fig. 10 (**a**) Oxygen isotopic composition of martian meteorites. MFL = Mars Fractionation Line; TFL = Terrestrial Fractionation Line. The plot is based on a compilation of data for 98 martian meteorites. Since $\Delta^{17}O$ for the original analyses was calculated using a variety of slope factors all the data in the plot has been recalculated using $\Delta^{17}O = \delta^{17}O - 0.525\delta^{18}O$. The MFL value of $\Delta^{17}O = 0.283 \pm 0.078‰$ (2σ) is based on the average of all the analyses plotted in (**a**) with the exception of the polymict breccias (NWA 7034 and pairs). This value is within error of that obtained by Franchi et al. (1999). Date Sources: Clayton and Mayeda (1996), Franchi et al. (1999), Rumble and Irving (2009), Basu Sarbadhikari et al. (2009), Irving et al. (2010), Filiberto et al. (2012), Agee et al. (2013), Llorca et al. (2013), Schwenzer et al. (2013), Wittmann et al. (2015), Ali et al. (2016), Meteoritical Bulletin Database. (**b**) The oxygen isotopic composition of martian meteorites shown in relation to the composition of carbonate extracted from ALH 84001, Nakhla and Lafayette (Farquhar et al. 1998; Farquhar and Thiemens 2000; Shaheen et al. 2015). Data sources for martian samples as per references in caption to (**a**). MFL = Mars Fractionation Line; TFL = Terrestrial Fractionation Line

meteorite, generally referred to as either a basaltic or polymict breccia (Fig. 10a) (Agee et al. 2013; Humayun et al. 2013; MacArthur et al. 2019).

In addition to petrographic-based classifications, the shergottites are subdivided geochemically in terms of their bulk REE abundances into Slightly, Moderately and Heavily Depleted groups, revealing a range of mantle source compositions for the associated primary basaltic melts (Bridges and Warren 2006). The major element compositions of the shergottites have frequently been used to represent a major compositional type representative of the martian crust e.g. McLennan (2003). The martian meteorites provide an essential comparison for igneous rocks identified by Mars landing missions. The Adirondack class basalts from Gusev Crater analysed by MER Spirit have a similar high Fe and low alkali composition (McSween et al. 2008). In contrast Gale Crater igneous float rocks are more alkali-rich than the shergottites and include feldspathic cumulates and trachybasalts (Cousin et al. 2017; Edwards et al. 2017; Sautter et al. 2015).

Martian meteorites cover a range of ages from nearly 4.5 Ga down to 130 Ma, although most ages fall within the Amazonian era between 150 and 650 Ma (Nyquist et al. 2001). However, recently, late-Amazonian <0.5 Ga (Darling et al. 2016; Moser et al. 2013) and early Amazonian >2.0 Ga (Herd et al. 2017; Lapen et al. 2017) ages for shergottite meteorites and the martian breccia NWA 7034 and pairs, have been identified. Zircons identified in martian breccia samples have been dated at 4.43–4.35 Gyr (Humayun et al. 2013; McCubbin et al. 2016) and a mineral isochron yielded a 4.39 Ga Sm-Nd age (Nyquist et al. 2016).

The $\delta^{18}O$ of martian meteorites falls in the range 3.4 to 5.7‰ (Fig. 10a) and is similar to that found in terrestrial basalts and gabbros. However, the triple oxygen isotope compositions of martian meteorites, excluding polymict breccias (see below), is highly distinctive with an average $\Delta^{17}O$ value of 0.283 ± 0.078‰ (2σ) (Fig. 10a). This value is within error of that obtained by Franchi et al. (1999). The relatively homogeneous oxygen isotope composition displayed by martian meteorites is consist with their derivation from a parent body that underwent large-scale melting and mixing. This evidence is consistent with the formation of a magma ocean on Mars early in its history (Zeff and Williams 2019).

A group of meteorites appear to be regolith breccias from Mars (Agee et al. 2013; Humayun et al. 2013). MacArthur et al. (2019) reported that the NWA 8114 martian breccia (paired with NWA 7034) is composed of mineral clasts, including pyroxenes, plagioclase and alkali feldspar, with minor volumes of iron oxides, and chlorapatite, as well as feldspar veins and aureoles. Pyroxene exsolution textures and feldspar cryptoperthite textures reveal slow cooling and a record of plutonic events, prior to the impact-related melting processes. An approximate ^{40}Ar-^{39}Ar maximum age of 1.13–1.25 Ga was found on an individual, separated, augite clast. Together with HRTEM (high-resolution transmission electron microscopy) evidence for oxidative breakdown of the pyroxene, this suggests the regolith within which shock melting occurred was an oxidizing, possibly water-rich environment.

These meteorites are also distinctive in having ferromagnesian minerals with $\Delta^{17}O$ of +0.30‰ but with bulk $\Delta^{17}O$ values of up +0.65‰ (Fig. 10a) (Ziegler et al. 2013). The oxygen isotope ratio of bulk martian breccia water shows it is not terrestrial contamination, with $\Delta^{17}O$ above the terrestrial fractionation line (Agee et al. 2013).

One of the main topics of research into martian meteorites is the presence of secondary mineral assemblages in the nakhlites and ALH 84001. As mentioned above, martian breccias also show isotopic and mineralogical signs of consolidation within a water-rich regolith environment. The 10 nakhlites contain variable amounts of a unique Fe-rich carbonate, ferric saponite, ferric serpentine and salts assemblage in veins within olivine and the mesostasis e.g. (Bridges et al. 2019; Hicks et al. 2014). Their truncation in places by fusion crust has established their martian origin (Gooding et al. 1991). A K-Ar age suggest formation at ages of $\leq$ 670 Ma (Swindle et al. 2010). Karlsson et al. (1992) and Farquhar and Thiemens (2000)

demonstrated that the nakhlite secondary assemblage minerals have $\Delta^{17}O$ of +0.32‰ but they are not in mass-dependent equilibrium with the silicate minerals. Thus, they record a valuable record of atmosphere-crust interaction. The $\delta^{18}O$ of the carbonate in Nakhla and Lafayette is notably high being 31.5 and 27.6‰ respectively (Fig. 10b) (Farquhar and Thiemens 2000). The $\Delta^{17}O$ of carbonates in martian meteorites is significantly elevated with respect to bulk rock values of the igneous martian meteorites, but overlaps the values measured in the basaltic breccias (Fig. 10b). This evidence indicates that the hydrosphere, lithosphere and atmosphere on Mars are not in isotopic equilibrium (Farquhar and Thiemens 2000).

The other secondary mineral assemblage of bona fide martian origin is the Ca-Mg-Fe carbonate grains which comprise ~1% of ALH84001. The martian origin of these carbonate 'rosettes' was established on the basis of preterrestrial shear zones that cut them (Mittlefehldt 1994). The carbonate may have formed at lower temperatures (<50 °C) than the nakhlite carbonate (Bridges and Schwenzer 2012), but both in metastable, rapidly cooled conditions (Bridges et al. 2001, 2019). ALH 84001 experienced subsequent shock-induced recrystallization. These carbonate grains are hosts to putative evidence of ancient martian life (McKay et al. 1996), a stimulating hypothesis but which has not been generally accepted e.g. (Bradley et al. 1998; Treiman 2005; Treiman and Essene 2011).

The stable isotopic compositions of the ALH 84001 carbonates vary widely, for the most part in concert with their elemental compositions. The $\delta^{18}O$ of carbonates correlate with Mg/Fe (Leshin et al. 1998; Eiler et al. 2002; Holland et al. 2005; Saxton et al. 1998), as do their $^{13}C/^{12}C$ ratios (Niles et al. 2005). Both of these isotopic ratios suggest incorporation of C and O from the martian atmosphere. The carbonate $\Delta^{17}O$ is also characteristic of the martian atmosphere rather than its interior, at +0.03 to +0.75‰ (Fig. 10b; Farquhar et al. 1998; Shaheen et al. 2015). For a detailed review of carbonates and their isotopic compositions in martian meteorites see Bridges et al. (2019).

4.2.3 Lunar Samples and Meteorites

Between July 1969 and December 1972 six manned Apollo missions to the lunar surface successfully returned to Earth over two thousand samples of Moon rock, with a total mass of 382 kg. In addition to this material, over 300 g of surface samples were collected on the Moon and returned by three Russian robotic Luna probes during the period 1970 to 1976. Alan Hills 81005, collected in 1982 in Antarctica, was recognised by Brian Mason of the Smithsonian Institution as having characteristics similar to Apollo samples and was the first identified lunar meteorite (Marvin 1983). There are currently 394 individual lunar meteorite samples listed on the Meteoritical Bulletin Database, although many of these are likely to be paired.

The intense period of scientific activity that followed the Apollo landings led to the development of two key concepts concerning the formation and early evolution of the Moon. Based on the results of the initial examination of lunar rocks, it was suggested by two groups that a relatively deep magma ocean had been present on the Moon immediately after its formation (Smith et al. 1970; Wood et al. 1970). Later it was suggested independently by Hartmann and Davis (1975) and Cameron and Ward (1976) that the Moon formed as a consequence of a planetary-scale collision. These two key concepts remain central to current lunar research.

A collisional formation origin for the Moon was refined by Canup and Asphaug (2001). Their classic Moon-forming giant impact model was constrained by the present angular momentum of the Earth-Moon system and the small relative mass of the Moon's core ($\leq$ 3%

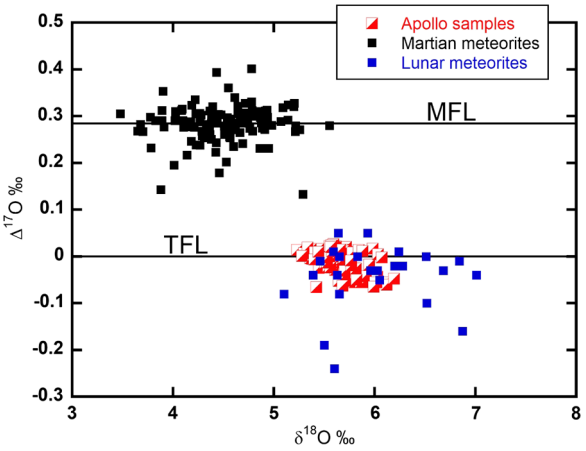

Fig. 11 Oxygen isotope compositions of lunar meteorites and Apollo samples shown in relation to martian meteorites (Fig. 9a). MFL = Mars Fractionation Line; TFL = Terrestrial Fractionation Line. Since $\Delta^{17}O$ for the original analyses was calculated using a variety of slope factors all the data in the plot have been recalculated using $\Delta^{17}O = \delta^{17}O - 0.525\delta^{18}O$. Data sources: Apollo samples—Wiechert et al. (2001), Spicuzza et al. (2007), Hallis et al. (2010), Herwartz et al. (2014), Young et al. (2016), Greenwood et al. (2018); Meteorite samples - Clayton and Mayeda (1996), Meteoritical Bulletin Database

of its total mass). Their model proposed a relatively low energy, oblique impact between the proto-Earth and a Mars-sized impactor, often referred to as Theia. Numerical simulations based on this model suggested that the Moon would have accreted from a debris disc containing approximately 70% impactor-derived material. As a result of this prediction, high-precision oxygen isotope analysis of lunar samples became an important test of the giant impact scenario. Given that Solar System bodies show significant oxygen isotopic variation with respect to $\Delta^{17}O$ (e.g. Fig. 6), the impactor would most likely have had a different oxygen isotopic composition to the proto-Earth. This signature should therefore be present in lunar rocks. However, high precision oxygen isotope studies have failed to detect significant differences between terrestrial and lunar rocks with respect to $\Delta^{17}O$ (Fig. 11) (Wiechert et al. 2001; Spicuzza et al. 2007; Hallis et al. 2010; Young et al. 2016; Greenwood et al. 2018). The small, ppm-level $\Delta^{17}O$ differences between terrestrial and lunar materials that have been detected (Herwartz et al. 2014; Greenwood et al. 2018), most likely relate to post formational processes (Greenwood et al. 2018).

Silicon and titanium isotope studies have also revealed that there are no significant differences between the Earth and Moon (Armytage et al. 2012; Zhang et al. 2012); while tungsten isotope studies indicate that both bodies initially had a closely similar ^{182}W composition (Dauphas et al. 2014). The lack of oxygen isotopic differences between the two bodies has been explained by a model involving post-impact isotopic equilibration within a hot melt-vapour disc (Pahlevan and Stevenson 2007).

A reassessment of the angular momentum constraints of the Earth-Moon system, has led to the formulation of new high-energy Moon-forming impact models, with essentially complete mixing of target and impactor-derived materials (Ćuk and Stewart 2012; Canup 2012; Lock et al. 2018). These scenarios would have involved near total isotopic homogenization. In contrast to such high energy models, it has been pointed out that the inner Solar system was likely to have been well mixed by the time of the giant impact and so the level of isotopic variability may have been small (Dauphas et al. 2014; Dauphas 2017).

As a consequence, Theia and proto-Earth might have been very close isotopically, hence relaxing the objections to the classic giant impact model (Dauphas 2017). This possibility raises the scientific importance, despite the technical difficulties involved, of sample return from either Venus or Mercury (Stevenson and Halliday 2014; Greenwood and Anand 2020). At present we have samples from relatively small (e.g. Moon), or distal (Mars) inner Solar System bodies. However, to test the possibility that the inner Solar System was isotopically well-mixed requires material from one of the other large inner Solar system bodies. Venus would be the preferred candidate being approximately the same size as Earth (Stevenson and Halliday 2014; Greenwood and Anand 2020).

As can be seen in Fig. 11, lunar meteorites show considerably more compositional scatter than lunar samples. This probably reflects a combination of factors, particularly terrestrial weathering, as well as analytical and calibration artefacts. In comparison, analyses of returned lunar samples show less variability. However, a compilation of lunar data of the type shown in Fig. 11 will overestimate the intrinsic level of isotopic variability due to calibration differences between labs (Rumble et al. 2007; Pack and Herwartz 2014; Miller et al. 2015, 2020). To date, returned lunar samples have been collected from a relatively restricted region corresponding to the Procellarum KREEP Terrane. It remains possible that samples recovered from other regions of the Moon will have oxygen isotopic compositions that are distinct from that of our existing sample collection. However, from our current perspective, as informed by the twin concepts of the giant impact and lunar magma ocean, this seems unlikely. Further sample return is required to test and refine these concepts.

4.3 Presolar Grains and Stellar Sources

The discovery of large variations in ^{16}O in CAIs was originally interpreted as representing admixture of grains from a distinctive nucleosynthetic source, likely a supernova. However, the lack of isotopic anomalies in different elements at the same scale as oxygen suggests that CAIs are not themselves of presolar origin. The discovery of hydrogen, carbon, and nitrogen isotope anomalies in interstellar dust particles (McKeegan et al. 1985) validated the notion that presolar material had survived in at least some materials coming from the primordial molecular cloud through the solar nebula to the planetary system. Ultimately the search for presolar grains based on progressive concentration of noble gases led to the discovery of a variety of carbonaceous carriers—SiC, graphite, and diamond, which were found to have distinctive C and N isotopic compositions (Anders and Zinner 1993; Zinner 1998).

These grains are small, really small. While the SiC grains can rarely get up to 30 μm, typically they, and the graphite grains, are less than 5 μm. The nanodiamonds are as they are named, with particle sizes of only a few nanometers. Despite these small sizes, isotopic analyses of multiple elements have been carried out on single grains of SiC (e.g., Ávila et al. 2012, 2013a, 2013b) and graphite (e.g., Jadhav et al. 2013). Then, the development of the Cameca nanoSIMS allowed the analyses of small areas (down to 50 nm across) within individual grains (Stadermann et al. 2005). However, as the size of the grains goes down, so does the absolute number of atoms that can be analysed. These presolar grains can be analysed because their isotopic anomalies are so large that even with the limitations of counting statistics they can be shown to be anomalous. Graphite, diamond, and silicon carbide are carbon-rich and this is the reason they survived the acid digestion used to concentrate them.

However, our solar system is oxygen-rich, not carbon-rich. Some indications of strange oxygen isotope compositions are found in carbon-rich grains. Stadermann et al. (2005) analysed submicron TiC crystals in a 10 μm graphite grain that appears to be sourced from a

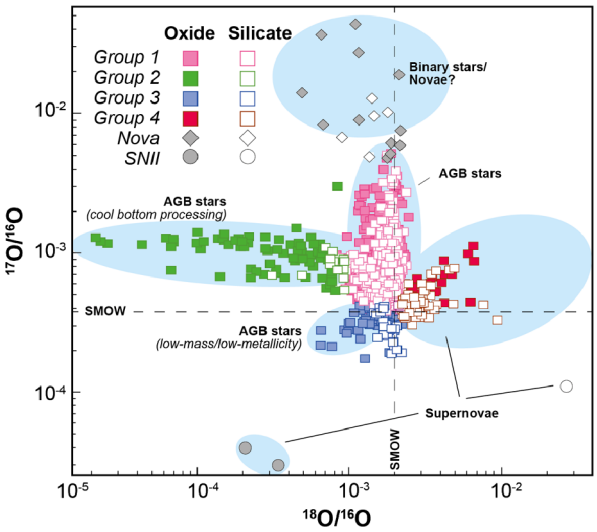

Fig. 12 Oxygen isotope compositions of presolar oxides and silicates. Most of the grains appear to be derived from AGB stars, but the grains show distinctive nucleosynthetic pathways labelled as Groups 1 to 4 of Nittler (1997). Compositions or rare supernovae grains, and compositions inferred to be from Binary stars or Novae are also shown. Data for presolar oxides and silicates from the Presolar Grain Database (https://presolar.physics.wustl.edu/presolar-grain-database/). Note logarithmic scale for the compositional range. Terrestrial SMOW composition shown for reference

supernova. These TiC inclusions had high oxygen concentrations and extreme $^{18}O/^{16}O$ enrichments (up to a factor of 20× solar), but curiously no $^{17}O/^{16}O$ anomalies. These oxygen isotope anomalies are completely different to the anomalies found in CAIs.

Notwithstanding the anomalies in the TiC, detailing oxygen isotope anomalies in silicates and oxides is of more relevance to the source of oxygen in our solar system. Some resilient oxide grains (hibonite, corundum, spinel) were found to have survived the acid treatment used to isolate the carbonaceous grains. Again, these grains have extremely large and variable O isotopic anomalies compared to any solar system materials (Nittler 1997; Nittler and Ciesla 2016). One of the signatures identified is a large excess of $^{17}O/^{16}O$, up to four times the terrestrial abundance, but with $^{18}O/^{16}O$ values similar to terrestrial (Group 1, Fig. 12). Other grains have large depletions in $^{18}O/^{16}O$ and enhanced $^{17}O/^{16}O$ ratios (Group 2). Grains from Group 3 show slight depletions in $^{17}O/^{16}O$ and $^{18}O/^{16}O$ values. These compositions have been interpreted largely as originating in red giant low-mass AGB stars. A small percentage of oxide and silicate grains have isotopic compositions pointing to an origin in Type II supernovae (Group 4). These grains are mostly ^{18}O-rich with variable $^{17}O/^{16}O$ ratios. Only two grains show large ^{16}O excess, the typical isotopic signature expected for supernova condensates (Nittler et al. 1998; Gyngard et al. 2010).

Discovering oxygen isotope anomalies in silicate minerals has been likened to finding a needle in a haystack, when your needle is also composed of straw. As such, the destructive techniques used to find carbonaceous presolar grains are completely inappropriate for identifying presolar silicate grains. The methodology adopted was through the painstaking examination of small regions of interplanetary dust particles with the Cameca NanoSIMS and chondrite matrix with the Cameca ims-1270 (Messenger et al. 2003; Nagashima et al. 2004). The search protocol was based on ion images of $^{16}O^-$, $^{17}O^-$ and $^{18}O^-$ and their reconstruction into isotope ratios. These images showed that extremely small regions were present in extraterrestrial materials and these had large oxygen isotopic anomalies. Many of the silicates have compositions in line with the oxide compositions, Nittler (1997) and are therefore likely related to dust ejected from AGB stars (Fig. 12).

The search for oxygen isotope anomalies has also been carried out based on isotopic anomalies in other elements. In seeking the source of ^{54}Cr isotopic anomalies that had been

discovered during acid leaching of meteorite matrices, Qin et al. (2011) found sub-200 nm chromite grains with ^{54}Cr anomalies exceeding 1500‰. Despite the extreme ^{54}Cr anomalies, the oxygen isotopic compositions of these grains could not be resolved from terrestrial, as opposed to other oxide grains that were discovered during ion imaging.

As such, oxygen in the solar system appears to be mainly sourced from AGB stars, not supernovae. Other sources may exist, but the absence of grains might also suggest that these have either been fragmented coming in to the molecular cloud, or have otherwise been destroyed in solar nebula processing, leaving their chemical memory but not the grains.

5 Sample-Return Missions

Four extraterrestrial sample return missions have been successful, the targets being the Moon, the Sun, a comet, and an asteroid.

5.1 Apollo (and Luna)—Moon

Over 380 kg or rock and dust were delivered back to Earth by the Apollo missions of 1969 to 1972. In addition, around 0.3 kg of lunar soils were returned to Earth from the robotic Luna missions (USSR). The similarities of the oxygen isotope systematics of the Moon and Earth have been covered above in Sect. 4.2.3. The key issue here is that the recognition of lunar meteorites would not have been possible without the return of the Apollo samples. With progressive improvement in analytical techniques, the Apollo samples and lunar meteorites are revisited with a view to resolving the potential for ever decreasing differences. Herein lies the importance and massive advantage of sample return missions, samples can be retained and reanalysed as desired.

5.2 Genesis—Sun

The NASA Genesis mission was designed to obtain a sample of the solar wind and return it to Earth (Burnett et al. 2003). Genesis took off in 2003 to orbit the Sun-Earth Lagrange L1 point and exposed high-purity collectors to the solar wind. The solar wind is ionised atmosphere of the Sun accelerated to a velocity of ca. 400 km/s. With such energy, solar wind particles are implanted into the collectors and oxygen atoms reside some 50–100 nm below the collector surface and even less in non-concentrator samples as the concentrator boosted impact energy by typically 40 to 60 keV, depending on ionization level. A variety of collector compositions were flown so as to allow a variety of different elements to be analysed. An electrostatic solar wind concentrator was used to focus the solar wind and implant into four quadrants of an independent collector to increase the resulting concentration of selected light elements by 20 fold. Genesis returned to Earth in 2005. After atmospheric re-entry, it was intended that the capsule would be intercepted by a helicopter gathering the parachute so as to avoid possible terrestrial contamination. However, the capsule came in without the parachute release and crashed into the Utah desert, fragmenting the solar wind collectors (Burnett and Genesis Science Team 2011). Fortunately the concentrator targets largely remained intact. Such a crash and resulting contamination could have been the end of analysing the solar wind composition. The contamination introduced during the impact could, to first order, be removed by standard cleaning techniques, although persistent levels of microparticles still need to be avoided during analysis (McKeegan et al. 2011). Of a more

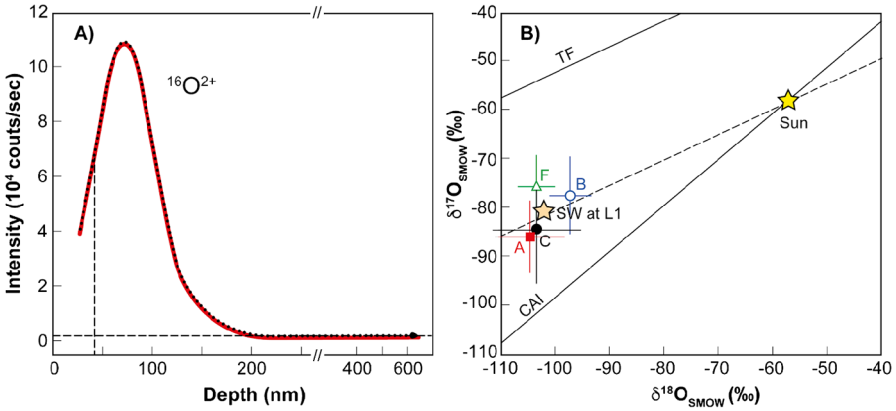

Fig. 13 MegaSIMS analysis of Genesis concentrator targets. Solar wind has a typical velocity of around 400 km/s resulting in the implantation of oxygen to a depth of around 50 nm. Additional acceleration from the electrostatic concentrator implants the solar wind at a higher energy. The depth profile obtained for $^{16}O^{2+}$ is consistent a mean implantation depth of around 80 nm (A). Oxygen isotope analyses across the concentrator, and corrected for variable electrostatic fractionation, indicate a composition for Solar Wind at L1 having a $\Delta^{17}O$ of approximately $-28‰$. Solar wind is known to be isotopically light (through mass dependent fractionation mechanism(s)) and so the inferred composition of the Sun lies at $\delta^{17}O \approx \delta^{18}O \approx -56‰$. After McKeegan et al. (2011)

insidious nature was a brown stain over the collectors. The brown stain was apparently related to glue outgassing from the spacecraft and being redeposited on to the clean collectors where it was affected by solar wind and UV radiation to form a very resistant film some 50 nm think. Analysis of the collectors was therefore compromised both by small adhering particles, likely related to terrestrial contamination, and the brown stain on the surface.

Oxygen isotope analysis of solar wind was the prime objective of the Genesis mission (Burnett et al. 2003). The energy of the solar wind results in implantation of oxygen below the surface of the collector. The means of analysing this oxygen are provided by an exceptional analytical instrument, MegaSIMS, which marries secondary ion mass spectrometry with accelerator mass spectrometry (McKeegan et al. 2004). This instrument was designed and constructed as part of the Genesis Mission. The issue in the analysis of solar wind oxygen is the high intrinsic concentration of hydrogen which results in a large OH^- fraction with SIMS analysis, which needs to be accommodated for the oxygen isotope analysis. The means of doing this is through accelerator mass spectrometry. The sputtered O^- and OH^- ions are recombined and passed into a gas stripper to produce an O^{2+} ion beam which is mass separated into the respective isotopes for analysis.

For the MegaSIMS oxygen isotope analysis, concentrator targets were used which had the highest concentration of oxygen. Progressive ablation of the sample demonstrated a rise in the O^{2+} counts consistent with the implantation of oxygen (Fig. 13a). Isotope ratios were determined from the depth profiles of the individual isotopes acquired simultaneously (with a multicollector). The oxygen is mass dependently fractionated as well as ^{16}O enriched, i.e. lying below the TFL (Fig. 13b). The $\delta^{18}O$ values of the solar wind are around $-100‰$. This mass dependent component appears to be related to a combination of gravitational settling in the solar photosphere as well as ionisation in the solar wind (see Burnett et al. 2003). The magnitude of the ^{16}O enrichment is approximately $56 \pm 3‰$ ($\delta^{17}O \approx \delta^{18}O \approx -56‰$; $\Delta^{17}O \approx -28‰$), which places it in a region similar to oxygen from refractory inclusions. This value exceeds the ^{16}O enrichment of Allende inclusions ($\Delta^{17}O \approx -20‰$; Clayton et al.

1977), but it does correspond to the extreme ^{16}O enrichments of Murchison hibonite grains (Δ^{17}O down to $\approx -30‰$; Ireland et al. 1992; Liu et al. 2009; Kööp et al. 2016). Thus, it is demonstrated that the Sun and Earth differ in their oxygen isotope compositions.

5.3 Stardust—Comet

The Stardust mission collected dust particles from a Jupiter Family Comet, 81P/Wild 2 (Brownlee et al. 2006). Comet Wild 2 was discovered in 1978, but it has been estimated that the comet had an encounter with Jupiter, approaching to within 0.0061 AU, in 1974 shifting the comet into a short-period orbit of 6.4 years within the inner solar system, with perihelion and aphelion distances of 1.49 AU and 5.24 AU respectively, and an inclination of 3.3° (Sekanina 2003). Thus it is probably a relatively fresh comet. The mission launched in 1999 and passed through the coma of comet Wild 2 (in 2006) with a differential velocity of around 6 km/s. Being a sample return mission, the spacecraft had to maintain a velocity that allowed it to return to Earth, and so matching the orbital speed of the comet was not an option (as opposed to the ESA Rosetta mission to comet P67 where a matched speed was required to allow landing of Philae). The high velocity of the spacecraft relative to the comet required a new type of collector that would allow for deceleration of particles without total vaporisation and destruction. The material chosen was aerogel, a lightweight glass composed of silica which approaches the density of air (Kistler 1931). Over 100 individual aerogel collectors were cast in an aluminium frame. Prior to the encounter, the detectors were faced backwards to avoid contamination.

Stardust passed through the Wild 2 coma on 02 Jan 2006. Remote sensing of the dust encounter was provided by the Dust Flux Monitor and the Cometary and Interstellar Dust Analyzer (CIDA). CIDA is a TOF-MS that was used to analyse particle compositions during the encounter (Kissel et al. 2004; Green et al. 2007). Most of the compositions appear to be dominated by organics. The CIDA instrument used on Stardust was identical to that used on Giotto and Vega 1 and 2 during the 1P/Halley comet encounter.

The Stardust sample capsule was returned to Earth on 14 Jan 2006 during Earth flyby. There was some worry about the re-entry because the same accelerometer timing system that had failed on Genesis was used on Stardust. However, the Stardust re-entry was nominal. The Stardust spacecraft was then redeployed as the NeXT mission to view the crater on comet Tempel created by the Deep Impact mission.

Examination of the Stardust collectors showed substantial (up to tens of μm in size) particles at the end of tracks. These included familiar inner solar system materials that looked like chondrule fragments, and even refractory inclusion-like materials (Brownlee et al. 2006) in elongated mm-length tracks which were classified as Type A tracks (Hörz et al. 2006; Burchell et al. 2008). In total, *Stardust* collected thousands of particles, 1–300 μm in size, totalling an estimated $\sim 3 \times 10^{-4}$ g in mass (Hörz et al. 2006; Burchell et al. 2008). Oxygen isotopic analysis of particles confirmed the inner solar system chondritic affinities with the chondrule fragments near the TFL, and the refractory particles enriched in ^{16}O relative to terrestrial (McKeegan et al. 2006; Bridges et al. 2012; Nakamura et al. 2008; Fig. 14). Zolensky et al. (2006), Joswiak et al. (2014), and Ishii et al. (2008) also reported a varied mineralogy, including olivines and low-Ca pyroxenes, Fe-Ni sulphides, Fe-Ni metal, and accessory phases. The presence of these particles has been interpreted as indicating substantial recycling of material from inner to outer solar system when the solar system was forming, and in particular, in the regions where comets accreted.

Type B, and C tracks are more bulbous and are thought to contain material analogous to fine grained chondrite matrix and organics (Burchell et al. 2008). In general, the large

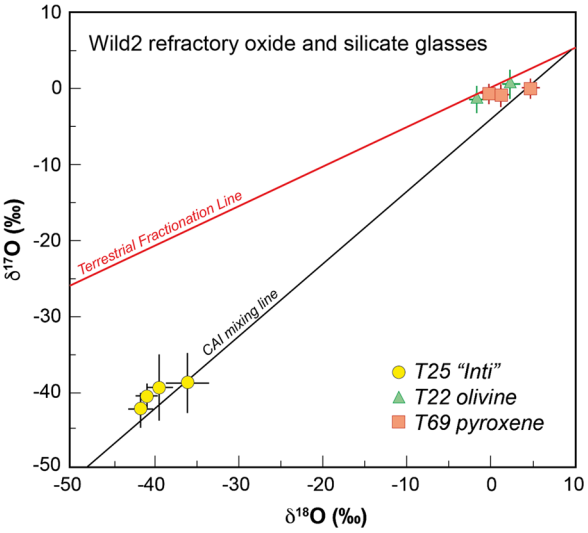

Fig. 14 Stardust grain fragments include materials that appear similar to chondrule and CAI derived minerals. Their oxygen isotope compositions is also similar to chondrule and CAI materials from chondrites suggesting that the comet forming region has been "polluted" with inner solar system materials likely transported out through jets or winds (Figure adapted from McKeegan et al. 2006)

particles at track ends have undergone less thermal processing during capture by the spacecraft from the coma, and so have been most useful for reconstructing the Wild2 mineralogy. The carbonaceous chondrite affinities are evident in the mineralogy. In addition to chondrule and CAI fragments, magnetite identified by Hicks et al. (2017) in Stardust tracks, reveals evidence for hydrous alteration on the cometary parent body.

In addition to the cometary particles, seven candidate interstellar grains were identified with the help of a 'Citizen Science' project by Westphal et al. (2014).

5.4 Asteroids

An asteroid sample return mission was, and is, premised on establishing the relationships between asteroids and meteorites. Infrared Spectroscopic characterisation of asteroids leads to two main types: S (17% abundance) and C (75%) (Tholen and Barucci 1989). The S-type asteroid spectrum has moderate albedo (c. 20%) and is further characterised by absorption features related to ferromagnesian silicate minerals (olivine, pyroxene). The C-type asteroid spectrum has a low albedo (<10%) with no features apparent. It is therefore tempting to relate the S-class spectrum to meteorites rich in ferromagnesian minerals such as ordinary chondrites or pallasites, and the C-class asteroids to carbonaceous chondrites. However, while C-type asteroids are the most abundant, carbonaceous chondrites are relatively uncommon (<5%). As such, there appears to be a flip in the apparent abundances of S- and C-class asteroids, and the abundance of stony meteorites and carbonaceous chondrites.

One successful sample return mission to an asteroid has been completed and two further missions are currently underway.

5.4.1 Hayabusa Mission to 25143 Itokawa (S Class Asteroid)

The Japanese Aerospace Exploration Agency (JAXA) Hayabusa mission began as the Muses-C mission, a technology demonstration to reach an asteroid and bring a sample back to Earth (Kawaguchi et al. 2008). This mission involved the use of autonomous navigation, ion engines, and a novel sampling device. Hayabusa was a 510 kg spacecraft about the size

of a large refrigerator. It had a variety of imaging cameras (optical, infrared) as well as LIDAR (Light Detection and Ranging) altimeter. The sampling was based on the touchdown of a sample collection horn. When the horn touched the surface, a 5 g tantalum bullet was fired, and the resulting ejecta was to be transferred up the horn to the sample chamber. Immediately after touchdown, thrusters were activated to take the spacecraft away from the surface. As such, the touchdown and sampling is almost instantaneous and the operation is akin to a Peregrine falcon (Hayabusa in Japanese) hovering, catching prey, and returning to hovering.

The target asteroid was 1998SF36, which was subsequently formally renamed 25143 Itokawa. This asteroid was estimated to be around 500 m across and has an S-type reflectance spectrum. Hayabusa launched on 9 May 2003 with an August 2007 return planned. In the early stages of the voyage to Itokawa, two of the gyroscopic reaction wheels ceased operation. Spacecraft attitude was then only able to be controlled by the one reaction wheel and operation of the ion engine and thrusters. Despite this setback, Hayabusa arrived at Itokawa in September 2005.

Itokawa was observed to be a rubble pile asteroid ($535 \times 294 \times 209$ m) with many boulders apparent on the surface (Fujiwara et al. 2006; Saito et al. 2006). The asteroid is peanut shaped, apparently formed by a low speed merger of two objects. Following a program of imaging, the first touchdown was scheduled to occur in the smooth Muses Sea region of the asteroid, a region in the middle of the asteroid largely free of boulders. A target marker was dropped to guide the touchdown location. The spacecraft appeared to touch down on the surface of the asteroid before the interlocks on the sampling gun had been removed and so touchdown proceeded without the gun firing. In addition, the thrusters to power the spacecraft back to the home position did not operate and it appeared Hayabusa had not only touched down, it had actually landed on the surface of Itokawa. After establishing that the spacecraft was fully operational, the thrusters were used to take the spacecraft back to a hovering position. A second touchdown was scheduled and operation appeared nominal. However, after the touchdown an incident occurred that took the spacecraft out of communication with Earth. This appeared to be related to the chemical thrusters all firing, setting the spacecraft into chaotic tumbling. With the Hayabusa spacecraft out of control, it was decided that the August 2007 return was not possible, and so Hayabusa would stay near Itokawa for another orbit of the solar system. After 6 months, full communications with Hayabusa were recovered. Hayabusa then left to return to Earth. Issues with the ion engines and charge neutralisation required a reconfiguration, but overall the return journey was uneventful. However, it was felt that the extra 3 years in space may have affected the state of the battery on the return capsule that was required for the operation of the drogue parachute and the "beeper" used to locate the spacecraft. It was decided to separate the capsule and mother spacecraft as late as possible (to maximise battery power coming from the mother craft) leading to the spectacular reentry of both return capsule and space craft. The re-entry was nominal and the capsule was quickly located within 400 m of the nominal target at the Woomera Range in South Australia, and then recovered.

Around 150 grains were collected from the sample rooms of the return capsule in the first year, since then ca. 1000 grains have been recovered. This is consistent with the non-firing of the gun on Hayabusa, and the grains obtained simply reflect the slow speed impact of the spacecraft with the asteroid surface. The largest grains were hundreds of micrometers across but most are in the 10–30 μm size fraction. Petrographic examination determined that the grains were predominantly composed of olivine and pyroxene, and the chemistry is consistent with an equilibrated LL chondrite (Nakamura et al. 2011). The oxygen isotope composition was also consistent with L/LL chondrites (Yurimoto et al. 2011; Fig. 15). The

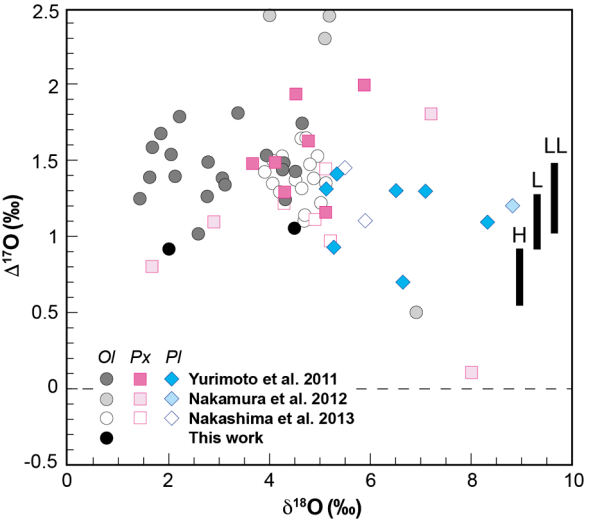

Fig. 15 Oxygen isotope composition of Itokawa grains including the Hayabusa preliminary examination team measurements by Yurimoto et al. (2011), Nakamura et al. (2012), Nakashima et al. (2013), and unpublished SHRIMP data. These analyses confirm the extraterrestrial compositions of these grains and the direct association of Itokawa with LL chondrites

exposure ages of the grains are young, less than 8 Ma based on ^{21}Ne accumulation and may reflect ongoing grinding of mineral surfaces on the asteroid, or assembly of the asteroid body (Nagao et al. 2011). It is established that Itokawa is an S-type asteroid and an LL ordinary chondrite parent body.

5.4.2 Hayabusa2 Mission to Ryugu (C Class Asteroid)

The success of the Hayabusa mission led to a swift turnaround and the building of Hayabusa 2. The short preparation time led to a similar retinue of instrumentation but with some added capability, and in particular to obtain close up images of the surface. The target asteroid of Hayabusa 2 is 1999JU3 now termed 162173 Ryugu. This is a C-type asteroid, which made it difficult to observe from Earth because of the low albedo.

Hayabusa 2 launched on 4 Dec 2014 and had an uneventful journey to Ryugu, arriving in June 2018. Ryugu is determined to have near equant dimensions at $1.04 \times 1.02 \times 0.88$ km (Watanabe et al. 2019). At home position, Ryugu appears as diamond shaped in profile and is close to the shape of a spinning top (i.e. looking down the rotation axis it appears to be round). Like Itokawa, Ryugu is a rubble pile asteroid with low density, and the surface is covered in a poorly sorted mix of pebbles to boulders (Watanabe et al. 2019; Sugita et al. 2019). Targets for the sample touchdown generally comprised locations that had the fewest boulders. After detailed imaging, a sampling touchdown was carried out in February 2019. All feedback from the touchdown indicates nominal operation and a successful sample recovery.

Hayabusa 2 also carried an experiment called the Small Carry-on Impactor (SCI). Here the objective was to make an artificial crater so that fresh sample free of space weathering could be obtained for analysis. The SCI was successfully deployed. A touchdown to the crater then followed in July 2019. At this stage, the sample capsule has been closed. Hayabusa left Ryugu in Dec 2019 for a Dec 2020 return to Earth at Woomera, South Australia.

5.4.3 OSIRIS-REx Mission to Bennu (C Class Asteroid)

Effectively in parallel with the JAXA Hayabusa 2 mission, the NASA OSIRIS-REx mission has targeted another C-class asteroid, 101955 Bennu. Bennu is the second spinning top rubble pile asteroid observed (Lauretta et al. 2019). Bennu is remarkably similar to Ryugu in terms of overall shape, although in detail there are differences in surface morphology. Touchdown evaluation is currently underway, with an expected sampling planned for December 2019. OSIRIS-REx will return to Earth in 2023.

6 Remote Analysis Missions (for Oxygen Isotopes)

Mass spectrometers have been flown frequently on space missions. However, the specific science goals of many of these mass spectrometers have been directed towards determining plasma elemental compositions for which low mass resolutions (tens to hundreds in terms of M/ΔM) are suitable. The drawbacks of flying with mass spectrometers with higher mass resolving power and high sensitivity are related to instrument mass and power consumption. Missions related to determining plasma compositions are not covered here; see a review by Yokota (2018). The discussion below is not intended to be definitive, but rather to exemplify the range of techniques used in space missions to date. The main focus of this section is to examine the ability of mass spectrometers to determine oxygen isotopic compositions.

A remote mass spectrometer must either rely on the presence of plasma as the source of ions for analysis, or the ions must be generated from neutrals related to gas or dust. Ionisation can be active (e.g. electron bombardment), or can be "passive" (e.g. secondary ions caused by the impact of energetic particles). The environment around comets, in particular, is quite suitable for mass spectrometric analysis because of the abundant presence of gas and dust species with high relative velocity causing ionisation.

6.1 Halley's Comet

The return of comet 1P/Halley in 1986 generated an immense interest in the nature of comets. The Halley Armada consisted of five spacecraft: Giotto from the European Space Agency, two spacecraft from U.S.S.R. (Vega1 and Vega2), and two spacecraft from Japan (Sakigake and Suisei). The Giotto mission to Comet Halley included three mass spectrometers (for neutrals, ions and dust; Reinhard 1986). Giotto passed the nucleus of Halley on 14 March 1986 at a distance of less than 600 km and a relative velocity of 68 km/s. Balsiger et al. (1986) used the ion mass spectrometer to measure positive ion spectra during the encounter. The mass spectra are dominated by OH species (OH^+, H_2O^+ and H_3O^+). The dominant presence of these species makes it impossible to measure isotopologues to estimate O isotopic abundances. In addition, the $^{16}O^+$ signal at 1000 c/s is too low to provide accurate information on the $^{18}O^+$ abundance, or the $^{17}O^+$ abundance.

Kissel et al. (1986) reported dust impact data from the PUMA time-of-flight mass spectrometer on board the Vega 1 spacecraft. Dust particles impacted on to a silver conversion plate and positive ions generated are accelerated into the mass spectrometer. The mass spectra are quite detailed and complicated. The mass resolution appears to be around 50 (M/DM) allowing mass peaks at unity separation to be resolved below mass 50. The main species detected are H, C, O, with smaller peaks of Mg and Si of variable abundance, confirming the nature of comets as predominantly ice and silicate dust mixes. Mass resolution is not sufficient to resolve minor isotopes or molecular species from atomic.

The Cometary Impact Dust Analyzer (CIDA) is a similar instrument to the PUMA mass spectrometer that was flown on Stardust (Kissel et al. 2004). During the fly-through of the Wild 2 coma the particles were predominantly organic.

6.2 Rosetta at Comet 67P/Churyumov-Gerasimenko

The Rosetta mission to Comet 67P/Churyumov-Gerasimenko was the first mission to match the velocity of the comet in an attempt to place a lander (Philae) on the surface (Taylor et al. 2015). Comet 67P/C-G is a Jupiter-family comet with an orbital period of 6.45 years with a perihelion of 1.24 a.u. and so the velocity requirements were not as extreme as for longer period comets. Comet 67P/C-G is around 4 km across and Rosetta orbited for two years from 2014 to 2016. The closeup images of the comet are outstanding and include detailed images of pits associated with jets and other features associated with gas loss by sublimation (Sierks et al. 2015). On board Rosetta was a mass spectrometer system for analysing released gases. The Rosetta Orbiter Spectrometer for Ion and Neutral Analysis (ROSINA) consists of two mass spectrometers, being a double focussing mass spectrometer (DFMS), and a Reflectron time-of-flight (RTOF). The DFMS is particularly exciting because it has high mass resolution capabilities sufficient for separating H-O isotopologues with M/ΔM of 3000 (for ΔM at 1% peak height; Hässig et al. 2013). This enabled a determination of the D/H ratio (from the $HD^{16}O/H_2^{16}O$) of 5.3 (± 0.7) $\times 10^{-4}$ (Altwegg et al. 2015), approximately 3 times the terrestrial value, and precluding cometary water such as this as a major source of water for the Earth's oceans. The DFMS also had the capability to measure $^{18}O/^{16}O$ and $^{17}O/^{16}O$ through the measurement of H_2O species at masses 18, 19, 20 (viz. $H_2^{16}O$, $H_2^{17}O$, and $H_2^{18}O$). Low count rates lead to large uncertainties and the ratios could not be resolved from terrestrial with $^{17}O/^{16}O = 3.7\ (\pm 0.9) \times 10^{-4}$ and $^{18}O/^{16}O = 1.8\ (\pm 0.2) \times 10^{-3}$. The uncertainty in $^{17}O/^{16}O$ corresponds to approximately 250‰, approximately the entire range of oxygen found in stony materials in the solar system (Ireland 2012). Nevertheless, this represents the first three oxygen isotope analysis from an operating spacecraft.

The Philae lander also included two mass spectrometers. The COmetary SAmpling and Composition (COSAC) instrument was a combined gas chromatograph and time-of-flight mass spectrometer designed to determine volatile abundances and species, particularly of organic compounds (Goesmann et al. 2007). Most of the ingenuity (and mass) of this device lies in the gas handling and chromatograph system. The mass spectrometer is a comparatively simple TOF-MS designed for M/ΔM of 350 at mass 70.

The second mass spectrometer system, Ptolemy, was an instrument capable of measuring stable isotope ratios of key volatiles on the comet's nucleus (Wright et al. 2007). Ptolemy utilises an ion trap mass spectrometer that can be regulated to either long mass ranges (for compound characterisation), or short range for isotope compositions. In an ion trap, ions are first captured and then released into the cyclotron in a pulse for analysis. This is a similar concept to a Time-of-Flight MS except the ions are constrained in a circular orbit until ejection for analysis. The instrumentation has been miniaturised to a level where the entire instrument weighs only 5 kg. Samples were to be delivered to ovens where volatiles would be released and then purified before being analysed in the mass spectrometer. However, with the difficulties associated with Philae's landing, Ptolemy did not get the opportunity to operate in its intended fashion and only analysed gas emanating from the surface.

6.3 Cassini at Saturn

The Cassini spacecraft carried the Ion and Neutral Mass Spectrometer (INMS), a dual ion source quadrupole mass spectrometer. INMS was used to analyse the gas ejected from Enceladus (Waite et al. 2006). An electron impact source was used to ionise the gas. The mass

spectrometer has effectively unit mass resolution and was capable of recognising the major gas species H_2O, CO_2, and CH_4, at masses 18, 44, and 16 respectively, although the interpretation of mass 28 is ambiguous in this type of analysis as being either CO or N_2.

6.4 Curiosity Rover on Mars

The Mars Curiosity Rover carries the SAM (Sample Analysis at Mars) system for determining chemical and isotopic compositions, particularly with reference to possible life habitats. Three instruments can be utilised as part of the characterisation including a Gas Chromatograph, a Quadrupole Mass Spectrometer, and a Tunable Laser Spectrometer. The total weight of this system is (a massive) 40 kg, but the capabilities are extensive. The quadrupole MS is similar to that carried on Cassini in that it uses electron bombardment and effectively has unit mass separation. Atmospheric samples can be directly input to the source (Mahaffy et al. 2013). Dust, soil, and rock samples can also be prepared for analysis through high temperature ovens (up to 1000 °C), as well as chemical solvents for wet chemistry experiments. This capability has been used for carrying out geochronological analysis of Mars surface materials (Cohen et al. 2019).

For the Mars atmosphere H, C, and O isotopes are dominated by atmospheric loss processes and water-rock reactions with its surface such as sulphate, clay and carbonate formation. SAM's measurements of the atmospheric isotope ratios of D/H ($\delta D = 4950 \pm 1080‰$), O ($\delta^{18}O = 48 \pm 5‰$) and C isotopes ($\delta^{13}C = 46 \pm 4‰$), have been interpreted on the basis that the martian reservoirs of CO_2 and H_2O were largely established by about 4 billion years ago, and that atmosphere was subsequently lost (Webster et al. 2013).

7 The Solar System

7.1 An Historical Perspective

In 1969, man landed on the moon and brought back the first samples collected from an extraterrestrial object. In that same year, two large carbonaceous chondrites landed on Earth making this a serendipitous year for obtaining samples relevant to our understanding of the solar system.

Fifty years ago, our view of the solar system was quite different to what it is now. It had been realized for some time that a key to understanding the provenance of our solar system was the search for isotopic anomalies produced during nucleosynthesis of the elements. B^2FH (Burbidge et al. 1957) showed that the abundances of the nuclides in the solar system could be described in eight nucleosynthetic processes and that the solar system elemental abundances had to be averages of multiple nucleosynthetic inputs. Hence, apparent isotopic anomalies are key to locating individual sources. However, prior to 1969, only a few elements had shown any isotopic variations and these were primarily for volatile species (H, and noble gases). Isotopic anomalies in the rock-forming elements were not known. One way of homogenising the elemental isotopic compositions is to completely evaporate everything in the solar nebula and then condense the rocky elements (Grossman 1972). Thus, the solar nebula was regarded by meteoriticists as extremely hot.

On 8 February 1969, two tons of the Allende (CV3) carbonaceous chondrite fell to Earth in Mexico. This was a propitious event in terms of having an abundance of extraterrestrial material available for testing analytical protocols for the upcoming lunar sample return. For

this purpose a 2 kg aliquot of Allende was ground up and made available as a reference material by the Smithsonian Institution (Jarosewich et al. 1987). Allende also contained large (up to 25 mm across) and varied CAIs (Grossman 1975). Oxygen isotope analysis of these inclusions were the first indication of substantial isotopic heterogeneity in solar system materials (Clayton et al. 1973). With the ready availability of material, isotopic anomalies were sought in many other elements. Of particular interest were anomalies in ^{26}Mg correlated with ^{27}Al indicating the presence of live ^{26}Al in the early solar system with a $(^{26}Al/^{27}Al)_0$ abundance of 5×10^{-5} (Lee et al. 1976). At this level, radioactive decay of ^{26}Al is a suitable heat source for planetesimals. Also of importance were anomalies in the Fe group of elements. Isotopic anomalies were first discovered in the heaviest isotope ^{50}Ti, suggesting the addition of neutron-rich material (Heydegger et al. 1979). The correlated excesses of ^{16}O, ^{26}Al, (and ^{50}Ti) supported the late stage SuperNova Injection model, where these nuclides were ejected from a supernova proximal to the early solar nebula, potentially causing the collapse of the molecular cloud leading to the solar nebula (Cameron and Truran 1977).

The Murchison (CM2) meteorite provided a different and perhaps complementary view to that of Allende (Ireland and Fegley 2000). On 28 September 1969, around 120 kg of Murchison were recovered in and around the township of Murchison, Victoria, Australia. The matrix of Murchison has seen aqueous alteration but not the metamorphism evident in the matrix of Allende. This cold matrix was found to contain a large variety of organic molecules, including amino acids. Murchison also contains its own suite of refractory inclusions. These are typically very small (less than 0.5 mm) and so analysis of these materials required a different approach to analysis of the larger Allende inclusions. They are also characterised by the common presence of a highly refractory mineral hibonite ($CaAl_{12}O_{19}$), which forms at higher temperatures than Allende CAI minerals and therefore might contain more of the initial heterogeneity of the solar system (Fahey et al. 1985). The isotopic analysis of these inclusions was possible because of the development of ion microprobes capable of in situ analysis while resolving various isobaric interferences including ^{48}Ca and ^{48}Ti ($M/\Delta M \approx 10000$; Zinner et al. 1986). These analyses showed a similar variability in oxygen isotope compositions from close to the terrestrial fractionation line to around a 6% enrichment in ^{16}O, and a similar maximum initial $(^{26}Al/^{27}Al)_0$ of 5×10^{-5}. However, anomalies in Ti and Ca were greatly increased with excesses in ^{50}Ti and ^{48}Ca of up to +27% and +10% respectively (Ireland 1990). The lack of correspondence between ^{48}Ca-^{50}Ti anomalies and ^{16}O anomalies was used to argue against the late supernova injection model (Fahey et al. 1987).

7.2 Origins of Isotopic Anomalies

Variations in isotopic abundances (isotopic anomalies) were initially thought to be solely produced through nuclear processes, such as stellar nucleosynthesis, in addition to radioactive decay. However, a variety of chemical processes are now thought to produce isotope variability beyond that solely expected from mass dependent fractionation. This is particularly important for oxygen.

7.2.1 Nuclear Inheritance

The direct incorporation of dust grains ejected from other stars manifests itself as isotopically anomalous material in our solar system. These grains predate our solar system and so are often referred to as presolar grains. The source of these grains can be related to the big dust producers in the galaxy, namely AGB stars and supernovae (Zinner 2003).

In terms of oxygen isotope diversity in solar system materials, the most striking anomaly is the ^{16}O abundance variation seen in CAIs. However, a general mineral carrier for this anomaly has not been found. Most of the presolar oxide and silicate grains are distinctive and appear to be related to AGB stars, just like the carbonaceous grains (Nittler 1997; Floss and Haenecour 2016).

Moreover, the solar system oxygen isotope signature is striking in that it is planet Earth which is anomalous relative to the Sun (Clayton 2002; McKeegan et al. 2011). In this case, what would a nucleosynthetic carrier actually represent at the scale of these two bodies? The big issue with oxygen is that it is a major element in the solar system and that the variability is in the major isotope requiring exchange of a large number of atoms to manifest change.

7.2.2 Chemical Fractionations

The lack of a viable means of describing the solar system oxygen isotope composition with carriers of nucleosynthetic anomalies leaves us with the possibility that the anomalies are induced by chemical speciation and non-mass-dependent isotope fractionation.

The production of ozone in the atmosphere induces an isotope shift because the available energy levels for asymmetric molecules are more plentiful than for molecules of a single isotope. Such a mechanism can be readily envisaged for the solar system through various reactions, and was postulated very early in the interpretation of oxygen isotope anomalies (Thiemens and Heidenreich 1983; Thiemens 1999). However, making such a scheme operable in the early solar system brings up a number of challenges. For the oxygen-ozone exchange reaction, both species are in the gas phase. We see that the compositions are different because we can physically separate the oxygen from the ozone and measure them separately. So for CAI it is tempting to envisage the same mechanism because the isotopic composition ranges up to $+50‰$ for $\delta^{17}O$ and $\delta^{18}O$ in Earth's stratospheric oxygen, at the same scale as anomalies in CAI. However, in the case of CAI, we only have a solid phase. Hence any fractionation must be transferable to the solid phase and the gas then would be expected to be isotopically heavy.

7.2.3 Predissociation and Self-Shielding

While chemical fractionations along the lines of molecular asymmetry need more explicit development, another type of chemical fractionation is well known in the cosmos. Predissociation of CO by UV photons leads ultimately to dissociation of CO in to C and O (Bally and Langer 1982; Lada et al. 1994). The predissociation is subject to self-shielding because the photon stream is attenuated through absorption by the CO molecules. Furthermore, for a cold molecular cloud, the predissociation energy is quantised with a narrow energy window. The different isotopologues of CO, each have a different associated energy for predissociation. Thus photons relevant for the dissociation of $^{12}C^{16}O$ are absorbed at a short optical depth whereas photons for dissociating $^{12}C^{17}O$ and $^{12}C^{18}O$ can penetrate deeper into the core of the molecular cloud. Hence the core of a molecular cloud can have CO, which is highly enriched in ^{16}O, because $C^{17}O$ and $C^{18}O$ are dissociated and the ^{17}O and ^{18}O react with abundant H to eventually form ^{17}O-, ^{18}O-enriched water ice. This is consistent with what is observed in molecular clouds where the $C^{16}O/C^{18}O$ can be measured optically (Bally and Langer 1982).

The possibility of predissociation and self-shielding (PSS) in the early solar system was initially considered for molecular oxygen by Navon and Wasserburg (1985). These authors discounted predissociation and self-shielding because of the likely low abundance of free

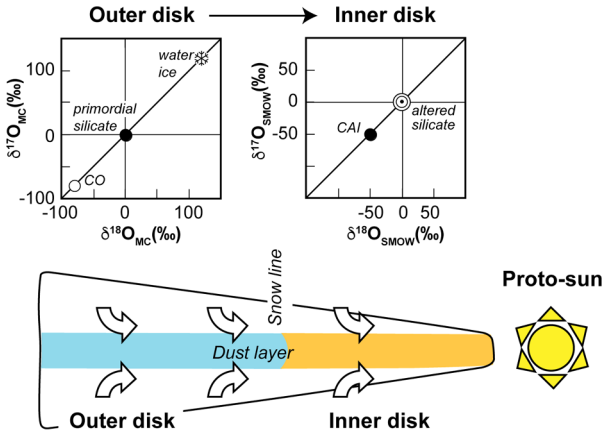

Fig. 16 The predissociation and self-shielding model of Yurimoto and Kuramoto (2004). In the primordial molecular cloud, UV photons cause predissociation of CO (i.e. CO -> C + O). The predissociation is subject to self-shielding because of the high relative abundance of $C^{16}O$, leading to rapid attenuation of photons that can predissociate $C^{16}O$. Predissociation of $C^{17}O$ and $C^{18}O$ can take place deeper in the molecular cloud and following reaction with H, can lead to water highly enriched in $H_2^{17}O$ and $H_2^{18}O$, while the associated CO is enriched in $C^{16}O$ (upper left). The primordial silicate composition is interpreted to represent the bulk molecular cloud composition and is also the starting CO composition ($\delta^{18}O$ of the molecular cloud, $\delta^{18}O_{MC} = 0$). When this assemblage arrives in the inner solar system, the water ice reacts with the original silicates to form an altered silicate reservoir, which represents the solids in the inner solar system including Earth ($\delta^{18}O$ of the inner solar system, $\delta^{18}O_{SMOW} = 0$). In normalising to the altered silicate composition of Earth, CAIs therefore appear anomalous, but they represent a remnant of the primordial dust composition. This model therefore suggests that the silicates in the inner solar system will differ from those of the outer solar system, and outer solar system silicates should reflect a composition close to CAIs. Figure based on Yurimoto and Kuramoto (2004)

gaseous oxygen. They did suggest CO as a more promising molecule. However, the concept languished until it was taken up by Robert Clayton (2002), who was the original advocate for a nucleosynthetic component carrying oxygen isotope anomalies (Clayton et al. 1973). Clayton (2002) suggested that PSS of CO occurred in the inner solar system and silicates reacted with the ^{17}O and ^{18}O preferentially released in the region of the terrestrial planets. Clayton (2002) importantly predicted that the solar composition would be relatively enriched in ^{16}O relative to Earth. However, Lyons and Young (2005) noted that an inner solar system locale is somewhat problematic because of the thermal line broadening that would occur in the inner solar system, which would affect the isotope selectivity and quickly erase the effects. Lyons and Young (2005) preferred a cold outer solar system location. Yurimoto and Kuramoto (2004) suggested that a molecular cloud setting was the most appropriate because this is where PSS is actually observed to occur. In their model, the ^{17}O and ^{18}O reacted with H to form OH and ultimately H_2O ice which would stick on dust grains (Fig. 16). On heating in the evolving solar system, water is released and reacts with dust to form an altered silicate reservoir, which is the process responsible for the terrestrial oxygen isotope composition.

One manifestation of this can be the large mineral specific oxygen isotopic fractionations and related mixing lines identified in ordinary chondrites (Sect. 4.1.1). The outer solar system would have silicates and oxides with the solar composition (i.e. similar to CAIs) while the water ice would be isotopically heavy (i.e. ^{17}O, ^{18}O-rich). Notwithstanding the specific location of the fractionation, these models all advocate a solar oxygen isotope composi-

tion which is enriched in ^{16}O, as has indeed been found by analysis of the Genesis targets (McKeegan et al. 2011).

7.3 Astrophysical Context

7.3.1 Formation of Solar Systems

Around 4568 million years ago, a molecular cloud was in the process of consolidation and forming new stellar systems. One of these stellar systems became our solar system. With the development of Hubble, Spitzer, Kepler, and other telescopes, we now have quite a detailed view of how stellar and planetary systems develop. Still, we cannot resolve down to inner solar system scales, nor get direct insight into the development of high temperature objects such as chondrules and CAIs around other stars. Understanding the formation of these objects is key to the formation of our solar system because the chemistry of the solar system is largely established at this time.

With the collapse of the molecular cloud, the solar nebula began to accrete and flatten into a disk due to conservation of angular momentum. Dust would be retained in Keplerian orbits but gas would be able to move quickly inwards to the growing protoSun. Dust would be accreted to form protoplanets and this must have occurred very early on if the gas giants were to be able to accrete H and He atmospheres before the gas disappeared into the Sun.

The present solar system shows a distinct difference between the inner solar system (terrestrial planets) and the outer solar system (gas and ice giants). This has been attributed to a snow line inside the orbit of Jupiter where water existed in the gas phase inside the line, and as water ice outside. In the simplest terms, a thermal gradient is indicated. This can be readily seen in calculations based on a minimum mass solar nebula. The temperatures in the disk are relatively low and are consistent with the presence of matrices in primitive meteorites that have not seen high temperatures. However, within that cold matrix are the high temperature chondrules and CAIs. Nowhere in a minimum mass nebula are temperatures high enough to melt silicates, which is required to form chondrules and CAIs (Salmeron and Ireland 2012b).

High temperature processing in the early solar system must be extensive but remains enigmatic. Chondrules are so prevalent in the solar system that they have to be formed in a general process of planetary systems. A full review is not warranted here but we will address some aspects that are pertinent to the thermal structure of the solar system that might be recorded. The key issue in this context is whether a thermal gradient can be seen in the processing of high temperature objects that would have implications for the temperature structure of the solar nebula.

CAIs are enriched in refractory elements and show characteristics of chemical fractionations at high temperatures such as overall high abundance of refractory elements, fractionation of ultra-refractory trace elements, and a lack of Fe metal. The lack, or low abundance, of Fe metal suggests a specific temperature range that CAIs formed within and that is above the condensation temperature of Fe; this is supported by the isotopic fractionation of Mg in CAIs (Richter et al. 2002). The lack of Fe^{2+}, except from secondary addition, suggests that CAIs formed in a reducing environment. The formation of CAIs must have occurred at extremely high temperature, and under quite restrictive temperature intervals such that the lanthanide elements could fractionate from each other. Furthermore, the isotopic variability in CAIs shows that they formed from precursors that weren't entirely homogenised. The most likely scenario is that CAIs formed close to the Sun and were then transported out into the accreting disk through jets, or winds, and/or turbulence.

The formation of chondrules appears to be quite distinct from the formation of CAIs. Chondrules appear to have formed in an oxidising region because of the presence of Fe^{2+}. They still require high temperatures to melt, but there is a distinct possibility that chondrules did not form in the same process/region as CAIs because CAIs appear to have formed under reducing conditions. A large number of the models for forming chondrules have been proposed.

Probably the mechanisms most widely accepted is that chondrules were melted in shock waves generated by gravitational instabilities in the protoplanetary disk (Desch and Connolly 2010). However, aggregates of appropriate size must be produced prior to entering the shock front. In addition, the nature of this process would suggest that partially shocked materials intermediate between the aggregates and chondrules should exist, but these do not appear to be common. Collisions between planetesimals is another likely scenario in the early solar system (Wakita et al. 2017), but again the record lacks the range of intermediate materials that might be expected if chondrules were formed by this process. Formation and transport in magnetohydrodynamic jets and winds have been modelled as suitable mechanisms to melt chondrules, either by direct solar radiation in close proximity to the Sun to for CAIs (Shu et al. 1996), or forming chondrules at 1 a.u. through friction generated between the wind and particles in a disc wind (Salmeron and Ireland 2012a,b). A drawback to these models is that chondrules would form and then have to be incorporated into matrix in rather specific proportions to yield chondritic abundances.

Chronology of the high temperature objects provides no definitive answers as to whether CAIs and chondrules formed in distinctly different processes. CAIs are the oldest material known from the early solar system and formed in a very narrow time window at 4567.3 ± 0.3 Myr; the oldest chondrules are close to the same age, but then record a much longer formation interval with ages up to ca. 4 Myr younger (Connelly et al. 2017). This time period is very similar to the observed duration of disks around young stars. It is also likely that Jupiter was largely formed before the chondrule forming event finished.

7.3.2 Oxygen Isotopes and the Structure of the Solar System

Oxygen isotopic compositions of chondrules and CAIs are similar in some aspects but different in others. Both indicate the presence of a ^{16}O-rich reservoir referred to as *solar*, and both indicate a reservoir closer to the TFL, referred to as *planetary* by Ireland (2012). These compositions are effectively those of the Sun, and the silicate dust composition, respectively.

CAIs and chondrules differ in the proportions of these components. CAI minerals hibonite, spinel, and pyroxene typically show oxygen isotope compositions with Δ^{17}O of -30 to -20‰ whereas melilite and anorthite can be variable but typically closer to the TFL. As such, these systematics are consistent with CAI formation close to the Sun with a solar gas composition mixing with solids during evaporation and condensation. It is debated as to whether the presence of melilite close to the TFL is a nebula product or a parent body product but either can be accommodated. The nebula could become more enriched as silicate evaporates, or, the parent body water could be equilibrated with its silicates.

As noted in Sect. 4.1, chondrules typically have compositions closer to the TFL than CAIs. Bulk compositions are within a few permil of TFL for Δ^{17}O for typical chondrule olivine in ordinary chondrites. Forsterite-rich relics are present, which frequently appear to have a greater ^{16}O-rich component in them (Kita et al. 2010). Chondrules in carbonaceous chondrites typically show larger ^{16}O enrichments. Noteworthy is chondrule a006 from the Acfer 214 carbonaceous chondrite, which has the largest ^{16}O excess ever recorded at $\Delta^{17}\text{O} \approx -40$‰ (Kobayashi et al. 2003). This composition is even more enriched in ^{16}O

than solar, which is not predicted for the primordial dust in the solar system. Potentially this is an important inclusion because its composition suggests reaction with a gas enriched in ^{16}O that might be associated with the otherwise lost CO reservoir.

In the PSS model, oxygen isotope compositions of H_2O-bearing species can be ^{17}O-^{18}O-rich (nebula water). Such compositions are uncommon but have been found. Ireland et al. (2006) found $\Delta^{17}O \approx +25‰$ in the surfaces of lunar metal grains, and while originally interpreted as related to solar wind, could be related to late stage water addition from cometary material. Sakamoto et al. (2007) documented a cosmic symplectite, an intergrowth of Fe, Ni-metal and sulphides apparently oxidised by water, in the Acfer 094 carbonaceous chondrite. This assemblage was found to have $\Delta^{17}O \approx +90‰$ and was interpreted as representing nebula water from the early solar system. Even heavier oxygen isotope ratios have come from organic-rich residues with $\Delta^{17}O$ up to $\approx 250‰$ (Hashizume et al. 2011).

The PSS model provides a context for understanding these oxygen isotope compositions in the solar system. The prediction that the Earth should be ^{17}O, ^{18}O-rich compared to the Sun appears to be borne out (Clayton 2002; McKeegan et al. 2011). PSS indicates that the nebula water composition becomes enriched in ^{17}O and ^{18}O, and the compositions above indicate that this isotopically heavy nebula water indeed appears to be present in the solar system. In the model of Yurimoto and Kuramoto (2004), this water reacts with dust to create an altered dust reservoir in the inner solar system. The corollary to this interpretation is that outer solar system dust and rocky material should be isotopically solar in the oxygen isotopes, like CAIs.

We have only a few indications of oxygen isotopes from the outer solar system. The analyses of particles from comets (McKeegan et al. 2006) determined that the same range in oxygen isotopes exists in the outer solar system as is found in the inner solar system. Interplanetary dust particles also show oxygen isotope compositions that have olivine close to the inner solar system planetary reservoir, and refractory minerals consistent with the CAI composition (McKeegan 1987). Even from this admittedly limited database, we are not seeing the variability in dust compositions that might be expected if outer solar system rocks were ^{16}O-rich relative to the inner solar system.

An alternative scenario could be postulated based on the uniformity of the planetary oxygen isotope composition, such as that indicated for Earth, Mars, and Vesta. These bodies have formed over large radial distances and yet their oxygen isotopes show only small subpermil differences. If these compositions were formed by interaction between the heavy nebula water reservoir and dust of solar composition, then it could be expected that larger variability in altered dust compositions would be apparent. The mixing of the solar and nebula water reservoirs, separated by around 250‰, would need to be thoroughly equilibrated with almost no variability in the mixing proportions to get such a specific oxygen isotope composition in planetary material (e.g. by the chondrule formation heating in the inner solar nebula; Yurimoto and Kuramoto 2004). An alternative interpretation might be that the planetary reservoir does represent the average dust from the molecular cloud and is only affected to a small degree by mixing with nebula water. Any interpretation of course awaits detailed analysis of materials including ice and rock from the outer solar system.

7.3.3 The Warren Gap

In assessing isotopic variability in planetary materials, Warren (2011) made an extraordinary observation that in plotting $\Delta^{17}O$ relative to $\delta^{54}Cr$, there are essentially two populations of material, with a distinct gap between (Fig. 17). This gap is perhaps the moreremarkable because there is no distinct gap in oxygen isotope compositions, and the Cr isotope compositions are near continuous in the plot. It is the correlation between oxygen and chromium

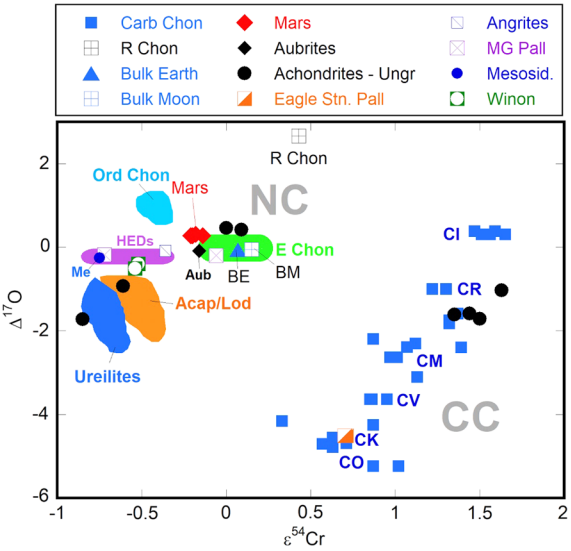

Fig. 17 A distinct separation exists between carbonaceous chondrites and non-carbonaceous chondrite-related meteorites. The separation of these compositions has recently been interpreted as due to the presence of Jupiter causing distinct inner and outer solar system reservoirs (Kruijer et al. 2017). However, this dichotomy is primarily represented by a shift in the chromium isotopic composition rather than oxygen. This is perhaps surprising given the large scale variability in oxygen isotope compositions in the inner solar system and particularly in inclusions in these meteorites. After Greenwood et al. (2017) and Warren (2011)

isotopes that produces the gap. The two groups are essentially related to ordinary chondrites and achondrites on one hand, versus carbonaceous chondrites on the other. The carbonaceous chondrites also show a positive correlation between δ^{54}Cr and Δ^{17}O indicating a fundamental relationship in this group between these two apparently unrelated elements.

An interpretation for this dichotomy has come forward based on the ALMA images of HL-Tau (ALMA Partnership 2015), that is that giant planets act as a road block for material accreting to the nebula (Dipierro et al. 2015). The HL-Tau image is effectively showing the dust distribution and it is clear the an annulus exists and that the most likely explanation is that a giant planet has accreted the dust coming in through the accretion disk and it acts as a block to material coming in to accrete on to any inner planets.

For our solar system, the explanation for the gap can then be posited in terms of the formation of Jupiter. Kruijer et al. (2017) used W and Mo isotopes to show that the gap exists for heavy elements and this can be interpreted as a difference in the accretion history of ordinary and carbonaceous chondrites, representing inner and outer solar system provenance. Once Jupiter had formed it would stop material flowing through the disk thereby allowing distinct reservoirs to exist. Scott et al. (2018) noted that refractory inclusions would come from the inner solar system via jets or winds and were aggregated into cosmic breccias in the outer solar system. Yet, the oxygen isotopic compositions of these outer solar system rocks remains largely "planetary" despite the potential presence of δ^{17}O, δ^{18}O rich water ice in the outer solar system. On the other hand, Yurimoto and Kuramoto (2004) predict isotopically light (solar) solids in the outer solar system. Such paradoxical relationships can only be resolved by sampling the outer solar system.

8 Outstanding Issues

Over a fifty year time frame, we have obtained close up images of all the planets, the dwarf planets—Ceres and Pluto, as well as an ever increasing number of asteroids and comets, and even a Kuiper Belt Object (Arrokoth). From a geologist's perspective these images show morphological features that can be described in terms of processes that have affected the surface. These processes are clearly many and varied, and have occurred in response to different temperatures, atmospheric pressures, and compositions. The radial change to first order in the compositions of planetary objects is quite striking in passing from the rocky and heavily cratered world of Mercury to the ice dominated Pluto. However, simply seeing the different morphologies is not enough. Every time an image is displayed, a planetary scientist wants to know the isotope compositions and formation and exposure ages. The only way of doing this is by remotely analysing it or by bringing a sample back to Earth.

8.1 Inner Solar System

8.1.1 Mercury

The visit by the orbital Messenger spacecraft allowed detailed mapping of the surface, as well as some chemical characterisation, which was limited by the low X-ray flare activity of the Sun. The upcoming Bepi-Colombo mission will revisit a number of the aspects discovered by Messenger but this remains a remote sensing mission. There will be no touchdown and no future touchdowns are planned.

8.1.2 Venus

The isotopic composition of Venus atmosphere was measured in two experiments during the Pioneer mission. During mission periapsis, upper atmosphere samples were analysed with the on-board neutral quadrupole mass spectrometer. It was found that $^{18}O/^{16}O$ and $^{17}O/^{16}O$ are within $\pm 5\%$ uncertainty of terrestrial (Niemann et al. 1979). Similar results were obtained with the single focussing magnetic sector mass spectrometer. Hoffman et al. (1979) reported that the $^{18}O/^{16}O$ of CO_2 was found to be within 1% of terrestrial but with a large uncertainty of $\pm 5\%$. The uncertainties of these measurements effectively cover the full range of terrestrial compositions and so refinement of these abundances is required.

Ten probes have landed on Venus. Of note were the 1978 Venera 9 and 10 spacecraft, which managed to transmit images of the Venusian surface back to Earth. Of most geochemical interest was the Venera 13 and 14 surface landers, which carried an XRF for soil analysis and a mass spectrometer for determining the atmospheric composition. Venus is covered by surface basalts of predicted age less than c. 500 Ma based on radar observations and crater counting. No current plans are in place to land and sample Venus, or to return a sample.

8.1.3 Mars

Mars is our most attractive planetary neighbour being readily accessible every two years with a relatively small Δv. Many landers have sampled the atmosphere and lithosphere with increasingly sophisticated methodologies. Despite all the successful missions, we are still left with a nagging question—Are SNC meteorites really from Mars? While the D/H

and planetary gas compositions suggest they are, it won't be satisfactorily resolved in many geochemical minds until a rock demonstrably from Mars is shown to have $\Delta^{17}O$ of $+0.30‰$.

It is certain from lander, orbiter missions and secondary mineral assemblages in martian meteorites that Mars has likely had an active hydrological cycle in the past and so detailed comparisons with the terrestrial water cycle are eagerly anticipated. ExoMars and the NASA Mars2020 missions are the latest to head to Mars in the search for life. Mars2020 is expected to obtain and sequester a number of samples for a prospective future return to Earth by 2032.

8.1.4 Asteroids

One asteroid, the S-type 25103 Itokawa, has been visited and a sample collected and returned to Earth for analysis. The result was that Itokawa has been clearly identified as a parent body of equilibrated LL chondrite meteorites. The oxygen isotope compositions of the returned samples is uniform at around $\Delta^{17}O$ of $+1.2‰$.

Hayabusa 2 surveyed the asteroid Ryugu for a year and a half and took samples. It left the asteroid in November 2019. OSIRIS-REx arrived at Bennu in December 2018 and is currently mapping the asteroid in detail. Samples are expected to return in late 2020 and 2023 respectively. Returned samples will resolve some of the issues relating C-type asteroids to carbonaceous chondrites. Oxygen isotopes will provide a strong context for relating the mineralogies described to samples within the existing meteorite catalog.

In terms of a sample return mission to a well-defined and scientifically important achondritic parent body, asteroid 4 Vesta is undoubtedly a prime target. Remote sensing studies by the NASA Dawn spacecraft have already furnished a wealth of information about this body (Russell et al. 2015). With well over 2000 officially recognised specimens, the HED meteorites are by far and away the most important achondrite group (∼75% of all achondritic meteorites). HEDs also have a diagnostic oxygen isotope composition (Greenwood et al. 2017). With the exception of planetary achondrites (see below), sample return from Vesta would validate, or otherwise, what appears to be the strongest meteorite-parent body relationship so far delineated. A returned sample would also help define the extent of oxygen isotope homogenization on Vesta. Basaltic achondrites with anomalous oxygen isotope compositions are presumed to be from differentiated asteroids other than Vesta (Greenwood et al. 2017). However, this remains an untested assumption and it is possible that Vesta is significantly more isotopically heterogeneous than is currently thought to be the case. A sample return mission to Vesta would directly address this issue.

8.1.5 Comets (Jupiter Class)

The Stardust mission performed a flyby with samples returned to Earth. These samples showed that comets were not as pristine as we thought, and oxygen isotopes showed that inner solar system material was transported out to the outer solar system when the comet parent bodies were forming.

The Rosetta-Philae mission to 67P/Churyumov-Gerasimenko provided a wealth of new data concerning the makeup of comets. However, the Philae touchdown did not proceed as planned. The anchor screws did not connect sending Philae bouncing over the surface in an uncontrolled manner. As such, high precision mass spectrometry of the comet surface was not obtained and analysing cometary ice remains a priority.

8.2 Outer Solar System

8.2.1 Gas and Ice Giants, and Pluto

The determination of isotopic compositions on Jupiter, Saturn, Uranus and Neptune is simply an issue of atmospheric sampling. No solid surfaces exist on these planets. Missions have mainly included flybys, but the atmospheric sampler on Galileo and the Huygens probe to the surface of Titan demonstrate that in situ analysis is possible.

8.2.2 Moons

The moons of the outer solar system planets offer a far more compelling case for geochemical analysis. From the basalt volcanoes on Io to the cryovolcanoes on Enceladus and Triton, much could be learned from detailed sampling concerning rock and water ice oxygen isotope compositions. From the Jupiter system alone, silicates from Io and ice compositions on Europa, Ganymede, Callisto would be of fundamental importance. The imaging of the surface of Titan shows a highly varied landscape and any mass spectrometric measurements on the surface of Titan would inform regarding the hydrocarbon cycle. The fly through of cryovolcanic ejecta on Enceladus indicated the presence of water ice.

8.2.3 Comets and KBOs

Obtaining samples from outer solar system comets and KBOs would provide a new constraint on the radial distribution of oxygen isotopes in the solar system. Ice alone would provide new constraints on the role of PSS in determining oxygen isotope compositions in the early solar system. Even a bulk sample of the silicates would prove invaluable in constraining the nature of dust and dust processing in the solar nebula.

9 Samples and Analysis

9.1 Priorities

The main priority to be addressed here is determining the oxygen isotope structure of our solar system. The PSS model provides a strong interpretative model for understanding oxygen isotope fractionations and obtaining analyses of water and silicate dust is essential. The clear element that is missing in this context is water and dust oxygen isotope compositions in the outer solar system. But, we also need better constraints on inner solar system planetary bodies.

The NASA mantra of “follow the water” is entirely attractive in this context. Water is the most common molecular compound in the solar system and its abundance reflects the gross thermal structure of the solar system. In terms of solar system structure, the ability to make oxygen isotope analyses is key. Water is routinely analysed by several forms of mass spectrometry, however, the key to unlocking the structure of our solar system is the ability to make three oxygen isotope measurements at high precision and accuracy. In addition, the coupled measurements of analysis of silicate dust is important in providing an understanding of the history of the solar system. These coupled measurements place stringent requirements on both remote analysis and sample return.

9.2 Remote Analysis

The issues concerning analysis of three oxygen isotopes relate to an integration of sample preparation and mass spectrometry. The key for remote analysis is to have a relatively light, low power consumption device capable of high resolution and high precision of triple oxygen isotopes.

Many of the systems that have been flown rely on the analysis of gas (and related ion) species that are formed in the outgassing of objects such as comets and outer solar system moons. Dust analysis has relied largely on the evaporation upon high energy collision with a conversion plate. However, in order to analyse silicate dust and to raise the signals to achieve high precision analysis, a means of direct sampling is required.

In terrestrial laboratories, the sample preparation has been based on obtaining a sample of pure oxygen to eliminate the isobaric interferences inherent in CO_2 mass spectrometry commonly used for $^{18}O/^{16}O$ analysis. This is achieved by reacting silicates with fluorine reagents (F_2, BrF_5), which are extremely difficult to handle. For mass spectrometry, the fundamental requirement is to analyse the $^{18}O/^{16}O$ ratio (at and abundance ratio of 1/500) and $^{17}O/^{16}O$ (at $1/2500$). This may not seem a big difference in the ratio, but getting sufficient sample to generate a high signal to noise makes this quite a difficult measurement. In magnetic sector mass spectrometry, the ion beam can be brought into optimized collectors to allow simultaneous measurement of the three isotopes to high precision. This is used in gas source mass spectrometry and secondary ion mass spectrometry. However, a heavy magnetic sector mass spectrometer is not well suited to space flight.

Despite these obstacles, many elements of a successful triple oxygen isotope analysis have already flown on space flights. For water analysis, the double-focussing mass spectrometer in ROSINA was capable of getting to high mass resolution to separate water isotopologues (ca. 3000 $M/\Delta M$), but in doing so gaussian peak shapes were produced, which are not amenable to high precision/accuracy measurements. On Philae, the sample preparation system SD2 included an elaborate chemical laboratory with multiple ovens and reaction vessels (Finzi et al. 2007); unfortunately this could not be operated because of the landing difficulties experienced by Philae.

There are a number of specific modifications that could be made to improve versatility and reliability. Flying fluorine reagents is potentially problematic in terms of valve operation. An alternative methodology could be based on reaction of evaporated/pyrolyzed oxygen with graphite, which could be purified ^{12}C as was used in the Genesis wafers, to avoid the ^{13}C isobars in mass spectrometric analysis. This would potentially work well for both dust and ice analysis.

With chemical separation available, a low mass resolution magnetic sector mass spectrometer is capable of separating the oxygen-bearing ions, without the high resolution required for water ion analysis. A lighter magnetic sector mass spectrometer would be the best system for this type of analysis with the demonstrated capability of high precision and high accuracy.

TOF has been the preferred method of mass spectrometry in space because of low overall weight and a relatively simple electronic configuration. An example of an upcoming TOF-MS is the MASPEX instrument to fly on Europa Clipper (Brockwell et al. 2016). It has a flight weight of 8 kg. This TOF-MS is capable of high sensitivity and 30000 $M/\Delta M$. The main objective is to be able to identify different organic compounds based on their small mass differences. This then has the mass resolution capabilities for carrying out oxygen three isotopes, but obtaining high precision isotope measurements on TOF-MS systems remains a tricky prospect. Other forms of mass spectrometers based around time of flight

include cyclotrons and the MULTUM II (a multi-turn TOF MS; Tonotani et al. 2016). But these are still based on bunches of a relatively small number of ions whereas high precision measurement requires a large number of ions to satisfy counting statistics.

Cavity Ring Down Spectrometry is a different type of measurement technology, based on optical spectroscopy and can be used in the field on Earth. Still, operation in space is a different story to operating on Earth and it remains to be seen if the instrumentation is sufficiently stable and robust to be capable of remote analysis. Ice measurement through water analysis is a definite possibility. If silicate oxygen could be released to form water, or CO_2, this would extend this capability.

9.3 Sample Return

The benefits of sample return in terms of analysis and sample documentation are immense. Hayabusa brought back 1500 grains of dust from Itokawa; this was sufficient to fully document a wide range of petrology, morphology, as well as isotopic systems. A timely approach to analysis can be carried out maximising the benefit of a single sample or indeed a single grain. Sample return allows optimised analytical conditions to get high precision and accuracy. Contamination can be assessed. Another important advantage of sample return is repeatability of measurements. Analysing a similar aliquot remotely is likely not possible with current technology.

The limitations to sample return are related to the logistics of bringing a sample capsule back to Earth. The asteroid return samples show that this is practical, and even the Stardust mission to a comet brought back the first solid mineral fragments thereof. However, these are all ostensibly inner solar system missions and with Δv back to Earth at a reasonable level.

The Hayabusa mission to Itokawa involved a Δv of only 0.5 km/s which was achievable through the ion engines. In coming back to Earth, the additional velocity was allowed for in the re-entry of the sample capsule. All sample return missions achieved so far are the same method. Even the return of Stardust followed this approach. The Earth re-entry already starts at 11 km/s and a small increment on top of this is not a major issue.

So a Mars return is feasible from the Earth reentry point of view. The difficulty for Mars sample return lies in the entry and exit from Mars itself. Getting samples from the Mars surface is currently being planned but remains a difficult and expensive logistical task.

For the asteroid belt, a potential Δv of 5 km/s becomes more daunting for direct re-entry. As such some form deceleration will likely be required either through engines, or through progressive atmospheric braking in Earth's or another planet's gravity well. The issue then becomes the duration of the mission. The Dawn mission lifted off in 2007 and took four years to get to Vesta; Dawn arrived at Ceres in 2015 and the mission was terminated in 2018. If a sample return mission was launched to Ceres a sample return would likely require at least 10 years depending on orbital alignment and profligacy of fuel expenditure.

It took Juno 5 years to reach Jupiter orbit. A mission to sample the Galilean Moons and return would be difficult not only for the entry and exit of Jupiter's gravitational well, but also the radiation coming from Jupiter. Add to this the issues of taking off from a sizeable planetary body. Potentially a mission to Callisto would be energetically more favourable but this would likely only result in the return of ice, and potentially contaminated with Trojan dust. A mission to Io, home of the furthest silicate volcanism from the Sun, would be highly desirable, but may be a step too far at this stage.

Inward from Earth are Venus and Mercury. A sample return from Venus involves many difficulties related to Venus mass, heavy atmosphere, surface heat, and then an uphill run

home. Mercury might be easier on all fronts to land and take a sample, but it also represents a major difficulty in coming out of Mercury and coming back to Earth.

10 Concluding Remarks

Sampling extraterrestrial bodies is an essential ingredient in understanding the provenance of our solar system. While much material is available to us for free through meteorites, obtaining the details of location and history of the particular source body is essential to reconstruct distributions of materials in the early solar system. Still, meteorites have shown us a lot, and oxygen isotope analysis has proven to be a particularly powerful classification tool because individual parent bodies can have a unique identifier in their triple oxygen isotope compositions. The source of these anomalies are likely related to chemical speciation of oxygen isotope carriers and specifically silicate dust, nebular water and carbon monoxide through predissociation and self-shielding likely in the primordial molecular cloud. This is supported by the Genesis mission where the Earth has been shown to be enriched in ^{17}O and ^{18}O relative to the Sun. Another prediction of this model is that outer solar system silicates should be closer to solar oxygen in isotope composition and should be accompanied by isotopically heavy oxygen (^{17}O, ^{18}O-rich) water ice. There is also evidence in chondrites for ^{16}O-poor hydrous activity on the asteroidal parent bodies from the inner Solar System. However, mineralogical and oxygen isotopic analyses of material returned by the Stardust mission from the coma of 81P/Wild2 hint at the complexities recorded in material from the earliest Solar System. Wild2 grains have chondrite-like mineral assemblages and isotopic characteristics.

Obtaining remote triple oxygen isotope analyses of water in the outer solar system appears achievable in the medium term. This would allow some further context to be placed on the oxygen isotope systematics of the entire solar system. However, a silicate analysis would require a completely new chemical separation procedure, as well as new methodologies to measure the triple oxygen isotope abundance. Sample return from the outer solar system would allow a direct test of some of the predictions of the PSS model, but is energy and time expensive. Sample return from the inner solar system planets will allow material to be analysed with the best analytical capability and precision, as well as allowing characterisation of the samples with an arsenal of analytical techniques. Studies of martian meteorites have established that such samples will not only reveal the details of crustal oxygen and other isotopic reservoirs but also a record of atmospheric interactions.

Acknowledgements TRI and RCG acknowledge ISSI support to attend the Europlanet & International Space Science Institute Workshop on the *Role of Sample Return in Addressing Major Outstanding Questions in Planetary Sciences* held in Bern, Switzerland, 5-9 February 2018. We are grateful to the two reviewers whose suggestions significantly improved the manuscript and to the patience of Mahesh Anand. RCG is funded through a Consolidated Grant from the Science and Technology Facilities Council (STFC), UK Grant Number: ST/L000776/1. LJH and JCB are funded by STFC grant ST/S000429/1. TRI was supported by Australian Research Council Discovery Project Grant DP190102760. Thanks to all our friends and colleagues at ESA, JAXA, and NASA.

References

C.B. Agee, N.V. Wilson, F.M. McCubbin, K. Ziegler, V.J. Polyak, Z.D. Sharp, Y. Asmerom, M.H. Nunn, R. Shaheen, M.H. Thiemens, A. Steele, M.L. Fogel, R. Bowden, M. Glamoclija, Z. Zhang, S.M. Elardo,

Unique meteorite from early Amazonian Mars: Water-rich basaltic breccia Northwest Africa 7034. Science **339**, 780–785 (2013). https://doi.org/10.1126/science.1228858
C.M.O'D. Alexander, D.J. Barber, R. Hutchison, The microstructure of Semarkona and Bishunpur. Geochim. Cosmochim. Acta **53**, 3045–3057 (1989). https://doi.org/10.1016/0016-7037(89)90180-4
A. Ali, I. Jabeen, D. Gregory, R. Verish, N.R. Banerjee, New triple oxygen isotope data of bulk and separated fractions from SNC meteorites: Evidence for mantle homogeneity of Mars. Meteorit. Planet. Sci. **51**, 981–995 (2016). https://doi.org/10.1111/maps.12640
ALMA Partnership et al., The 2014 ALMA long baseline campaign: First results from high angular resolution observations toward the HL Tau region. Astrophys. J. Lett. **808**, L3 (2015). https://doi.org/10.1088/2041-8205/808/1/L3
K. Altwegg et al., 67P/Churyumov-Gerasimenko, a Jupiter family comet with a high D/H ratio. Science **347**, 1261952 (2015). https://doi.org/10.1126/science.1261952
E. Anders, E. Zinner, Interstellar grains in primitive meteorites: Diamond, silicon carbide, and graphite. Meteoritics **28**, 490–514 (1993). https://doi.org/10.1111/j.1945-5100.1993.tb00274.x
R.M.G. Armytage, R.B. Georg, H.M. Williams, A.N. Halliday, Silicon isotopes in lunar rocks: Implications for the Moon's formation and the early history of the Earth. Geochim. Cosmochim. Acta **77**, 504–524 (2012). https://doi.org/10.1016/j.gca.2011.10.032
J.N. Ávila, M. Lugaro, T.R. Ireland, F. Gyngard, E. Zinner, S. Cristallo, P. Holden, J. Buntain, S. Amari, A. Karakas, Tungsten isotopic compositions in Stardust SiC grains from the Murchison meteorite: Constraints on the s-process in the Hf-Ta-W-Re-Os region. Astrophys. J. **744**, 49–62 (2012). https://doi.org/10.1088/0004-637X/744/1/49
J.N. Ávila, T.R. Ireland, F. Gyngard, E. Zinner, G. Malmann, P. Holden, S. Amari, Barium isotopic compositions in large Stardust SiC grains from the Murchison meteorite: A cautionary tale of unresolved mass interferences. Geochim. Cosmochim. Acta **120**, 628–647 (2013a). https://doi.org/10.1016/j.gca.2013.03.039
J.N. Ávila, T.R. Ireland, M. Lugaro, F. Gyngard, E. Zinner, S. Cristallo, P. Holden, T. Rauscher, Europium s-process signature at close-to-solar metallicity in Stardust SiC grains from asymptotic giant branch stars. Astrophys. J. Lett. **768**, L18 (2013b). https://doi.org/10.1088/2041-8205/768/1/L18
J.N. Ávila, T.R. Ireland, P. Holden, P. Lanc, A. Latimore, N. Schram, J. Foster, I.S. Williams, L. Loiselle, B. Fu, High-precision, high-accuracy oxygen isotope measurements of zircon reference materials with the SHRIMP-SI. J. Geostand. Geoanal. Res. (2020, in press). https://doi.org/10.1111/ggr.12298
P. Baertschi, Absolute ^{18}O content of standard mean ocean water. Earth Planet. Sci. Lett. **31**, 341–344 (1976). https://doi.org/10.1016/0012-821X(76)90115-1
P. Baertschi, S.R. Silverman, The determination of relative abundances of the oxygen isotopes in silicate rocks. Geochim. Cosmochim. Acta **1**, 317–328 (1951). https://doi.org/10.1016/0016-7037(51)90006-3
J. Bally, W.D. Langer, Isotope-selective photodissociation of carbon monoxide. Astrophys. J. **255**, 143–148 (1982). https://doi.org/10.1086/159812
H. Balsiger, K. Altwegg, F. Bühler, J. Geiss, A.G. Ghielmetti, B.E. Goldstein, R. Goldstein, W.T. Huntress, W.-H. Ip, A.J. Lazarus, A. Meier, M. Neugebauer, U. Rettenmund, H. Rosenbauer, R. Schwenn, R.D. Sharp, E.G. Shelley, E. Ungstrup, D.T. Young, Ion composition and dynamics at comet Halley. Nature **321**, 330–334 (1986). https://doi.org/10.1038/321330a0
S.L.L. Barker, G.M. Dipple, F. Dong, D.S. Baer, Use of laser spectroscopy to measure the $^{13}C/^{12}C$ and $^{18}O/^{16}O$ compositions of carbonate minerals. Anal. Chem. **83**, 2220–2226 (2011). https://doi.org/10.1021/ac103111y
J-A. Barrat, R.C. Greenwood, K. Keil, M.L. Rouget, J.S. Boesenberg, B. Zanda, I.A. Franchi, The origin of aubrites: Evidence from lithophile trace element abundances and oxygen isotopic compositions. Geochim. Cosmochim. Acta **192**, 29–48 (2016). https://doi.org/10.1016/j.gca.2016.07.025
A. Basu Sarbadhikari, J.M.D. Day, Y. Liu, D. Rumble, L.A. Taylor, Petrogenesis of olivine-phyric shergottite Larkman Nunatak 06319: Implications for enriched components in martian basalts. Geochim. Cosmochim. Acta **73**, 2190–2214 (2009). https://doi.org/10.1016/j.gca.2009.01.012
A. Bischoff, M. Horstmann, A. Pack, M. Laubenstein, S. Haberer, Asteroid 2008 TC3—Almahata Sitta: A spectacular breccia containing many different ureilitic and chondritic lithologies. Meteorit. Planet. Sci. **45**, 1638–1656 (2010). https://doi.org/10.1111/j.1945-5100.2010.01108.x
A. Bischoff, N. Vogel, J. Roszjara, The Rumuruti chondrite group. Geochemistry **71**, 101–133 (2011). https://doi.org/10.1016/j.chemer.2011.02.005
A. Bischoff, M. Horstmann, J-A. Barrat, M. Chaussidon, A. Pack, D. Herwartz, D. Ward, C. Vollmer, S. Decker, Trachyandesitic volcanism in the early Solar System. Proc. Natl. Acad. Sci. USA **111**, 12689–12692 (2014). https://doi.org/10.1073/pnas.1404799111
J. Bradley, H. McSween, R. Harvey, Epitaxial growth of nanophase magnetite in martian meteorite Allan Hills 84001: Implications for biogenic mineralization. Meteorit. Planet. Sci. **33**, 765–773 (1998). https://doi.org/10.1111/j.1945-5100.1998.tb01682.x

A.J. Brearley, R.H. Jones, Chondritic meteorites, in *Planetary Materials*, ed. by J.J. Papike. Reviews in Mineralogy, vol. 36 (1998), pp. 3-1–3-398
J.C. Bridges, T.R. Ireland, Oxygen isotope analyses by SHRIMP of chondrules in highly unequilibrated Ll3 chondrites, in *Lunar and Planetary Science Conference XLVI* (2015), abstract #1674
J.C. Bridges, S.P. Schwenzer, The nakhlite hydrothermal brine on Mars. Earth Planet. Sci. Lett. **359–360**, 117–123 (2012). https://doi.org/10.1016/j.epsl.2012.09.044
J.C. Bridges, P.H. Warren, The SNC meteorites: Basaltic igneous processes on Mars. J. Geol. Soc., Lond. **163**, 229–251 (2006). https://doi.org/10.1144/0016-764904-501
J.C. Bridges, I.A. Franchi, R. Hutchison, A.D. Morse, J.V.P. Long, C.T. Pillinger, Cristobalite- and tridymite-bearing clasts in Parnallee (LL3) and Farmington (L5). Meteoritics **30**, 715–727 (1995). https://doi.org/10.1111/j.1945-5100.1995.tb01169.x
J.C. Bridges, I.A. Franchi, A.S. Sexton, C.T. Pillinger, Mineralogical controls on the oxygen isotopic compositions of UOCs. Geochim. Cosmochim. Acta **63**, 945–951 (1999). https://doi.org/10.1016/S0016-7037(98)00317-2
J.C. Bridges, D.C. Catling, J.M. Saxton, T.D. Swindle, I.C. Lyon, M.M. Grady, Alteration assemblages in martian meteorites: Implications for near-surface processes, in *Evolution of Mars*, ed. by R. Kallenbach, J. Geiss, W.K. Hartmann (Kluwer, Dordrecht, 2001), pp. 365–392. https://doi.org/10.1023/A:101196582 [also published in Space Sci. Rev. **96**, 365–392 (2001)]
J.C. Bridges, H.G. Changela, S. Nayakshin, N.A. Starkey, I.A. Franchi, Chondrule fragments from Comet Wild2: Evidence for high temperature processing in the outer solar system. Earth Planet. Sci. Lett. **341–344**, 186–194 (2012). https://doi.org/10.1016/j.epsl.2012.06.011
J.C. Bridges, L.J. Hicks, A. Treiman, Carbonates on Mars, in *Volatiles in the Martian Crust*, ed. by J. Filiberto, S.P. Schwenzer (Elsevier, Amsterdam, 2019), pp. 89–118. https://doi.org/10.1016/B978-0-12-804191-8.00005-2
T.G. Brockwell, K.J. Meech, K. Pickens, J.H. Waite, G. Miller, J. Roberts, J.I. Lunine et al., The mass spectrometer for planetary exploration (MASPEX), in *IEEE Aerospace Conference* (2016). https://doi.org/10.1109/AERO.2016.7500777
D. Brownlee et al., Comet 81P/Wild 2 under a microscope. Science **314**, 1711–1716 (2006). https://doi.org/10.1126/science.1135840
E.M. Burbidge, G.R. Burbidge, W.A. Fowler, F. Hoyle, Synthesis of the elements in stars. Rev. Mod. Phys. **29**, 547–650 (1957). https://doi.org/10.1103/RevModPhys.29.547
T. Burbine, *Asteroids: Astronomical and Geological Bodies*, Cambridge Planetary Science (Cambridge University Press, Cambridge, 2016). https://doi.org/10.1017/9781316156582
M.J. Burchell, S.A.J. Fairey, P. Wozniakiewicz, D.E. Brownlee, F. Hörz, A.T. Kearsley, T.H.S.P. Tsou, A. Westphal, S.F. Green, J.M. Trigo-Rodríguez, G. Domingúez, Characteristics of cometary dust tracks in Stardust aerogel and laboratory calibrations. Meteorit. Planet. Sci. **43**, 23–40 (2008). https://doi.org/10.1111/j.1945-5100.2008.tb00608.x
D.S. Burnett (Genesis Science Team), Solar composition from the Genesis Discovery Mission. Proc. Natl. Acad. Sci. **108**, 19147–19151 (2011). https://doi.org/10.1073/pnas.1014877108
D.S. Burnett, B.L. Barraclough, R. Bennett, M. Neugebauer, L.P. Oldham, C.N. Sasaki, D. Sevilla, N. Smith, E. Stansbery, D. Sweetnam, R.C. Wiens, Genesis discovery mission: Return of solar matter to Earth. Space Sci. Rev. **105**, 509–534 (2003). https://doi.org/10.1023/A:1024425810605
A.G.W. Cameron, J.W. Truran, The supernova trigger for formation of the solar system. Icarus **30**, 447–461 (1977). https://doi.org/10.1016/0019-1035(77)90101-4
A.G.W. Cameron, W.R. Ward, The origin of the Moon, in *7th Lunar and Planetary Science Conference*, vol. 7 (1976), pp. 120–122 (abstract)
R.M. Canup, Forming a Moon with an Earth-like composition via a giant impact. Science **338**, 1052–1055 (2012). https://doi.org/10.1126/science.1226073
R.M. Canup, E. Asphaug, Origin of the Moon in a giant impact near the end of the Earth's formation. Nature **412**, 708–712 (2001). https://doi.org/10.1038/35089010
C.D. Cappa, M.B. Hendricks, D.J. DePaolo, R.C. Cohen, Isotopic fractionation of water during evaporation. J. Geophys. Res., Atmos. **108**, 4525 (2003). https://doi.org/10.1029/2003JD003597
N.L. Chabot, H. Haack, Evolution of asteroidal cores, in *Meteorites and the Early Solar System II*, ed. by D.S. Lauretta, H.Y. McSween Jr. (University of Arizona Press, Tucson, 2006), pp. 747–771, 943 pp.
B.-G. Choi, K.D. McKeegan, A.N. Krot, J.T. Wasson, Extreme oxygen-isotope compositions in magnetite from unequilibrated ordinary chondrites. Nature **392**, 577–579 (1998). https://doi.org/10.1038/33356
R.N. Clayton, Oxygen isotopes in meteorites. Annu. Rev. Earth Planet. Sci. **21**, 15–149 (1993). https://doi.org/10.1146/annurev.ea.21.050193.000555
R.N. Clayton, Self-shielding in the solar nebula. Nature **415**, 860–861 (2002). https://doi.org/10.1038/415860b

R.N. Clayton, Oxygen isotopes in the solar system. Space Sci. Rev. **106**, 19–32 (2003). https://doi.org/10.1023/A:102466911

R.N. Clayton, T.K. Mayeda, The use of bromine pentafluoride in the extraction of oxygen from oxides and silicates for isotopic analysis. Geochim. Cosmochim. Acta **27**, 43–52 (1963). https://doi.org/10.1016/0016-7037(63)90071-1

R.N. Clayton, T.K. Mayeda, Oxygen isotope studies of achondrites. Geochim. Cosmochim. Acta **60**, 1999–2017 (1996). https://doi.org/10.1016/0016-7037(96)00074-9

R.N. Clayton, T.K. Mayeda, Oxygen isotope studies of carbonaceous chondrites. Geochim. Cosmochim. Acta **63**, 2089–2104 (1999). https://doi.org/10.1016/S0016-7037(99)00090-3

R.N. Clayton, L. Grossman, T.K. Mayeda, A component of primitive nuclear composition in carbonaceous meteorites. Science **182**, 485–488 (1973). https://doi.org/10.1126/science.182.4111.485

R.N. Clayton, N. Onuma, T.K. Mayeda, A classification of meteorites based on oxygen isotopes. Earth Planet. Sci. Lett. **30**, 10–18 (1976). https://doi.org/10.1016/0012-821X(76)90003-0

R.N. Clayton, N. Onuma, L. Grossman, T.K. Mayeda, Distribution of the pre-solar component in Allende and other carbonaceous chondrites. Earth Planet. Sci. Lett. **34**, 209–224 (1977). https://doi.org/10.1016/0012-821X(77)90005-X

R.N. Clayton, N. Onuma, Y. Ikeda, T.K. Mayeda, I.D. Hutcheon, E.J. Olsen, C. Molini-Velsko, Oxygen isotopic compositions of chondrules in Allende and ordinary chondrites, in *Chondrules and Their Origins*, ed. by E.A. King (1983), pp. 37–43

R.N. Clayton, T.K. Mayeda, A.E. Rubin, Oxygen isotopic compositions of enstatite chondrites and aubrites. J. Geophys. Res. **89**, 245–249 (1984). https://doi.org/10.1029/JB089iS01p0C245

R.N. Clayton, T.K. Mayeda, J.N. Goswami, E.J. Olsen, Oxygen isotope studies of ordinary chondrites. Geochim. Cosmochim. Acta **55**, 2317–2337 (1991). https://doi.org/10.1016/0016-7037(91)90107-G

P. Cloud, Paleoecological significance of the banded iron formation. Econ. Geol. **68**, 1135–1143 (1973). https://doi.org/10.2113/gsecongeo.68.7.1135

B.A. Cohen, C.A. Malespin, K.A. Farley, P.E. Martin, Y. Cho, P.R. Mahaffy, In situ geochronology on Mars and the development of future instrumentation. Astrobiology **19**(11), 1303–1314 (2019). https://doi.org/10.1089/ast.2018.1871

J.N. Connelly, J. Bollard, M. Bizzarro, Pb–Pb chronometry and the early Solar System. Geochim. Cosmochim. Acta **201**, 345–363 (2017). https://doi.org/10.1016/j.gca.2016.10.044

H.C. Connolly Jr., R.H. Jones, Chondrules: The canonical and noncanonical views. J. Geophys. Res., Planets **121**, 1885–1899 (2016). https://doi.org/10.1002/2016JE005113

A. Cousin, V. Sautter, V. Payré, O. Forni, N. Mangold, O. Gasnault, L. Le Deit, J. Johnson, S. Maurice, M. Salvatore, R.C. Wiend, P. Gasda, W. Rapin, Classification of igneous rocks analyzed by ChemCam at Gale crater, Mars. Icarus **288**, 265–283 (2017). https://doi.org/10.1016/j.icarus.2017.01.014

H. Craig, Standard for reporting concentrations of deuterium and oxygen-18 in natural waters. Science **133**, 1833–1834 (1961). https://doi.org/10.1126/science.133.3467.1833

M. Ćuk, S.T. Stewart, Making the Moon from a fast-spinning Earth: A giant impact followed by resonant despinning. Science **338**, 1047–1052 (2012). https://doi.org/10.1126/science.1225542

W. Dansgaard, Stable isotopes in precipitation. Tellus **16**, 436–468 (1964). https://doi.org/10.1111/j.2153-3490.1964.tb00181.x

J.R. Darling, D.E. Moser, I.R. Barker, K.T. Tait, K.R. Chamberlain, A.K. Schmitt, B.C. Hyde, Variable microstructural response of baddeleyite to shock metamorphism in young basaltic shergottite NWA 5298 and improved U–Pb dating of Solar System events. Earth Planet. Sci. Lett. **444**, 1–12 (2016). https://doi.org/10.1016/j.epsl.2016.03.032

N. Dauphas, The isotopic nature of the Earth's accreting material throughout time. Nature **541**, 521–524 (2017). https://doi.org/10.1038/nature20830

N. Dauphas, C. Burkhardt, P.H. Warren, F-Z. Teng, Geochemical arguments for an Earth-like Moon-forming impactor. Philos. Trans. R. Soc. Lond. A **372**, 20130244 (2014). https://doi.org/10.1098/rsta.2013.0244

F.E. DeMeo, R.P. Binzel, S.M. Slivan, S.J. Bus, An extension of the Bus asteroid taxonomy into the near-infrared. Icarus **202**, 160–180 (2009). https://doi.org/10.1016/j.icarus.2009.02.005

S.J. Desch, H.C. Connolly Jr., A model of the thermal processing of particles in solar nebula shocks: Application to the cooling rates of chondrules. Meteorit. Planet. Sci. **37**, 183–207 (2010). https://doi.org/10.1111/j.1945-5100.2002.tb01104.x

G. Dipierro, D. Price, G. Laibe, K. Hirsh, A. Cerioli, G. Lodato, On planet formation in HL Tau. Mon. Not. R. Astron. Soc. **453**, L73–L77 (2015). https://doi.org/10.1093/mnrasl/slv105

P.H. Edwards, J.C. Bridges, R.C. Wiens, R. Anderson, D. Dyar, M. Fisk, L. Thompson, P. Gasda, J. Filiberto, S.P. Schwenzer, D. Blaney, I. Hutchinson, Basalt-trachybasalt samples in gale crater, Mars. Meteorit. Planet. Sci. **52**, 2391–2410 (2017). https://doi.org/10.1111/maps.12953

J.M. Eiler, N. Kitchen, L. Leshin, M. Strausberg, Hosts of hydrogen in Allan Hills 84001: Evidence for hydrous martian salts in the oldest martian meteorite? Meteorit. Planet. Sci. **37**, 395–405 (2002). https://doi.org/10.1111/j.1945-5100.2002.tb00823.x

S. Epstein, R.P. Sharp, A.J. Gow, Six-year record of oxygen and hydrogen isotope variations in South Pole Firn. J. Geophys. Res. **70**, 1809–1814 (1965). https://doi.org/10.1029/JZ070i008p01809

A.J. Fahey, J.N. Goswami, K.D. McKeegan, E. Zinner, Evidence for extreme Ti-50 enrichments in primitive meteorites. Astrophys. J. Lett. **296**, L17–L20 (1985). https://doi.org/10.1086/184539

A.J. Fahey, J.N. Goswami, K.D. McKeegan, E.K. Zinner, O-16 excesses in Murchison and Murray hibonites—A case against a late supernova injection origin of isotopic anomalies in O, Mg, Ca, and Ti. Astrophys. J. Lett. **323**, L91–L95 (1987). https://doi.org/10.1086/185064

J. Farquhar, M.H. Thiemens, Oxygen cycle of the martian atmosphere-regolith system: Δ^{17}O of secondary phases in Nakhla and Lafayette. J. Geophys. Res., Planets **105**, 11991–11997 (2000). https://doi.org/10.1029/1999JE001194

J. Farquhar, M.H. Thiemens, T. Jackson, Atmosphere-surface interactions on Mars: Δ^{17}O measurements of carbonate from ALH 84001. Science **280**, 1580–1582 (1998). https://doi.org/10.1126/science.280.5369.1580

J. Farquhar, H. Bao, M. Thiemens, Atmospheric influence of Earth's earliest sulfur cycle. Science **289**, 756–758 (2000). https://doi.org/10.1126/science.289.5480.756

G. Faure, *Principles of Isotope Geology*, 2nd edn. (Wiley, New York, 1986), 589 pp.

J. Filiberto, E. Chin, J.M.D. Day, I.A. Franchi, R.C. Greenwood, J. Gross, S.C. Penniston-Dorland, S.P. Schwenzer, A.H. Treiman, Geochemistry of intermediate olivine-phyric shergottite Northwest Africa 6234, with similarities to basaltic shergottite Northwest Africa 480 and olivine-phyric shergottite Northwest Africa 2990. Meteorit. Planet. Sci. **47**, 1256–1273 (2012). https://doi.org/10.1111/j.1945-5100.2012.01382.x

A.E. Finzi, F.B. Zazzera, C. Dainese, F. Malnati, P.G. Magnani, E. Re, P. Bologna, S. Espinasse, A. Olivieri, SD2—How to sample a comet. Space Sci. Rev. **128**, 281–299 (2007). https://doi.org/10.1007/s11214-006-9134-6

C. Floss, P. Haenecour, Presolar silicate grains: Abundances, isotopic and elemental compositions, and the effects of secondary processing. Geochem. J. **50**, 3–25 (2016). https://doi.org/10.2343/geochemj.2.0377

I.A. Franchi, I.P. Wright, A.S. Sexton, C.T. Pillinger, The oxygen-isotopic composition of Earth and Mars. Meteorit. Planet. Sci. **34**, 657–661 (1999). https://doi.org/10.1111/j.1945-5100.1999.tb01371.x

A. Fujiwara, J. Kawaguchi, D.K. Yeomans, M. Abe, T. Mukai, T. Okada, J. Saito, H. Yano, M. Yoshikawa, D.J. Scheeres, O. Barnouin-Jha, A.F. Cheng, H. Demura, R.W. Gaskell, N. Hirata, H. Ikeda, T. Kominato, H. Miyamoto, A.M. Nakamura, R. Nakamura, S. Sasaki, K. Uesugi, The rubble-pile asteroid Itokawa as observed by Hayabusa. Science **312**, 1330–1334 (2006). https://doi.org/10.1126/science.1125841pmid:16741107

G.D. Garlick, S. Epstein, Oxygen isotope ratios in coexisting minerals of regionally metamorphosed rocks. Geochim. Cosmochim. Acta **31**, 181–214 (1967). https://doi.org/10.1016/S0016-7037(67)80044-9

B.J. Giletti, M.P. Semet, R.A. Yund, Studies in diffusion- III. Oxygen in feldspars: An ion microprobe determination. Geochim. Cosmochim. Acta **42**, 45–58 (1978). https://doi.org/10.1016/0016-7037(78)90215-6

F. Goesmann, H. Rosenbauer, R. Roll, C. Szopa, F. Raulin, R. Sternberg, G. Israel, U. Meierhenrich, W. Thiemann, G. Munoz-Caro, COSAC, the COmetary SAmpling and Composition experiment on Philae. Space Sci. Rev. **128**, 257–280 (2007). https://doi.org/10.1007/s11214-006-9000-6

J.L. Gooding, S.J. Wentworth, M.E. Zolensky, Aqueous alteration of the Nakhla meteorite. Meteoritics **26**, 135–143 (1991). https://doi.org/10.1111/j.1945-5100.1991.tb01029.x

S.F. Green, N. McBride, M.T.S.H. Colwell, J.A.M. McDonnell, A.J. Tuzzolino, T.E. Economou, B.C. Clark, Z. Sekanina, P. Tsou, D. Brownlee, Stardust Wild 2 dust measurements, in *Proc. "Dust in Planetary Systems" ESA SP-64*, ed. by H. Krueger, A. Graps (2007), pp. 35–44

R.C. Greenwood, I.A. Franchi, A. Jambon, J.A. Barrat, T.H. Burbine, Oxygen isotope variation in stony-iron meteorites. Science **313**, 1763–1765 (2006). https://science.sciencemag.org/content/313/5794/176

R.C. Greenwood, I.A. Franchi, J.M. Gibson, G.K. Benedix, Oxygen isotope variation in primitive achondrites: The influence of primordial, asteroidal and terrestrial processes. Geochim. Cosmochim. Acta **94**, 146–163 (2012). https://doi.org/10.1016/j.gca.2012.06.025

R.C. Greenwood, J-A. Barrat, E.R.D. Scott, H. Haack, P.C. Buchanan, I.A. Franchi, A. Yamaguchi, D. Johnson, A.W.R. Bevan, T.H. Burbine, Geochemistry and oxygen isotope composition of main-group pallasites and olivine-rich clasts in mesosiderites: Implications for the "Great Dunite Shortage" and HED-mesosiderite connection. Geochim. Cosmochim. Acta **169**, 115–136 (2015). https://doi.org/10.1016/j.gca.2015.07.023

R.C. Greenwood, T.H. Burbine, M.F. Miller, I.A. Franchi, Melting and differentiation of early-formed asteroids: The perspective from high precision oxygen isotope studies. Chem. Erde **77**, 1–43 (2017). https://doi.org/10.1016/j.chemer.2016.09.005

R.C. Greenwood, J-A. Barrat, M.F. Miller, M. Anand, N. Dauphas, I.A. Franchi, P. Sillard, N.A. Starkey, Oxygen isotopic evidence for accretion of Earth's water before a high-energy Moon-forming giant impact. Sci. Adv. **4**, eaao5928 (2018). https://doi.org/10.1126/sciadv.aao5928

R.C. Greenwood, M. Anand, What is the oxygen isotope composition of Venus? The scientific case for sample return from Earth's "sister" planet. Space Sci. Rev. (2020, accepted)

R.C. Greenwood, T.H. Burbine, I.A. Franchi, Linking asteroids and meteorites to the primordial planetesimal population. Geochim. Cosmochim. Acta (2020, accepted). https://doi.org/10.1016/j.gca.2020.02.004

L. Grossman, Condensation in the primitive solar nebula. Geochim. Cosmochim. Acta **36**, 597–619 (1972). https://doi.org/10.1016/0016-7037(72)90078-6

L. Grossman, Petrography and mineral chemistry of Ca-rich inclusions in the Allende Meteorite. Geochim. Cosmochim. Acta **39**, 433–454 (1975). https://doi.org/10.1016/0016-7037(75)90099-X

J.N. Grossman, C.M.O'D. Alexander, J. Wang, A.J. Brearley, Bleached chondrules: Evidence for widespread aqueous processes on the parent asteroids of ordinary chondrites. Meteorit. Planet. Sci. **35**, 467–486 (2000). https://doi.org/10.1111/j.1945-5100.2000.tb01429.x

F. Gyngard, E. Zinner, L.R. Nittler, A. Morgand, F.J. Stadermann, K.M. Hynes, Automated NanoSIMS measurements of spinel Stardust from the Murray meteorite. Astrophys. J. **717**, 107–120 (2010). https://doi.org/10.1088/0004-637X/717/1/107

M.K. Haba, J-F. Wotzlaw, Y-J. Lai, A. Yamaguchi, M. Schönbächler, Mesosiderite formation on asteroid 4 Vesta by a hit-and-run collision. Nat. Geosci. **12**, 510–515 (2019). https://doi.org/10.1038/s41561-019-0377-8

L.J. Hallis, M. Anand, R.C. Greenwood, M.F. Miller, I.A. Franchi, S.S. Russell, The oxygen isotope composition, petrology and geochemistry of mare basalts: Evidence for large-scale compositional variation in the lunar mantle. Geochim. Cosmochim. Acta **74**, 6885–6899 (2010). https://doi.org/10.1016/j.gca.2010.09.023

B. Hapke, Space weathering from Mercury to the asteroid belt. J. Geophys. **106**, 10039–10074 (2001). https://doi.org/10.1029/2000JE001338

W.K. Hartmann, D.R. Davis, Satellite-sized planetesimals and lunar origin. Icarus **24**, 504–514 (1975). https://doi.org/10.1016/0019-1035(75)90070-6

K. Hashizume, N. Takahata, H. Naraoka, Y. Sano, Oxygen isotope anomaly with a solar origin detected in meteoritic organics. Nat. Geosci. **4**, 165–168 (2011). https://doi.org/10.1038/NGEO1070

M. Hässig, K. Altwegg, H. Balsiger, J.J. Berthelier, U. Calmonte, M. Combi, J. De Keyser, B. Fiethe, S.A. Fuselier, M. Rubin, ROSINA/DFMS capabilities to measure isotopic ratios in water at comet 67P/Churyumov–Gerasimenko. Planet. Space Sci. **84**, 148–152 (2013). https://doi.org/10.1016/j.pss.2013.05.014

J.E. Heidenreich III, M.H. Thiemens, A non-mass-dependent oxygen isotope effect in the production of ozone from molecular oxygen: The role of molecular symmetry in isotope chemistry. J. Chem. Phys. **84**, 2129 (1986). https://doi.org/10.1063/1.450373

C.D.K. Herd et al., The Northwest Africa 8159 martian meteorite: Expanding the martian sample suite to the early Amazonian. Geochim. Cosmochim. Acta **218**, 1–26 (2017). https://doi.org/10.1016/j.gca.2017.08.037

D. Herwartz, A. Pack, B. Friedrichs, A. Bischoff, Identification of the giant impactor Theia in lunar rocks. Science **344**, 1146–1150 (2014). https://doi.org/10.1126/science.1251117

H.R. Heydegger, J. Foster, W. Compston, Evidence of a new isotopic anomaly from titanium isotopic ratios in meteoric materials. Nature **278**, 704–707 (1979). https://doi.org/10.1038/278704a0

L.J. Hicks, J.C. Bridges, S.J. Gurman, Ferric saponite and serpentine in the nakhlite martian meteorites. Geochim. Cosmochim. Acta **136**, 194–210 (2014). https://doi.org/10.1016/j.gca.2014.04.010

L.J. Hicks, J. MacArthur, J.C. Bridges, M. Price, J. Wickham-Eade, M. Burchell, G. Hansford, A. Butterworth, S.J. Gurman, S. Baker, Magnetite in Comet Wild 2: Evidence for parent body aqueous alteration. Meteorit. Planet. Sci. **52**, 2075–2096 (2017). https://doi.org/10.1111/maps.12909

J. Hoefs, *Stable Isotope Geochemistry*, 6th edn., vol. 285 (Springer, Berlin, 2009)

J.H. Hoffman, R.R. Hodges Jr., M.B. McElroy, T.M. Donahue, M. Kolpin, Composition and structure of the Venus atmosphere: Results from pioneer Venus. Science **205**, 49–52 (1979). https://doi.org/10.1126/science.205.4401.49

H. Holland, The oxygenation of the atmosphere and oceans. Philos. Trans. R. Soc. B **361**, 903–915 (2006). https://doi.org/10.1098/rstb.2006.1838

G. Holland, J.M. Saxton, I.C. Lyon, G. Turner, Negative δ^{18}O values in Allan Hills 84001 carbonate: Possible evidence for water precipitation on Mars. Geochim. Cosmochim. Acta **69**, 1359–1369 (2005). https://doi.org/10.1016/j.gca.2004.08.023

M. Horstmann, A. Bischoff, A. Pack, N. Albrecht, M. Weyrauch, H. Hain, L. Roggon, K. Schneider, Mineralogy and oxygen isotope composition of new samples from the Almahata Sitta strewn field, in *75th Annual Meeting of the Meteoritical Society, held August 12-17, 2012 in Cairns, Australia*. Published in Meteoritics and Planetary Science Supplement, id. 5052. http://adsabs.harvard.edu/abs/2012M&PSA..75.5052H

F. Hörz et al., Impact features on Stardust: Implications for Comet 81P/Wild 2 dust. Science **314**, 1716–1719 (2006). https://doi.org/10.1126/science.1135705

M. Humayun, A. Nemchin, B. Zanda, R.H. Hewins, M. Grange, A. Kennedy, J.-P. Lorand, C. Göpel, C. Fieni, S. Pont, D. Deldicque, Origin and age of the earliest martian crust from meteorite NWA 7533. Nature **503**, 513–516 (2013). https://doi.org/10.1038/nature12764

R. Hutchison, C.M.O'D. Alexander, D.J. Barber, The Semarkona meteorite: First recorded occurrence of smectite in an ordinary chondrite, and its implications. Geochim. Cosmochim. Acta **51**, 1875–1882 (1987). https://doi.org/10.1016/0016-7037(87)90178-5

R.B. Ickert, J. Hiess, I.S. Williams, P. Holden, T.R. Ireland, P. Lanc, N. Schram, J.J. Foster, S.W. Clement, Determining high precision, in situ, oxygen isotope ratios with a SHRIMP II: Analyses of MPI-DING silicate-glass reference materials and zircon from contrasting granites. Chem. Geol. **257**, 114–128 (2008). https://doi.org/10.1016/j.chemgeo.2008.08.024

T.R. Ireland, Presolar isotopic and chemical signatures in hibonite-bearing refractory inclusions from the Murchison carbonaceous chondrite. Geochim. Cosmochim. Acta **54**, 3219–3237 (1990). https://doi.org/10.1016/0016-7037(90)90136-9

T.R. Ireland, Oxygen isotope tracing of the solar system. Aust. J. Earth Sci. **59**, 225–236 (2012). https://doi.org/10.1080/08120099.2012.620626

T.R. Ireland, Ion microscopes and microprobes, in *Treatise on Geochemistry*, vol. 15, ed. by H.D. Holland, K.K. Turekian, 2nd edn. (Elsevier, Oxford, 2014), pp. 385–409

T.R. Ireland, B. Fegley Jr., The solar system's earliest chemistry: Systematics of refractory inclusions. Int. Geol. Rev. **42**, 865–894 (2000). https://doi.org/10.1080/00206810009465116

T.R. Ireland, E.K. Zinner, A.J. Fahey, T.M. Esat, Evidence for distillation in the formation of HAL and related hibonite inclusions. Geochim. Cosmochim. Acta **56**, 2503–2520 (1992). https://doi.org/10.1016/0016-7037(92)90205-W

T.R. Ireland, P. Holden, M.D. Norman, J. Clarke, Isotopic enhancements of ^{17}O and ^{18}O from solar wind particles in the lunar regolith. Nature **440**, 776–778 (2006). https://doi.org/10.1038/nature04611

T.R. Ireland, N. Schram, P. Holden, P. Lanc, J. Ávila, R. Armstrong, Y. Amelin, A. Latimore, D. Corrigan, S. Clement, J.J. Foster, W. Compston, Charge-mode electrometer measurements of S-isotopic compositions on SHRIMP-SI. Int. J. Mass Spectrom. **359**, 26–37 (2014). https://doi.org/10.1016/j.ijms.2013.12.020

A.J. Irving, S.M. Kuehner, C.D.K. Herd, M. Gellissen, R.L. Korotev, I. Puchtel, R.J. Walker, T. Lapen, D. Rumble, Petrologic, elemental and multi-isotopic characterization of permafic olivine-phyric shergottite northwest Africa 5789: A primitive magma derived from depleted martian mantle, in *41st Lunar and Planetary Science Conference* (2010), abstract #1547

H.A. Ishii, J.P. Bradley, Z.R. Dai, M. Chi, A.T. Kearsley, M.J. Burchell, N.D. Browning, F. Molster, Comparison of Comet 81P/WIld 2 dust with interplanetary dust from comets. Science **319**, 447–450 (2008). https://doi.org/10.1126/science.1150683

I. Jabeen, M. Kusakabe, Determination of δ^{17}O values of reference water samples VSMOW and SLAP. Chem. Geol. **143**, 115–119 (1997). https://doi.org/10.1016/S0009-2541(97)00109-5

M. Jadhav, E.K. Zinner, S. Amari, T. Maruoka, K.K. Marhas, R. Gallino, Multi-element isotopic analyses of presolar graphite grains from Orgueil. Geochim. Cosmochim. Acta **113**, 193–224 (2013). https://doi.org/10.1016/j.gca.2013.01.018

E. Jarosewich, R.S. Clarke Jr., J.N. Barrows, in *Allende Meteorite Reference Sample*. Smithsonian Contributions to the Earth Sciences, vol. 27 (1987), pp. 1–49. https://doi.org/10.5479/si.00810274.27.1

S. Johnsen, W. Dansgaard, H. Clausen et al., Oxygen isotope profiles through the Antarctic and Greenland ice sheets. Nature **235**, 429–434 (1972). https://doi.org/10.1038/235429a0

J.E. Johnson, A. Gerpheide, M.P. Lamb, W.W. Fischer, O_2 constraints from Paleoproterozoic detrital pyrite and uraninite. Geol. Soc. Am. Bull. **126**, 813–830 (2014). https://doi.org/10.1130/B30949

D.J. Joswiak, D. Nakashima, D.E. Brownlee, G. Matrajt, T. Ushikubo, N.T. Kita, S. Messenger, M. Ito, Terminal particle from Stardust track 130: Possible Al-rich chondrule fragment from comet Wild 2. Geochim. Cosmochim. Acta **144**, 277–298 (2014). https://doi.org/10.1016/j.gca.2014.08.017

H.R. Karlsson, R.N. Clayton, E.K. Gibson, T.K. Mayeda, Water in SNC meteorites—Evidence for a martian hydrosphere. Science **255**, 1409–1411 (1992). https://doi.org/10.1126/science.11537889

J. Kawaguchi, A. Fujiwara, T. Uesugi, Hayabusa—Its technology and science accomplishment summary and Hayabusa-2. Acta Astronaut. **62**, 639–647 (2008). https://doi.org/10.1016/j.actaastro.2008.01.028

Y. Kawai, T. Hondo, K.R. Jensen, M. Toyoda, K. Terada, Improved quantitative dynamic range of time-of-flight mass spectrometry by simultaneously waveform-averaging and ion-counting data acquisition. J. Am. Soc. Mass Spectrom. **29**, 1403–1407 (2018). https://doi.org/10.1007/s13361-018-1967-1

J. Kissel et al., Composition of comet Halley dust particles from Vega observations. Nature **321**, 280–282 (1986). https://doi.org/10.1038/321280a0

J. Kissel, F.R. Krueger, J. Silén, B.C. Clark, The Cometary Impact Dust Analyzer (CIDA). Science **304**, 1774–1776 (2004). https://doi.org/10.1126/science.1098836

S.S. Kistler, Coherent expanded aerogels and jellies. Nature **127**, 741 (1931). https://doi.org/10.1038/127741a0

N. Kita, T. Ushikubo, B. Fu, J. Valley, High precision SIMS oxygen isotope analysis and the effect of sample topography. Chem. Geol. **264**, 43–57 (2009). https://doi.org/10.1016/j.chemgeo.2009.02.012

N.T. Kita, H. Nagahara, S. Tachibana, S. Tomomura, M.J. Spicuzza, J.H. Fournelle, J.W. Valley, High precision SIMS oxygen three isotope study of chondrules in LL3 chondrites: Role of ambient gas during chondrule formation. Geochim. Cosmochim. Acta **74**, 6610–6635 (2010). https://doi.org/10.1016/j.gca.2010.08.011

S. Kobayashi, H. Imai, H. Yurimoto, New extreme ^{16}O-rich reservoir in the early solar system. Geochem. J. **37**, 663–669 (2003). https://doi.org/10.2343/geochemj.37.663

L. Kööp, A.M. Davis, D. Nakashima, C. Park, A.N. Krot, K. Nagashima, T.J. Tenner, P.R. Heck, N.T. Kita, A link between oxygen, calcium and titanium isotopes in ^{26}Al-poor hibonite-rich CAIs from Murchison and implications for the heterogeneity of dust reservoirs in the solar nebula. Geochim. Cosmochim. Acta **189**, 70–95 (2016). https://doi.org/10.1016/j.gca.2016.05.014

A.N. Krot, K. Keil, E.R.D. Scott, C.A. Goodrich, M.K. Weisberg, Classification of meteorites and their genetic relationships, in *Meteorites and Cosmochemical Processes, vol. 1, Treatise on Geochemistry*, ed. by A.M. Davis, 2nd edn. (Elsevier, Oxford, 2014), pp. 1–63

A.N. Krot, K. Nagashima, K. Fintor, E. Pal-Molnar, Evidence for oxygen-isotope exchange in refractory inclusions from Kaba (CV3.1) carbonaceous chondrite during fluid-rock interaction on the CV parent asteroid. Geochim. Cosmochim. Acta **246**, 419–435 (2019). https://doi.org/10.1016/j.gca.2018.11.002

T.S. Kruijer, C. Burkhardt, G. Budde, T. Kleine, Dating the formation of Jupiter. Proc. Natl. Acad. Sci. **114**, 6712–6716 (2017). https://doi.org/10.1073/pnas.1704461114

C.J. Lada, E.A. Lada, D.P. Clemens, J. Bally, Dust extinction and molecular gas in the dark cloud IC 5146. Astrophys. J. **429**, 694–709 (1994). https://doi.org/10.1086/174354

T.J. Lapen et al., Two billion years of magmatism recorded from a single Mars meteorite ejection site. Sci. Adv. **3**(2), e1600922 (2017). https://doi.org/10.1126/sciadv.1600922

D.S. Lauretta et al., The unexpected surface of asteroid (101955) Bennu. Nature **568**, 55–60 (2019). https://doi.org/10.1038/s41586-019-1033-6

T. Lee, D.A. Papanastassiou, G.J. Wasserburg, Demonstration of ^{26}Mg excess in Allende and evidence for ^{26}Al. Geophys. Res. Lett. **3**, 41–44 (1976). https://doi.org/10.1029/GL003i001p00041

L.A. Leshin, K.D. McKeegan, P.K. Carpenter, R.P. Harvey, Oxygen isotopic constraints on the genesis of carbonates from martian meteorite ALH84001. Geochim. Cosmochim. Acta **62**, 3–13 (1998). https://doi.org/10.1016/S0016-7037(97)00331-1

W. Li, N. Baoling, J. Dequi, Z. Qinglian, Measurement of the absolute abundance of oxygen-17 in VSMOW. Chin. Sci. Bull. **33**, 1610–1613 (1988). https://doi.org/10.1360/sb1988-33-19-1610

M.C. Liu, K.D. McKeegan, J.N. Goswami, K.K. Marhas, S. Sahijpal, T.R. Ireland, A.M. Davis, Isotopic records in CM hibonites: Implications for timescales of mixing of isotope reservoirs in the solar nebula. Geochim. Cosmochim. Acta **73**, 5051–5079 (2009). https://doi.org/10.1016/j.gca.2009.02.039

J. Llorca, J. Roszjar, J. Roszjar, J.A. Cartwright, A. Bischoff, U. Ott, A. Pack, S. Merchel, G. Rugel, L. Fimiani, P. Ludwig, J.V. Casado, D. Allepuz, The Ksar Ghilane 002 shergottite—The 100th registered martian meteorite fragment. Meteorit. Planet. Sci. **48**, 493–513 (2013). https://doi.org/10.1111/maps.12074

S.J. Lock, S.T. Stewart, M.I. Petaev, Z. Leinhardt, M.T. Mace, S.B. Jacobsen, M. Ćuk, The origin of the Moon within a terrestrial synestia. J. Geophys. Res., Planets **123**, 910–951 (2018). https://doi.org/10.1002/2017JE005333

L. Loiselle, P. Holden, J.N. Ávila, P. Lanc, J.C. Bridges, J.L. MacArthur, T.R. Ireland, The O isotope composition of martian meteorites using SHRIMP SI: Evidence of multiple reservoirs in silicate minerals of the regolith breccia Northwest Africa 8114, in *50th Lunar and Planetary Science Conference* (2019), abstract #2648

J.R. Lyons, E.D. Young, CO self-shielding as the origin of oxygen isotope anomalies in the early solar nebula. Nature **435**, 317–320 (2005). https://doi.org/10.1038/nature03557

J. MacArthur, J.C. Bridges, L.J. Hicks, R. Burgess, K. Joy, M.J. Branney, G.M. Hansford, S.H. Baker, S.P. Schwenzer, S.J. Gurmand, N.R. Stephen, E.D. Steer, J.D. Piercy, T.R. Ireland, Mineralogical constraints

on the thermal history of martian regolith breccia Northwest Africa 8114. Geochim. Cosmochim. Acta **246**, 267–298 (2019). https://doi.org/10.1016/j.gca.2018.11.026

P.R. Mahaffy, C.R. Webster, S.K. Atreya, H. Franz, M. Wong, P.G. Conrad, D. Harpold, J.J. Jones, L.A. Leshin, H. Manning, T. Owen, R.O. Pepin, S. Squyres, M. Trainer (MSL Science Team), Abundance and isotopic composition of gases in the martian atmosphere from the curiosity rover. Science **341**, 263–266 (2013). https://doi.org/10.1126/science.1237966

U.B. Marvin, The discovery and initial characterization of Allan Hills 81005: The first lunar meteorite. Geophys. Res. Lett. **10**(9), 775–778 (1983). https://doi.org/10.1029/GL010i009p00775

Y. Matsuhisa, J.R. Goldsmith, R.N. Clayton, Mechanism of hydrothermal crystallization of quartz at 250 °C and 15 kbar. Geochim. Cosmochim. Acta **42**, 173–182 (1978). https://doi.org/10.1016/0016-7037(78)90130-8

P. Mayewski et al., Holocene climate variability. Quat. Res. **62**(3), 243–255 (2004). https://doi.org/10.1016/j.yqres.2004.07.001

T.B. McCord, J.B. Adams, T.V. Johnson, Asteroid Vesta: Spectral reflectivity and compositional implications. Science **168**, 1445–1447 (1970). https://doi.org/10.1126/science.168.3938.1445

F.M. McCubbin et al., Geologic history of martian regolith breccia Northwest Africa 7034: Evidence for hydrothermal activity and lithologic diversity in the martian crust. J. Geophys. Res., Planets **121**, 2120–2149 (2016). https://doi.org/10.1002/2016JE005143

D.S. McKay, E.K. Gibson, K.L. Thomas-Keprta, H. Vali, C.S. Romanek, S.J. Clemett, X.D. Chillier, C.R. Maechling, R.N. Zare, Search for past life on Mars: Possible relic biogenic activity in martian meteorite ALH84001. Science **273**, 924–930 (1996). https://doi.org/10.1126/science.273.5277.924

K.D. McKeegan, Oxygen isotopes in refractory stratospheric dust particles: Proof of extraterrestrial origin. Science **237**, 1468–1471 (1987). https://doi.org/10.1126/science.237.4821.1468

K.D. McKeegan, R.M. Walker, E. Zinner, Ion microprobe isotopic measurements of individual interplanetary dust particles. Geochim. Cosmochim. Acta **49**, 1971–1987 (1985). https://doi.org/10.1016/0016-7037(85)90091-2

K.D. McKeegan, C.D. Coath, P.H. Mao, G. Jarzebinski, D. Burnett, A high energy secondary ion mass spectrometer for the analysis of captured solar wind, in *36th Lunar and Planetary Science Conference* (2004), abstract #2000

K.D. McKeegan et al., Isotopic compositions of cometary matter returned by Stardust. Science **314**, 1724–1728 (2006). https://doi.org/10.1126/science.1135992

K.D. McKeegan, A. Kallio, V. Heber, G. Jarzebinski, P. Mao, C. Coath, T. Kunihiro, R. Wiens, J. Nordholt, R. Moses, D. Reisenfeld, A. Jurewicz, D. Burnett, The oxygen isotopic composition of the Sun inferred from captured solar wind. Science **332**, 1528–1532 (2011). https://doi.org/10.1126/science.1204636

S.M. McLennan, Large-ion lithophile element fractionation during the early differentiation of Mars and the composition of the martian primitive mantle. Meteorit. Planet. Sci. **38**, 895–904 (2003). https://doi.org/10.1111/j.1945-5100.2003.tb00286.x

H.Y. McSween, SNC meteorites: Are they martian rocks? Geology **12**, 3–6 (1984). https://doi.org/10.1130/0091-7613(1984)12%3C3:SMATMR%3E2.0.CO;2

H.Y. McSween, S.W. Ruff, R.V. Morris, R. Gellert, G. Klingelhöfer, P.R. Christensen, T.J. McCoy, A. Ghosh, J.M. Moersch, B.A. Cohen, A.D. Rogers, C. Schröder, S.W. Squyres, J. Crisp, A. Yen, Mineralogy of volcanic rocks in Gusev Crater, Mars: Reconciling Mössbauer, Alpha Particle X-Ray Spectrometer, and Miniature Thermal Emission Spectrometer spectra. J. Geophys. Res. **113**, E06S04 (2008). https://doi.org/10.1029/2007JE002970

H.Y. McSween, D.W. Mittlefehldt, A.W. Beck, R.G. Mayne, T.J. McCoy, HED meteorites and their relationship to the geology of Vesta and the dawn mission. Space Sci. Rev. **163**, 141–174 (2011). https://doi.org/10.1007/s11214-010-9637-z

S. Messenger, L.P. Keller, F.J. Stadermann, R.M. Walker, E. Zinner, Samples of stars beyond the solar system: Silicate grains in interplanetary dust. Science **300**, 105–108 (2003). https://doi.org/10.1126/science.1080576

M.F. Miller, Isotopic fractionation and the quantification of $\Delta^{17}O$ anomalies in the oxygen three-isotope system—An appraisal and geochemical significance. Geochim. Cosmochim. Acta **66**, 1881–1889 (2002). https://doi.org/10.1016/S0016-7037(02)00832-3

M.F. Miller, R.C. Greenwood, I.A. Franchi, Comment on "The triple oxygen isotope composition of the Earth mantle and understanding $\Delta^{17}O$ variations in terrestrial rocks and minerals" by A. Pack and D. Herwartz [Earth Planet. Sci. Lett. **390**, 138–145 (2014)]. Earth Planet. Sci. Lett. **418**, 181–183 (2015). https://doi.org/10.1016/j.epsl.2014.12.026

M.F. Miller, A. Pack, I.N. Bindeman, R.C. Greenwood, Standardizing the reporting of $\Delta^{17}O$ data from high precision oxygen triple-isotope ratio measurements of silicate rocks and minerals. Chem. Geol. (2020, accepted). https://doi.org/10.1016/j.chemgeo.2019.119332

D.W. Mittlefehldt, ALH84001, a cumulate orthopyroxenite member of the martian meteorite clan. Meteorit. Planet. Sci. **29**, 214–221 (1994). https://doi.org/10.1111/j.1945-5100.1994.tb00673.x

D.W. Mittlefehldt, T.J. McCoy, C.A. Goodrich, A. Kracher, Non-chondritic meteorites from asteroidal bodies, in *Planetary Materials*, ed. by J.J. Papike. Reviews in Mineralogy, vol. 36 (Mineralogical Society of America, Chantilly, 1998), pp. 4.1–4.195

D.E. Moser et al., Solving the martian meteorite age conundrum using micro-baddeleyite and launch-generated zircon. Nature **499**, 454–457 (2013). https://doi.org/10.1038/nature12341

K. Nagao et al., Irradiation history of Itokawa regolith material deduced from noble gases in the Hayabusa samples. Science **333**, 1128–1131 (2011). https://doi.org/10.1126/science.1207785

K. Nagashima, A.N. Krot, H. Yurimoto, Stardust silicates from primitive meteorites. Nature **428**, 921–924 (2004). https://doi.org/10.1038/nature02510

T. Nakamura, T. Noguchi, A. Tsuchiyama, T. Ushikubo, N.T. Kita, J.W. Valley, M.E. Zolensky, Y. Kakazu, K. Sakamoto, E. Mashio, K. Uesugi, T. Nakano, Chondrule-like objects in short-period Comet 81P/Wild 2. Science **321**, 1664–1667 (2008). https://doi.org/10.1126/science.1160995

T. Nakamura et al., Itokawa dust particles: A direct link between S-type asteroids and ordinary chondrites. Science **333**, 1113–1116 (2011). https://doi.org/10.1126/science.1207758

E. Nakamura, A. Makishima, T. Moriguti, K. Kobayashi, R. Tanaka, T. Kunihiro, T. Tsujimori, C. Sakaguchi, H. Kitagawa, T. Ota, Y. Yachi, T. Yada, M. Abe, A. Fujimura, M. Ueno, T. Mukai, M. Yoshikawa, J. Kawaguchi, Space environment of an asteroid preserved on micrograins returned by the Hayabusa spacecraft. Proc. Natl. Acad. Sci. USA **109**, E624–E629 (2012). https://doi.org/10.1073/pnas.1116236109

D. Nakashima, N.T. Kita, T. Ushikubo, T. Noguchi, T. Nakamura, J.W. Valley, Oxygen three-isotope ratios of silicate particles returned from asteroid Itokawa by the Hayabusa spacecraft: A strong link with equilibrated LL chondrites. Earth Planet. Sci. Lett. **379**, 127–136 (2013). https://doi.org/10.1016/j.epsl.2013.08.009

O. Navon, G.J. Wasserburg, Self-shielding in O_2—A possible explanation for oxygen isotopic anomalies in meteorites? Earth Planet. Sci. Lett. **73**, 1–16 (1985)

H.B. Niemann, R.E. Hartle, W.T. Kasprzak, N.W. Spencer, D.M. Hunten, G.R. Carignan, Venus upper atmosphere neutral composition: Preliminary results from the pioneer Venus orbiter. Science **203**, 770–772 (1979). https://doi.org/10.1126/science.203.4382.770

P.B. Niles, L. Leshin, Y. Guan, Microscale carbon isotope variability in ALH84001 carbonates and a discussion of possible formation environments. Geochim. Cosmochim. Acta **69**, 2931–2944 (2005). https://doi.org/10.1016/j.gca.2004.12.012

L.R. Nittler, Presolar oxide grains in meteorites. AIP Conf. Proc. **402**, 59–82 (1997). https://doi.org/10.1063/1.53320

L.R. Nittler, F. Ciesla, Astrophysics with extraterrestrial materials. Annu. Rev. Astron. Astrophys. **54**, 53–93 (2016). https://doi.org/10.1146/annurev-astro-082214-122505

L.R. Nittler, C.M.O'.D. Alexander, J. Wang, X. Gao, Meteoritic oxide grain from supernova found. Nature **393**, 222 (1998). https://doi.org/10.1038/30377

L.E. Nyquist, C.-Y. Shih, D.D. Bogard, Ages and geologic histories of martian meteorites, in *Chronology and Evolution of Mars*, ed. by R. Kallenbach, J. Geiss, W.K. Hartmann (Kluwer, Dordrecht, 2001), pp. 105–164

L.E. Nyquist, C-Y. Shih, F.M. McCubbin, A.R. Santos, C.K. Shearer, Z.X. Peng, P.V. Burger, C.B. Agee, Rb-Sr and Sm-Nd isotopic and REE studies of igneous components in the bulk matrix domain of martian breccia Northwest Africa 7034. Meteorit. Planet. Sci. **51**, 483–498 (2016)

A. O'Keefe, D.A.G. Deacon, Cavity ring-down Optical Spectrometer for absorption measurements using pulsed laser sources. Rev. Sci. Instrum. **59**, 2544 (1988). https://doi.org/10.1063/1.1139895

A. Pack, D. Herwartz, The triple oxygen isotope composition of the Earth mantle and understanding $\Delta^{17}O$ variations in terrestrial rocks and minerals. Earth Planet. Sci. Lett. **390**, 138–145 (2014). https://doi.org/10.1016/j.epsl.2014.01.017

K. Pahlevan, D.J. Stevenson, Equilibration in the aftermath of the lunar-forming giant impact. Earth Planet. Sci. Lett. **262**, 438–449 (2007). https://doi.org/10.1016/j.epsl.2007.07.055

A.A. Pavlov, J.F. Kasting, Mass-independent fractionation of sulfur isotopes in archean sediments: Strong evidence for an anoxic archean atmosphere. Astrobiology **2**, 27–41 (2002). https://doi.org/10.1089/153110702753621321

R. Pepin, Meteorites: Evidence of martian origins. Nature **317**, 473–475 (1985). https://doi.org/10.1038/317473a0

P.N. Peplowski, D.J. Lawrence, T.H. Prettyman, N. Yamashita, D. Bazell, W.C. Feldman, L. Le Corre, T.J. McCoy, V. Reddy, R.C. Reedy, C.T. Russell, M.J. Toplis, Compositional variability on the surface of 4 Vesta revealed through GRaND measurements of high-energy gamma rays. Meteorit. Planet. Sci. **48**, 2252–2270 (2013). https://doi.org/10.1111/maps.12176

L. Qin, L.R. Nittler, C.M.O'D. Alexander, J. Wang, F.J. Stadermann, R.W. Carlson, Extreme ^{54}Cr-rich nano-oxides in the CI chondrite orgueil—Implications for a late supernova injection into the solar system. Geochim. Cosmochim. Acta **75**, 629–644 (2011). https://doi.org/10.1016/j.gca.2010.10.017

R. Reinhard, The Giotto encounter with comet Halley. Nature **321**, 313–318 (1986). https://doi.org/10.1038/321313a0

F. Richter, A.M. Davis, D.S. Ebel, A. Hashimoto, Elemental and isotopic fractionation of Type B calcium-, aluminum-rich inclusions: Experiments, theoretical considerations, and constraints on their thermal evolution. Geochim. Cosmochim. Acta **66**, 521–540 (2002). https://doi.org/10.1016/S0016-7037(01)00782-7

D. Rumble, A.J. Irving, Dispersion of oxygen isotopic compositions among 42 martian meteorites determined by laser fluorination: Evidence for assimilation of (ancient) altered crust, in *40th Lunar and Planetary Science Conference* (2009), abstract #2293

D. Rumble, M.F. Miller, I.A. Franchi, R.C. Greenwood, Oxygen three-isotope fractionation line in terrestrial silicate minerals: An inter laboratory comparison of hydrothermal quartz and eclogitic garnet. Geochim. Cosmochim. Acta **71**, 3592–3600 (2007). https://doi.org/10.1016/j.gca.2007.05.011

D. Rumble, M.E. Zolensky, J.M. Friedrich, P. Jenniskens, M.H. Shaddad, The oxygen isotope composition of Almahata Sitta. Meteorit. Planet. Sci. **45**, 1765–1770 (2010). https://doi.org/10.1111/j.1945-5100.2010.01099.x

C.T. Russell, H.Y. McSween, R. Jaumann, C.A. Raymond, The dawn mission to Vesta and ceres, in *Asteroids IV*, ed. by P. Michel, F.E. DeMeo, W.F. Bottke (University of Arizona Press, Tucson, 2015), pp. 419–432. https://muse.jhu.edu/chapter/1705177

F.J. Ryerson, K.D. McKeegan, Determination of oxygen self-diffusion in åkermanite, anorthite, diopside, and spinel: Implications for oxygen isotopic anomalies and the thermal histories of Ca-Al-rich inclusions. Geochim. Cosmochim. Acta **58**, 3713–3734 (1994). https://doi.org/10.1016/0016-7037(94)90161-9

J. Saito et al., Detailed images of asteroid 25143 Itokawa from Hayabusa. Science **312**, 1341–1344 (2006). https://doi.org/10.1126/science.1125722

N. Sakamoto, Y. Seto, S. Itoh, K. Kuramoto, K. Fujino, K. Nagashima, A.N. Krot, H. Yurimoto, Remnants of the early solar system water enriched in heavy oxygen isotopes. Science **317**, 231–233 (2007). https://doi.org/10.1126/science.1142021

R. Salmeron, T.R. Ireland, Formation of chondrules in magnetic winds blowing through the proto-asteroid belt. Earth Planet. Sci. Lett. **327–328**, 61–67 (2012a). https://doi.org/10.1016/j.epsl.2012.01.033

R. Salmeron, T.R. Ireland, The role of protostellar jets in star formation and the evolution of the early solar system: Astrophysical and meteoritical perspectives. Meteorit. Planet. Sci. **47**, 1922–1940 (2012b). https://doi.org/10.1111/maps.12029

L. Sangély, B. Boyer, E. de Chambost, N. Valle, J.-N. Audinot, T. Ireland, M. Wiedenbeck, J. Aleon, H. Jungnickel, J.-P. Barnes, P. Bienvenu, U. Breuer, Secondary ion mass spectrometry, in *Sector Field Mass Spectrometry for Elemental and Isotopic Analysis* (The Royal Society of Chemistry, London, 2015), pp. 439–499. Chap. 15

V. Sautter, M.J. Toplis, R.C. Wiens, A. Cousin, C. Fabre, O. Gasnault, S. Maurice, O. Forni, J. Lasue, A. Ollila, J.C. Bridges, N. Mangold, S. Le Mouélic, M. Fisk, P.-Y. Meslin, P. Beck, P. Pinet, L. Le Deit, W. Rapin, E.M. Stolper, H. Newsom, D. Dyar, N. Lanza, D. Vaniman, S. Clegg, In situ evidence for continental crust on early Mars. Nat. Geosci. **8**, 605–609 (2015). https://doi.org/10.1038/ngeo2474

S.M. Savin, S. Epstein, The oxygen and hydrogen isotope geochemistry of clay minerals. Geochim. Cosmochim. Acta **34**, 25–42 (1970). https://doi.org/10.1016/0016-7037(70)90149-3

J. Saxton, I. Lyon, G. Turner, Correlated chemical and isotopic zoning in carbonates in the martian meteorite ALH84001. Earth Planet. Sci. Lett. **160**, 811–822 (1998). https://doi.org/10.1016/S0012-821X(98)00129-0

J.M. Saxton, I.C. Lyon, G. Turner, Oxygen isotopes in forsterite grains from Julesburg and Allende: Oxygen-16-rich material in an ordinary chondrite. Meteorit. Planet. Sci. **33**, 1017–1027 (2010). https://doi.org/10.1111/j.1945-5100.1998.tb01708.x

B. Schueler, J. Morton, K. Mauersberger, Measurement of isotopic abundances in collected stratospheric ozone samples. Geophys. Res. Lett. **17**, 1295–1298 (1990). https://doi.org/10.1029/GL017i009p01295

S.P. Schwenzer, R.C. Greenwood, S.P. Kelley, U. Ott, A.G. Tindle, R. Haubold, S. Herrmann, J.M. Gibson, M. Anand, S. Hammond, I.A. Franchi, Quantifying noble gas contamination during terrestrial alteration in martian meteorites from Antarctica. Meteorit. Planet. Sci. **48**, 929–954 (2013). https://doi.org/10.1111/maps.12110

E.R.D. Scott, K. Keil, J.L. Goldstein, E. Asphaug, W.F. Bottke, N.A. Moskovitz, Early impact history and dynamical origin of differentiated meteorites and asteroids, in *Asteroids IV*, ed. by P. Michel, F. DeMeo, W.F. Bottke (University of Arizona Press, Tucson, 2015), pp. 573–595

E.R.D. Scott, A.N. Krot, I.S. Sanders, Isotopic dichotomy among meteorites and its bearing on the protoplanetary disk. Astrophys. J. **854**, 164 (2018). https://doi.org/10.3847/1538-4357/aaa5a5

Z. Sekanina, A model for comet 81P/Wild 2. J. Geophys. Res., Planets **108**, 8112 (2003). https://doi.org/10.1029/2003JE002093
N. Shackleton, N. Opdyke, Oxygen isotope and palaeomagnetic stratigraphy of equatorial Pacific core V28-238: Oxygen isotope temperatures and ice volumes on a 10^5 year and 10^6 year scale. Quat. Res. **3**, 39–55 (1973). https://doi.org/10.1016/0033-5894(73)90052-5
R. Shaheen, P.B. Niles, K. Chong, C.M. Corrigan, M.H. Thiemens, Carbonate formation events in ALH84001 trace the evolution of the martian atmosphere. Proc. Natl. Acad. Sci. **112**, 336–341 (2015). https://doi.org/10.1073/pnas.1315615112
Z.D. Sharp, A laser-based microanalytical method for the in situ determination of oxygen isotope ratios in silicates and oxides. Geochim. Cosmochim. Acta **54**, 1353–1357 (1990). https://doi.org/10.1016/0016-7037(90)90160-M
F.H. Shu, H. Shang, T. Lee, Toward an astrophysical theory of chondrites. Science **271**, 1545–1552 (1996). https://doi.org/10.1126/science.271.5255.1545
M. Siddall, E. Rohling, A. Almogi-Labin et al., Sea-level fluctuations during the last glacial cycle. Nature **423**, 853–858 (2003). https://doi.org/10.1038/nature01690
H. Sierks et al., On the nucleus structure and activity of comet 67P/Churyumov-Gerasimenko. Science **347**, aaa1044 (2015). https://doi.org/10.1126/science.aaa1044
G. Skrzypek, D. Ford, The stable isotope analysis of saline water samples on a cavity ring–down spectroscopy instrument. Environ. Sci. Technol. **48**, 2827–2834 (2014). https://doi.org/10.1021/es4049412
J.V. Smith, A.T. Anderson, R.C. Newton, E.J. Olsen, P.J. Wyllie, A petrologic model for the Moon based on petrogenesis, experimental petrology, and physical properties. J. Geol. **78**, 381–405 (1970). https://doi.org/10.1086/627537
M.L. Spicuzza, J.M.D. Day, L.A. Taylor, J.W. Valley, Oxygen isotope constraints on the origin and differentiation of the Moon. Earth Planet. Sci. Lett. **253**, 254–265 (2007). https://doi.org/10.1016/j.epsl.2006.10.030
F. Stadermann, T.K. Croat, T.J. Bernatowicz, S. Amari, S. Messenger, R.M. Walker, E. Zinner, Supernova graphite in the NanoSIMS: Carbon, oxygen and titanium isotopic compositions of a spherule and its TiC sub-components. Geochim. Cosmochim. Acta **69**, 177–188 (2005). https://doi.org/10.1016/j.gca.2004.06.017
D.J. Stevenson, A.N. Halliday, The origin of the Moon. Philos. Trans. R. Soc., Math. Phys. Eng. Sci. **372**, 20140289 (2014). https://doi.org/10.1098/rsta.2014.0289
S. Sugita et al., The geomorphology, color, and thermal properties of Ryugu: Implications for parent-body processes. Science **364**, eaaw0422 (2019). https://doi.org/10.1126/science.aaw0422
T.D. Swindle, A.H. Treiman, D.J. Lindstrom, M.K. Burkland, B.A. Cohen, J.A. Grier, B. Li, E.K. Olson, Noble gases in iddingsite from the Lafayette meteorite: Evidence for liquid water on Mars in the last few hundred million years. Meteorit. Planet. Sci. **35**, 107–115 (2010). https://doi.org/10.1111/j.1945-5100.2000.tb01978.x
R. Tanaka, E. Nakamura, Determination of ^{17}O-excess of terrestrial silicate/oxide minerals with respect to Vienna Standard Mean Ocean Water (VSMOW). Rapid Commun. Mass Spectrom. **27**, 285–297 (2012). https://doi.org/10.1002/rcm.6453
H.P. Taylor, S. Epstein, Relationship between ^{18}O/^{16}O ratios in coexisting minerals of igneous and metamorphic rocks: Part 1: Principles and experimental results. Geol. Soc. Am. Bull. **73**, 461–480 (1962a). https://doi.org/10.1130/0016-7606(1962)73[461:RBORIC]2.0.CO;2
H.P. Taylor, S. Epstein, Relationship between ^{18}O/^{16}O ratios in coexisting minerals of igneous and metamorphic rocks: Part 2. Application to petrologic problems. Geol. Soc. Am. Bull. **73**, 675–693 (1962b). https://doi.org/10.1130/0016-7606(1962)73[675:RBORIC]2.0.CO;2
M.G.G.T. Taylor et al., Rosetta begins its Comet Tale. Science **347**, 387 (2015). https://doi.org/10.1126/science.aaa4542
M. Thiemens, Mass-independent isotope effects in planetary atmospheres and the early solar system. Science **283**, 341–345 (1999). https://doi.org/10.1126/science.283.5400.341
M. Thiemens, J.E. Heidenreich III, The mass-independent fractionation of oxygen: A novel isotope effect and its possible cosmochemical implications. Science **219**, 1073–1075 (1983). https://doi.org/10.1126/science.219.4588.1073
D.J. Tholen, M.A. Barucci, Asteroid taxonomy, in *Asteroids II; Proceedings of the Conference*, Tucson, AZ, Mar. 8–11, 1988 (A90-27001 10-91) (University of Arizona Press, Tucson, 1989), pp. 298–315. https://doi.org/10.1016/0012-821X(85)90030-5
A. Tonotani, K. Bajo, S. Itose, M. Ishihara, K. Uchino, H. Yurimoto, Evaluation of multi-turn time-of-flight mass spectrum of laser ionization mass nanoscope. Surf. Interface Anal. **48**, 1122–1126 (2016). https://doi.org/10.1002/sia.6112
A.H. Treiman, Olivine and carbonate globules in ALH84001: A terrestrial analog, and implications for water on Mars, in *36th Lunar and Planetary Science Conference XXXVI* (2005), abstract #1107

A.H. Treiman, E.J. Essene, Chemical composition of magnetite in martian meteorite ALH 84001: Revised appraisal from thermochemistry of phases in Fe–Mg–C–O. Geochim. Cosmochim. Acta **75**, 5324–5335 (2011). https://doi.org/10.1016/j.gca.2011.06.038

T. Ushikubo, M. Kimura, N.T. Kita, J.W. Valley, Primordial oxygen isotope reservoirs of the solar nebula recorded in chondrules in Acfer 094 carbonaceous chondrite. Geochim. Cosmochim. Acta **90**, 242–264 (2012). https://doi.org/10.1016/j.gca.2012.05.010

W.R. Van Schmus, J.A. Wood, A chemical-petrologic classification for the chondritic meteorites. Geochim. Cosmochim. Acta **31**, 747–754 (1967). https://doi.org/10.1016/S0016-7037(67)80030-9

J.H. Waite Jr., M.R. Combi, W.-H. Ip, T.E. Cravens, R.L. McNutt Jr., W. Kasprzak, R. Yelle, J. Luhmann, H. Niemann, D. Gell, B. Magee, G. Fletcher, J. Lunine, W.-L. Tseng, Cassini ion and neutral mass spectrometer: Enceladus plume composition and structure. Science **311**, 1419–1422 (2006). https://doi.org/10.1126/science.1121290

S. Wakita, Y. Matsumoto, S. Oshino, Y. Hasegawa, Planetesimal collisions as a chondrule forming event. Astrophys. J. **834**, 125 (2017). https://doi.org/10.3847/1538-4357/834/2/125

H. Wang, C. Lineweaver, T.R. Ireland, The volatility trend of protosolar and terrestrial elemental abundances. Icarus **328**, 287–305 (2019). https://doi.org/10.1016/j.icarus.2019.03.018

P. Warren, Stable-isotopic anomalies and the accretionary assemblage of the Earth and Mars: A subordinate role for carbonaceous chondrites. Earth Planet. Sci. Lett. **311**, 93–100 (2011). https://doi.org/10.1016/j.epsl.2011.08.047

S. Watanabe et al., Hayabusa2 arrives at the carbonaceous asteroid 162173 Ryugu—A spinning top—Shaped rubble pile. Science **364**, 268–272 (2019). https://doi.org/10.1126/science.aav8032

C.R. Webster, P.R. Mahaffy, G.J. Flesch, P.B. Niles, J.H. Jones, L.A. Leshin, S.K. Atreya, J.C. Stern, L.E. Christensen, T. Owen, H. Franz, R.O. Pepin, A. Steele (the MSL Science Team), Isotope ratios of H, C, and O in CO_2 and H_2O of the martian atmosphere. Science **341**, 260–263 (2013). https://doi.org/10.1126/science.1237961

M.K. Weisberg, M. Prinz, R.N. Clayton, T.K. Mayeda, M.M. Grady, I. Franchi, C.T. Pillinger, G.W. Kallemeyn, The K (Kakangari) chondrite grouplet. Geochim. Cosmochim. Acta **60**, 4253–4263 (1996). https://doi.org/10.1016/S0016-7037(96)00233-5

M.K. Weisberg, T.J. McCoy, A.N. Krot, Systematics and evaluation of meteorite classification, in *Meteorites and the Early Solar System II*, ed. by D.S. Lauetta, H.Y. McSween Jr. (University of Arizona Press, Tucson, 2006), pp. 19–52

A.J. Westphal et al., Evidence for interstellar origin of seven dust particles collected by the Stardust spacecraft. Science **345**, 786–791 (2014). https://doi.org/10.1126/science.1252496

U. Wiechert, A.N. Halliday, D-C. Lee, G.A. Snyder, L.A. Taylor, D. Rumble, Oxygen isotopes and the Moon-forming Giant Impact. Science **294**, 345–348 (2001). https://doi.org/10.1126/science.1063037

W.C. Wiley, I.H. McLaren, Time-of-flight mass spectrometer with improved resolution. Rev. Sci. Instrum. **26**, 1150 (1955). https://doi.org/10.1063/1.1715212

A. Wittmann, R.L. Korotev, B. Jolliff, A.J. Irving, D.F. Moser, I. Barker, D. Rumble, Petrography and composition of martian regolith breccia meteorite Northwest Africa 7475. Meteorit. Planet. Sci. **50**, 326–352 (2015). https://doi.org/10.1111/maps.12425

J.A. Wood, J.S. Dickey, U.B. Marvin, B.N. Powell, Lunar anorthosites. Science **167**, 602–604 (1970). https://doi.org/10.1126/science.167.3918.602

I.P. Wright, J. Barber, G.H. Morgan, A.D. Morse, S. Sheridan, D.J. Andrews, J. Maynard, D. Yau, T. Evans, M.R. Leese, J.C. Zarnecki, B.J. Kent, N.R. Waltham, M.S. Whalley, S. Heys, D.L. Drummond, R.L. Edeson, E.C. Sawyer, R.F. Turner, C.T. Pillinger, Ptolemy—An instrument to measure stable isotopic ratios of key volatiles on a cometary nucleus. Space Sci. Rev. **128**, 363–381 (2007). https://doi.org/10.1007/s11214-006-9001-5

S. Yokota, Isotope mass spectrometry in the solar system exploration. Mass Spectrom. **7**, S0076 (2018). https://doi.org/10.5702/massspectrometry.S0076

E.D. Young, S.S. Russell, Oxygen reservoirs in the early solar nebula inferred from an Allende CAI. Science **282**, 452–455 (1998). https://doi.org/10.1126/science.282.5388.452

E.D. Young, I.E. Kohl, P.H. Warren, D.C. Rubie, S.A. Jacobson, A. Morbidelli, Oxygen isotopic evidence for vigorous mixing during the Moon-forming giant impact. Science **351**, 493–496 (2016). https://doi.org/10.1126/science.aad0525

H. Yurimoto, Oxygen isotopes, in *Encyclopedia of Geochemistry: A Comprehensive Reference Source on the Chemistry of the Earth*, ed. by W.M. White (Springer, Cham, 2018), pp. 1129–1135

H. Yurimoto, K. Kuramoto, Molecular cloud origin for the oxygen isotope heterogeneity in the solar system. Science **305**, 1763–1766 (2004). https://doi.org/10.1126/science.1100989

H. Yurimoto, J.T. Wasson, Extremely rapid cooling of a carbonaceous-chondrite chondrule containing very ^{16}O-rich olivine and a ^{26}Mg-excess. Geochim. Cosmochim. Acta **66**, 4355–4363 (2002). https://doi.org/10.1016/S0016-7037(02)01218-8

H. Yurimoto, A.N. Krot, B. Choi, J. Aléon, T. Kunihiro, A.J. Brearley, Oxygen isotopes of chondritic components. Rev. Mineral. Geochem. **68**, 141–186 (2008)
H. Yurimoto et al., Oxygen isotopic compositions of asteroidal materials returned from Itokawa by the Hayabusa mission. Science **333**, 1116–1119 (2011). https://doi.org/10.1126/science.1207776
G. Zeff, Q. Williams, Fractional crystallization of martian magma oceans and formation of a thermochemical boundary layer at the base of the mantle. Geophys. Res. Lett. **46**, 10997–11007 (2019)
J. Zhang, N. Dauphas, A.M. Davis, I. Leya, A. Fedkin, The proto-Earth as a significant source of lunar material. Nat. Geosci. **5**, 251–255 (2012). https://doi.org/10.1038/ngeo1429
K. Ziegler, Z.D. Sharp, C.B. Agee, The unique NWA 7034 martian meteorite: Evidence for multiple oxygen isotope reservoirs, in *44th Lunar and Planetary Science Conference* (2013), abstract #2639
E. Zinner, Stellar nucleosynthesis and the isotopic composition of presolar grains from primitive meteorites. Annu. Rev. Earth Planet. Sci. **26**, 147–188 (1998). https://doi.org/10.1146/annurev.earth.26.1.147
E.K. Zinner, Presolar grains, in *Treatise on Geochemistry*, vol. 1, ed. by A.M. Davis, H.D. Holland, K.K. Turekian (Elsevier, Amsterdam, 2003), pp. 17–39. https://doi.org/10.1016/B0-08-043751-6/01144-0
E.K. Zinner, A.J. Fahey, J.N. Goswami, T.R. Ireland, K.D. McKeegan, Large ^{48}Ca anomalies are associated with ^{50}Ti anomalies in Murchison and Murray hibonites. Astrophys. J. Lett. **311**, L103–L106 (1986). https://doi.org/10.1086/184807
M. Zolensky et al., Mineralogy and petrology of Comet 81P/Wild 2 nucleus samples. Science **314**, 1735–1739 (2006). https://doi.org/10.1126/science.1135842